PHYSICAL REVIEW D **85,** 114032 (2012)

Charmed and strange baryon resonances with heavy-quark spin symmetry

O. Romanets,[1] L. Tolos,[2,1] C. García-Recio,[3] J. Nieves,[4] L. L. Salcedo,[3] and R. G. E. Timmermans[1]

[1]*KVI, University of Groningen, Zernikelaan 25, 9747AA Groningen, The Netherlands*

[2]*Institut de Ciències de l'Espai (IEEC/CSIC), Campus Universitat Autònoma de Barcelona, Facultat de Ciències, Torre C5, E-08193 Bellaterra, Spain*

[3]*Departamento de Física Atómica, Molecular y Nuclear, and Instituto Carlos I de Física Teórica y Computacional, Universidad de Granada, E-18071 Granada, Spain*

[4]*Instituto de Física Corpuscular (centro mixto CSIC-UV), Institutos de Investigación de Paterna, Apartado 22085, 46071, Valencia, Spain*

(Received 11 February 2012; published 20 June 2012)

We study charmed and strange baryon resonances that are generated dynamically by a unitary baryon-meson coupled-channel model which incorporates heavy-quark spin symmetry. This is accomplished by extending the SU(3) Weinberg-Tomozawa chiral Lagrangian to SU(8) spin-flavor symmetry plus a suitable symmetry breaking. The model produces resonances with negative parity from s-wave interaction of pseudoscalar and vector mesons with $1/2^+$ and $3/2^+$ baryons. Resonances in all the isospin, spin, and strange sectors with one, two, and three charm units are studied. Our results are compared with experimental data from several facilities, such as the CLEO, Belle or *BABAR* collaborations, as well as with other theoretical models. Some of our dynamically-generated states can be readily assigned to resonances found experimentally, while others do not have a straightforward identification and require the compilation of more data and also a refinement of the model. In particular, we identify the $\Xi_c(2790)$ and $\Xi_c(2815)$ resonances as possible candidates for a heavy-quark spin symmetry doublet.

DOI: 10.1103/PhysRevD.85.114032 PACS numbers: 14.20.Lq, 14.40.Lb, 11.10.St, 12.38.Lg

I. INTRODUCTION

In the last few decades there has been a growing interest in the properties of charmed hadrons in connection with many experiments such as CLEO, Belle, *BABAR*, and others [1–36]. Also, the planned experiments such as PANDA and CBM at the FAIR facility at Gesellschaft fuer Schwerionen Forschung [37,38], which involve the studies of charm physics, open the possibility for observation of more states with exotic quantum numbers of charm and strangeness in the near future. The observation of new states and the plausible explanation of their nature is a very active topic of research. The ultimate goal is to understand whether those states can be described with the usual three-quark baryon or quark-antiquark meson interpretation or, alternatively, qualify better as hadron molecules.

Recent approaches based on coupled-channels dynamics have proven to be very successful in describing the existing experimental data. In particular, unitarized coupled-channel methods have been applied in the baryon-meson sector with the charm degree of freedom [39–45], partially motivated by the parallelism between the $\Lambda(1405)$ and the $\Lambda_c(2595)$. In those references, the baryon-meson interaction in the charm sector is constructed using the t-channel exchange of vector mesons between pseudoscalar mesons and baryons. Other existing coupled-channel approaches are based on the Jülich meson-exchange model [46–48] or on the hidden gauge formalism [49].

However, those previous models are not consistent with heavy-quark spin symmetry [50–52], which is a proper QCD symmetry that appears when the quark masses, such as the charm mass, become larger than the typical confinement scale. Aiming to incorporate heavy-quark symmetry, an SU(8) spin-flavor symmetric model has recently been developed [53,54], which includes vector mesons similarly to the SU(6) approach developed in the light sector Refs. [55,56]. Following this scheme, baryon resonances in the charm sector have been studied, such as the s-wave states in the charm $C = 1$ and strangeness $S = 0$ sector [53], as well as $C = -1$ sectors [54], which are necessarily exotic.

The objective of this work is to continue those studies on dynamically-generated baryon resonances using heavy-quark spin symmetry constraints. We will focus on charm $C = 1$ and strangeness $S = -2$, -1 and 0, as well as on sectors with $C = 2$ and 3. We therefore use the model of Ref. [53], and as novelty we pay here special attention to the pattern of spin-flavor symmetry breaking. Flavor SU(4) is not a good symmetry in the limit of a heavy charm-quark, for this reason, instead of the breaking pattern SU(8) $\supset$ SU(4), in this work we consider the pattern SU(8) $\supset$ SU(6), since the light spin-flavor group [SU(6)] is decoupled from heavy-quark transformations. This allows us to implement heavy-quark spin symmetry in the analysis and to unambiguously identify the corresponding multiplets among the resonances generated dynamically. At the same time, we are also able to assign approximate heavy [SU(8)] and light [SU(6)] spin-flavor multiplet labels to the states.

We would like to devote a few words here to critically discuss the extension of the Weinberg-Tomozawa (WT)

interaction to vector mesons and to flavor SU(4) assumed in this work. Because at present we lack a robust scheme to systematically construct an effective field theory approach to study four flavor physics, one has to rely on models, including as many as possible known features of QCD. Most of the available models in the literature assume SU(4) flavor symmetry in one way or another and this is probably the weakest point of the whole approach, as well as some arbitrary pattern of symmetry breaking.

As usually understood, chiral symmetry refers only to the light-quark sector, i.e., at best to flavor SU(3), and it could very well be the case that no trace of it survives in sectors involving charm. However, spectroscopic data indicate that the large charm-quark mass acts mainly in an additive way on the hadron masses. This still leaves the possibility that the effect of the large quark mass introduces only moderate changes in other hadron properties. Chiral symmetry breaking fixes the strength of the lowest order interaction between Goldstone bosons and other hadrons (here baryons) in a model independent way; this is the WT interaction, but chiral symmetry does not fix the interaction between vector-mesons and baryons. On the other hand, heavy-quark spin symmetry (HQSS) connects vector and pseudoscalar mesons containing charmed quarks. It does not tell anything about mesons made out of light quarks. Nevertheless, there exist several predictions (relative closeness of baryon octet and decuplet masses, the axial current coefficient ratio $F/D = 2/3$, the magnetic moment ratio $\mu_p/\mu_n = -3/2$) which are remarkably well satisfied in nature [57], which suggests that spin symmetry could be a good approximate symmetry in the light sector. This is the spin-flavor SU(6) symmetry of the quark model already identified in the hadronic properties before the advent of QCD (see, for instance [58]). Moreover, in the large N_c limit (being N_c the number of colors) there exists an exact spin-flavor symmetry for ground state baryons [59]. In the meson sector, an underlying static chiral U(6) $\times$ U(6) symmetry has been advocated by Caldi and Pagels [60,61], in which vector mesons would be Goldstone bosons acquiring mass through relativistic corrections. This scheme solves a number of theoretical problems in the classification of mesons and also makes predictions which are in remarkable agreement with the experiment.

The number of couplings between low-lying hadrons with four flavors is very large, and the amount of available spectroscopic data is still reduced. It is clearly appealing to have a predictive model for four flavors including all basic hadrons (pseudoscalar and vector mesons, and $1/2^+$ and $3/2^+$ baryons) which reduces to the WT interaction in the sector where Goldstone bosons are involved and which incorporates heavy-quark symmetry in the sector where charm quarks participate. The model assumption in the present extension does not appear to be easy to justify directly from QCD, but, on the one hand, it is worth trying it in view of the reasonable semiqualitative outcome of the SU(6) extension in the three-flavor sector [62]. On the other hand, there is a formal plausibleness on how the SU(4) WT interaction in the charmed pseudoscalar meson-baryon sector did come out in the vector-meson exchange picture, as discussed in the t-channel vector model exchange (TVME) approach [42]. We just want to do a simple match making of the two, with the bonus that we improve on previous models since we incorporate spin symmetry HQSS in the charm sector.

The paper has been organized in the following way. In the next section a description of the theoretical model is given. The third section presents the results of our calculation, and in the last section we summarize the conclusions of this work. In Appendix A we show results incorporating a suppression factor for the charm-exchange transitions. The tables of the interaction matrices for the different baryon-meson channels are collected in Appendix B.

II. THEORETICAL FRAMEWORK

A. Spin-flavor and heavy-quark structure of the baryon-meson interaction

For the baryon-meson interaction we use the model of [53,54]. As mentioned, this model obeys SU(8) spin-flavor symmetry and also HQSS in the sectors studied in this work. The SU(6) version of the model has been also applied to the study of mesonic [63] and baryonic [62] light resonances.

The model is based on an extension of the WT SU(3) chiral Lagrangian to implement spin-flavor symmetry [56,64]. The channel space is augmented with vector mesons and $3/2^+$ baryons, in addition to pseudoscalar mesons and $1/2^+$ baryons. The interaction includes only s-wave, which is appropriate for the description of low-lying odd-parity baryon-meson resonances.

In the SU(8) spin-flavor scheme, the mesons, M, fall in the **63**-plet (adjoint irreductible representation) plus a singlet, while the baryons, B, are placed in the **120**-plet, which is fully symmetric. This refers to the lowest-lying hadrons with all quarks in relative s-wave. The extension of the WT Lagrangian is a contact interaction between baryon and meson modeling the zero-range t-channel exchange of mesons in the adjoint representation. Schematically,

$$\mathcal{L}_{\mathrm{WT}}^{\mathrm{SU(8)}} = \frac{1}{f^2}[[M^\dagger \otimes M]_{\mathbf{63_a}} \otimes [B^\dagger \otimes B]_{\mathbf{63}}]_{\mathbf{1}}. \qquad (1)$$

In the s-channel, the baryon-meson space reduces into the following SU(8) irreps:

$$\mathbf{63} \otimes \mathbf{120} = \mathbf{120} \oplus \mathbf{168} \oplus \mathbf{2520} \oplus \mathbf{4752}, \qquad (2)$$

therefore the single **63**-like coupling in the t-channel [see Eq. (1)] corresponds to four s-channel couplings. These are proportional to the following eigenvalues:

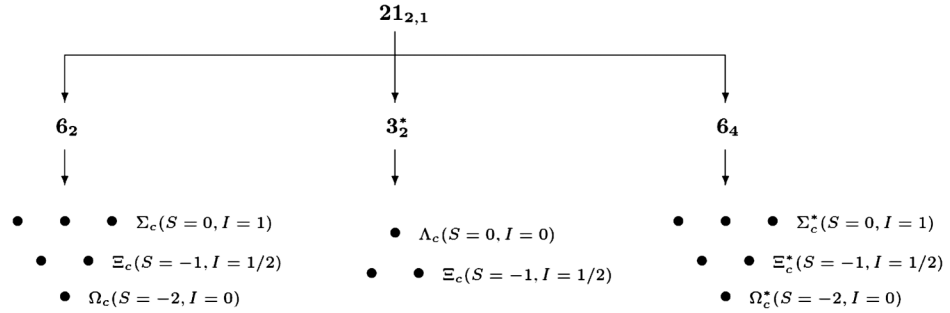

FIG. 1. SU(3) × SU(2) reduction of the $\mathbf{21_{2,1}}$ multiplet of SU(6) × $SU_C(2)$ × $U_C(1)$.

$$\lambda_{\mathbf{120}} = -16, \quad \lambda_{\mathbf{168}} = -22, \quad \lambda_{\mathbf{2520}} = 6, \quad \lambda_{\mathbf{4752}} = -2. \tag{3}$$

In our convention for the potential, a negative sign in the eigenvalues implies an attractive interaction. Then, from the eigenvalues, we find that the multiplets **120** and **168** are the most attractive ones while the **4752**-plet is weakly attractive and the **2520**-plet is repulsive. As a consequence, dynamically-generated baryon resonances are most likely to occur within the **120** and **168** sectors. States in other SU(8) irreps are necessarily exotic, as they cannot be obtained from qqq states, that is, from $\mathbf{4}\otimes\mathbf{4}\otimes\mathbf{4}$ in flavor SU(4).[1] It is also instructive to draw the attention here to some of the findings of Ref. [56] when the number of colors N_C departs from 3 [64]. There it is shown that, in the **168** SU(8) irreducible space, the SU(8) extension of the WT s-wave baryon-meson interaction scales as $\mathcal{O}(1)$. Note that SU(3) WT counterpart in some channels also scales as $\mathcal{O}(1)$ because of the coupling strength for some channels behaves as $\mathcal{O}(N_C)$, which compensates $\mathcal{O}(1/N_C)$ coming from the square of the meson decay constant [65]. However, the WT interaction behaves as $\mathcal{O}(1/N_C)$ within the **120** and **4752** baryon-meson spaces. This presumably implies that **4752** states do not appear in the large N_C QCD spectrum, since both excitation energies and widths grow with an approximate $\sqrt{N_C}$ rate.

To take into account the breaking of flavor symmetry introduced by the heavy charmed quark, we consider the reduction

$$\mathrm{SU}(8) \supset \mathrm{SU}(6) \times \mathrm{SU}_C(2) \times \mathrm{U}_C(1), \tag{4}$$

where SU(6) is the spin-flavor group for three flavors. $SU_C(2)$ is the rotation group of quarks with charm. We consider only s-wave interactions so $\boldsymbol{J}_C$ is just the spin carried by the charmed quarks or antiquarks. Finally, $U_C(1)$ is the group generated by the charm quantum number C.

The two main SU(8) multiplets have the following reductions:

$$\begin{aligned}\mathbf{120} &= \mathbf{56_{1,0}} \oplus \mathbf{21_{2,1}} \oplus \mathbf{6_{3,2}} \oplus \mathbf{1_{4,3}},\\ \mathbf{168} &= \mathbf{70_{1,0}} \oplus \mathbf{21_{2,1}} \oplus \mathbf{15_{2,1}} \oplus \mathbf{6_{1,2}} \oplus \mathbf{6_{3,2}} \oplus \mathbf{1_{2,3}}.\end{aligned} \tag{5}$$

For the right-hand side we use the notation $\boldsymbol{R}_{2J_C+1,C}$, where $\boldsymbol{R}$ is the SU(6) irrep label (for which we use the dimension), J_C is the spin carried by the quarks with charm, and C is the charm. Therefore, with $C = 1$ there are two $\mathbf{21_{2,1}}$: one from **120** and another from **168**, and one $\mathbf{15_{2,1}}$ only from **168**. With $C = 2$ there are two $\mathbf{6_{3,2}}$: one from each SU(8) irrep, and one $\mathbf{6_{1,2}}$ from **168**. Finally, there are two representations with $C = 3$: $\mathbf{1_{4,3}}$ and $\mathbf{1_{2,3}}$.

The SU(6) multiplets can be reduced under SU(3) × $SU_l(2)$. The factor $SU_l(2)$ refers to the spin of the light quarks (i.e., with flavors u, d, and s). In order to connect with the labeling (C, S, I, J) based on isospin multiplets (S is the strangeness, I the isospin, J the spin), we further reduce $SU_l(2) \times SU_C(2) \supset SU(2)$, where SU(2) refers to the total spin J, that is, we couple the spins of light and charmed quarks to form SU(3) multiplets with well-defined J. So, for instance, the multiplet $\mathbf{21_{2,1}}$ reduces as $\mathbf{6_2} \oplus \mathbf{3_2^*} \oplus \mathbf{6_4}$, where we use the notation $\boldsymbol{r}_{2J+1}$ and $\boldsymbol{r}$ stands for the SU(3) irrep.[2] The charmed SU(6) multiplets reduce as follows:

$$\begin{aligned}&\mathbf{21_{2,1}} = \mathbf{6_2} \oplus \mathbf{3_2^*} \oplus \mathbf{6_4}, \qquad \mathbf{15_{2,1}} = \mathbf{6_2} \oplus \mathbf{3_2^*} \oplus \mathbf{3_4^*},\\ &\mathbf{6_{3,2}} = \mathbf{3_2} \oplus \mathbf{3_4}, \qquad \mathbf{6_{1,2}} = \mathbf{3_2},\\ &\mathbf{1_{2,3}} = \mathbf{1_2}, \qquad \mathbf{1_{4,3}} = \mathbf{1_4}.\end{aligned} \tag{6}$$

The decomposition of the SU(6) × $SU_C(2)$ × $U_C(1)$ multiplets under SU(3) × SU(2) is shown in Figs. 1–3 for the multiplets in Eq. (5) with $C = 1, 2$, (the $C = 3$ singlets decomposition is not depicted). The further reduction into (C, S, I, J) multiplets is also displayed.

[1]The states in the **168** cannot be obtained from $\mathbf{8}\otimes\mathbf{8}\otimes\mathbf{8}$ of spin-flavor if a relative s-wave is assumed, but they appear by allowing p-wave states, so exotic is better defined with regards to flavor.

[2]The $\mathbf{21_{2,1}}$ irrep can be realized by a baryon with quark structure llc with the two light quarks in a symmetric spin-flavor state. In the light sector, and from the point of view of SU(3), this is $(\mathbf{3_2}\otimes\mathbf{3_2})_s = \mathbf{6_3} \oplus \mathbf{3_1^*}$, the subindex being $2J_l + 1$. The coupling of $J_l = 0, 1$ with $J_C = 1/2$ gives the decomposition quoted in the text. The $\mathbf{15_{2,1}}$ reduction follows similarly, but the pair ll is antisymmetric.

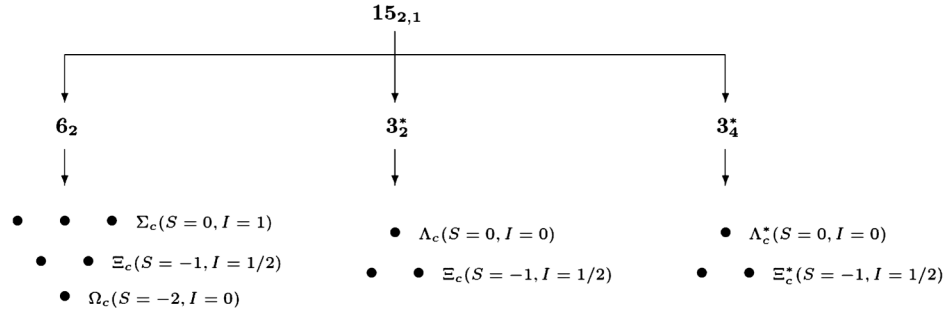

FIG. 2. SU(3) × SU(2) reduction of the $\mathbf{15_{2,1}}$ multiplet of SU(6) × $\mathrm{SU}_C(2)$ × $\mathrm{U}_C(1)$.

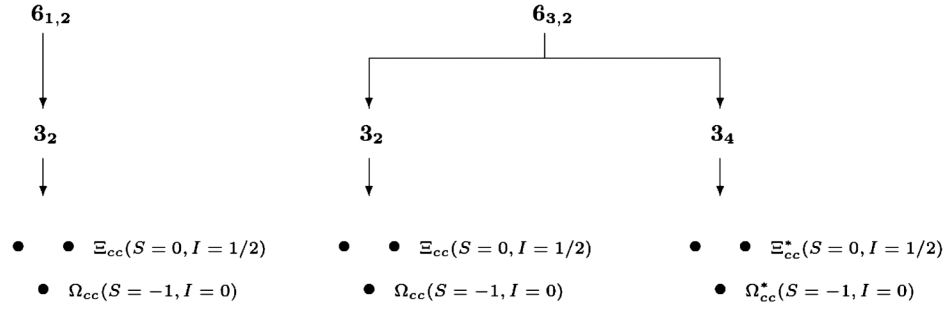

FIG. 3. SU(3) × SU(2) reduction of the multiplets $\mathbf{6_{3,2}}$ and $\mathbf{6_{1,2}}$ of SU(6) × $\mathrm{SU}_C(2)$ × $\mathrm{U}_C(1)$.

Collecting the various *CSIJ* multiplets in the strongly attractive representations **120** and **168**, we can estimate the expected number of dynamically-generated baryon-meson resonances. These expected numbers of states are shown in Table I. In the next section we find that none of these states for the sectors with charm goes to a wrong Riemann sheet in the complex s-plane, and so they can be identified with physical states.[3]

Heavy-quark spin operators are suppressed by the inverse mass of the heavy quark, therefore HQSS is a fairly good approximate symmetry of QCD [50,51] and it is mandatory to implement it in any hadronic model involving charmed quarks. HQSS implies conservation of the number of charmed quarks, N_c, and of the number of charmed antiquarks, $N_{\bar{c}}$, with corresponding symmetry group $\mathrm{U}_c(1) \times \mathrm{U}_{\bar{c}}(1)$. In addition, there is invariance under the group SU(2) × SU(2) of separate rotations of spin of c and $\bar{c}$. Although such invariance is not automatically ensured by requiring spin-flavor symmetry,[4] spin-flavor does imply HQSS whenever only heavy quarks are present (but not heavy antiquarks), or only heavy antiquarks are present (but not heavy quarks). This observation suggests a simple prescription to enforce HQSS in the interaction for the charmed sectors considered in this work, namely, to drop meson-baryon channels containing $c\bar{c}$ pairs. Specifically, we consider the sectors $(N_c, N_{\bar{c}}) = (1,0), (2,0), (3,0)$, for which the SU(8)-extended WT interaction fulfills HQSS. It should be noted that SU(8) is no longer an exact symmetry in the truncated coupled-channel space. Nevertheless, for the low-lying resonances, the omitted channels are kinematically suppressed anyway, due to their large mass. Charmless sectors with hidden charm are necessarily exotic. The study of these sectors is deferred for future work.

As a final comment, it should be noted that the SU(6) irrep $\mathbf{56_{1,0}}$ in Eq. (5) does not exactly coincide with the usual **56** irrep that one finds in spin-flavor with only u, d and s flavors. The latter is completely charmless, while the states in $\mathbf{56_{1,0}}$ contain hidden charm components in general. Actually, in the SU(8) case, there are further $\mathbf{56_{1,0}}$ irreps (in **2520** or **4752**). Using a suitable angle mixing [similar to the ideal mixing in SU(3)] one can recover the purely charmless $\mathbf{56_{1,0}}$ and construct another $\mathbf{56_{1,0}}$ of the form $|lll\rangle|c\bar{c}\rangle$ (l standing for light quarks). When the hidden charm components are dropped, one $\mathbf{56_{1,0}}$ combination remains while the other one disappears. These considerations can be extended to the other irreps in Eq. (5). This explains why, when dropping the hidden charm components, we still get the same number of expected states quoted in Table I, even if the total dimension of the full meson-baryon space is reduced.

[3]This is not always the case, for instance in [62,66]; some resonances move to unphysical regions of the Riemann surface after breaking of the symmetry.

[4]Spin-flavor symmetry ensures invariance under equal spin rotations of c and $\bar{c}$.

TABLE I. Expected number of baryonic resonances for the various *CSIJ* sectors.

				J^P	
C	S	I	State	$\frac{1}{2}^-$	$\frac{3}{2}^-$
1	0	0	Λ_c	3	1
	0	1	Σ_c	3	2
	−1	1/2	Ξ_c	6	3
	−2	0	Ω_c	3	2
2	0	1/2	Ξ_{cc}	3	2
	−1	0	Ω_{cc}	3	2
3	0	0	Ω_{ccc}	1	1

B. Unitarization in coupled channels

The tree-level baryon-meson interaction of the SU(8)-extended WT interaction, reads

$$V_{ij}(s) = D_{ij}\frac{2\sqrt{s} - M_i - M_j}{4f_i f_j}\sqrt{\frac{E_i + M_i}{2M_i}}\sqrt{\frac{E_j + M_j}{2M_j}}. \quad (7)$$

Here, i and j are the outgoing and incoming baryon-meson channels, respectively. M_i, E_i, and f_i stand, respectively, for the mass and the center-of-mass energy of the baryon and the meson decay constant in the i channel. D_{ij} are the matrix elements for the various *CSIJ* sectors considered in this work. They are displayed in Appendix B. The matrix elements can be evaluated using the method described in the Appendix A of Ref. [53], or using the Clebsch-Gordan coefficients computed in Ref. [67].

In order to calculate the scattering amplitudes, T_{ij}, we solve the on-shell Bethe-Salpeter equation in coupled channels using the interaction matrix V as kernel:

$$T(s) = \frac{1}{1 - V(s)G(s)}V(s). \quad (8)$$

$G(s)$ is a diagonal matrix containing the baryon-meson propagator for each channel. D, T, V, and G are matrices in coupled-channel space. All these matrices are symmetric and block diagonal in *CSIJ* sectors, producing the corresponding symmetric submatrices D^{CSIJ}, T^{CSIJ}, V^{CSIJ}, and G^{CSIJ}.

The bare loop function $G^0_{ii}(s)$ is logarithmically ultraviolet divergent and needs to be renormalized. This can be done by one-subtraction at a subtraction point $\sqrt{s} = \mu_i$,

$$G_{ii}(s) = G^0_{ii}(s) - G^0_{ii}(\mu_i^2). \quad (9)$$

Here we adopt the prescription of [42], namely, μ_i depends only on *CSI* and equals $\sqrt{m_{\rm th}^2 + M_{\rm th}^2}$, where $m_{\rm th}$ and $M_{\rm th}$ are, respectively, the masses of the meson and the baryon of the channel with the lowest threshold in the given *CSI* sector. G_{ii} is determined (see Eq. (14) of Ref. [62]) by the loop function $\bar{J}_0$ defined in the Appendix of Ref. [68] for the different relevant Riemann sheets.

An enlightening discussion on the dependence on the subtraction point has been presented in [69]. There, a "natural" value is introduced for the subtraction point, namely, the mass of the lightest baryon in the given coupled-channel sector (see [70] for an alternative definition of natural value). As argued in [69], the natural value needs not coincide with the phenomenological one, and a comparison between both provides valuable information on the nature of the resonances generated dynamically, to wit, quark vs molecular structures. In the present exploratory work the phenomenological values, obtained from reproducing experimental data on the position of the resonances, are not available in general. With regard to the prescription of Ref. [42], this choice was justified in [42] by guaranteeing an approximate crossing symmetry although, as noted in [53], such a claim appears somewhat dubious because crossing symmetry involves isospin mixtures. Thus choosing an alternative subtraction point might lead to yet another reasonable result. This prescription for the subtraction point was indeed used in the SU(6) model [62]. The SU(6) approach recovered previous results for the lowest-lying $1/2^-$ and $3/2^-$ baryon resonances appearing in the scattering of the octet of Goldstone bosons off the lowest baryon octet and decuplet given in Refs. [71,72], and lead to new predictions for higher energy resonances, giving a phenomenological confirmation of its plausibility.

In Ref. [53] the value of the subtraction point was slightly modified to obtain the position of the $\Lambda_c(2595)$ resonance. In the present work the value has not been modified because, on the one hand, results for the resonances in $C = 1$, $S = 0$ sector did not change substantially by varying the value of the subtraction point and, on the other hand, there is scarce experimental information about resonances in the other strange and charm sectors beyond $C = 1$, $S = 0$.

The dynamically-generated baryon resonances can be obtained as poles of the scattering amplitudes for given *CSIJ* quantum numbers. One has to check both first and second Riemann sheets of the variable $\sqrt{s}$. The poles of the scattering amplitude on the first Riemann sheet (FRS) on the real axis that appear below threshold are interpreted as bound states. The poles that are found on the second Riemann sheet (SRS) below the real axis and above threshold are called resonances. Poles on the SRS on, or below the real axis but below threshold, will be called virtual states. Poles appearing in different positions than the ones mentioned can not be associated with physical states and are, therefore, artifacts. For any *CSIJ* sector, there are as many branching points as channels involved, which implies a complicated geometry of the complex s-variable space [68].

The mass and the width of the resonance can be found from the position of the pole on the complex energy plane. Close to the pole, the T-matrix behaves as

TABLE II. Values of baryon masses, M_i, and meson masses, m_i, and decay constants, f_i, (in MeV) used throughout this work. The masses are taken from the PDG [73], except the masses for Ξ_{cc}^*, Ω_{cc}, Ω_{cc}^*, and Ω_{ccc}. While Ξ_{cc}^* is obtained from Ξ_{cc} summing 80 MeV, similar to the $\Xi_c' - \Xi_c^*$ mass splitting, the masses for Ω_{cc}, Ω_{cc}^* are given in Ref. [74] and for Ω_{ccc} in Ref. [75]. The decay constants f_i are taken from Ref. [53], except for f_{η_c} and $f_{J/\Psi}$. We take $f_{J/\Psi}$ from the width of the $J/\Psi \to e^- e^+$ decay and we set $f_{\eta_c} = f_{J/\Psi}$, as predicted by HQSS and corroborated in the lattice evaluation of Ref. [76]. The SU(6) $\times$ SU$_C$(2) $\times$ U$_C$(1) and SU(3) $\times$ SU(2) labels are also displayed. The last column indicates the HQSS multiplets. Members of a doublet are placed in consecutive rows.

Meson	Mass	Decay constant	SU(6)	SU(3)	HQSS	Baryon	Mass	SU(6)	SU(3)	HQSS
π	138.03	92.4	$\mathbf{35_{1,0}}$	$\mathbf{8_1}$	Singlet	N	938.92	$\mathbf{56_{1,0}}$	$\mathbf{8_2}$	Singlet
K	495.68	113.0	$\mathbf{35_{1,0}}$	$\mathbf{8_1}$	Singlet	Λ	1115.68	$\mathbf{56_{1,0}}$	$\mathbf{8_2}$	Singlet
η	547.45	111.0	$\mathbf{35_{1,0}}$	$\mathbf{8_1}$	Singlet	Σ	1193.15	$\mathbf{56_{1,0}}$	$\mathbf{8_2}$	Singlet
ρ	775.49	153.0	$\mathbf{35_{1,0}}$	$\mathbf{8_3}$	Singlet	Ξ	1318.11	$\mathbf{56_{1,0}}$	$\mathbf{8_2}$	Singlet
K^*	893.88	153.0	$\mathbf{35_{1,0}}$	$\mathbf{8_3}$	Singlet	Δ	1210.00	$\mathbf{56_{1,0}}$	$\mathbf{10_4}$	Singlet
ω	782.57	138.0	$\mathbf{35_{1,0}}$	Ideal	Singlet	Σ^*	1384.57	$\mathbf{56_{1,0}}$	$\mathbf{10_4}$	Singlet
ϕ	1019.46	163.0	$\mathbf{35_{1,0}}$	Ideal	Singlet	Ξ^*	1533.40	$\mathbf{56_{1,0}}$	$\mathbf{10_4}$	Singlet
η'	957.78	111.0	$\mathbf{1_{1,0}}$	$\mathbf{1_1}$	Singlet	Ω	1672.45	$\mathbf{56_{1,0}}$	$\mathbf{10_4}$	Singlet
D	1867.23	157.4	$\mathbf{6^*_{2,1}}$	$\mathbf{3^*_1}$	Doublet	Λ_c	2286.46	$\mathbf{21_{2,1}}$	$\mathbf{3^*_2}$	Singlet
D^*	2008.35	157.4	$\mathbf{6^*_{2,1}}$	$\mathbf{3^*_3}$	Doublet	Ξ_c	2469.45	$\mathbf{21_{2,1}}$	$\mathbf{3^*_2}$	Singlet
D_s	1968.50	193.7	$\mathbf{6^*_{2,1}}$	$\mathbf{3^*_1}$	Doublet	Σ_c	2453.56	$\mathbf{21_{2,1}}$	$\mathbf{6_2}$	Doublet
D_s^*	2112.30	193.7	$\mathbf{6^*_{2,1}}$	$\mathbf{3^*_3}$	Doublet	Σ_c^*	2517.97	$\mathbf{21_{2,1}}$	$\mathbf{6_4}$	Doublet
η_c	2979.70	290.0	$\mathbf{1_{1,0}}$	$\mathbf{1_1}$	Doublet	Ξ_c'	2576.85	$\mathbf{21_{2,1}}$	$\mathbf{6_2}$	Doublet
J/ψ	3096.87	290.0	$\mathbf{1_{3,0}}$	$\mathbf{1_3}$	Doublet	Ξ_c^*	2646.35	$\mathbf{21_{2,1}}$	$\mathbf{6_4}$	Doublet
						Ω_c	2697.50	$\mathbf{21_{2,1}}$	$\mathbf{6_2}$	Doublet
						Ω_c^*	2768.30	$\mathbf{21_{2,1}}$	$\mathbf{6_4}$	Doublet
						Ξ_{cc}	3519.00	$\mathbf{6_{3,2}}$	$\mathbf{3_2}$	Doublet
						Ξ_{cc}^*	3600.00	$\mathbf{6_{3,2}}$	$\mathbf{3_4}$	Doublet
						Ω_{cc}	3712.00	$\mathbf{6_{3,2}}$	$\mathbf{3_2}$	Doublet
						Ω_{cc}^*	3795.00	$\mathbf{6_{3,2}}$	$\mathbf{3_4}$	Doublet
						Ω_{ccc}	4799.00	$\mathbf{1_{4,3}}$	$\mathbf{1_4}$	Singlet

$$T_{ij}(s) \approx \frac{g_i g_j}{\sqrt{s} - \sqrt{s_R}}. \tag{10}$$

The mass and width of the resonance follow from $\sqrt{s_R} = m_R - i\Gamma_R/2$, while the dimensionless constant g_i is the coupling of the resonance to the i channel. Since the dynamically-generated states may couple differently to their baryon-meson components, we will examine the ij-channel independent quantity

$$\tilde{T}^{IJSC}(s) \equiv \max_j \sum_i |T_{ij}^{IJSC}(s)|, \tag{11}$$

which allows us to identify all the resonances within a given sector at once.

The matrix elements D_{ij} display exact SU(8) invariance, but this symmetry is severely broken in nature, so we implement various symmetry-breaking mechanisms. As said we only keep channels without charmed antiquarks, to comply with HQSS. This means to remove channels with extra $c\bar{c}$ pairs. Such channels are heavier than the basic ones so they would be kinematically suppressed anyway. However, the suppression introduced by HQSS in the matrix elements is more severe and we simply take the infinite c-quark mass limit in those would-be couplings (but, of course, not in the charmed hadron masses).

In addition, several soft symmetry-breaking mechanisms are introduced. In the present work we use physical values for the masses of the hadrons and for the decay constants of the mesons since we consider that meson-baryon states interact via a pointlike interaction given by the SU(8) model extension of the WT interaction. The values used in this work are quoted in Table II. We have checked in a previous work [62] that this approach leads to a reasonable description of the odd-parity light baryon resonances. Indeed, we found that most of the low-lying three- and four-star odd-parity baryon resonances with spin $1/2$ and $3/2$ can be dynamically-generated within this scheme.

Also in Appendix A we discuss the effects induced by a possible reduction in the matrix elements for which an exchange of charm between meson and baryon takes place. The introduction of these quenching factors does not spoil heavy-quark spin symmetry, however, it amounts to a further source of flavor breaking. In schemes formulated in terms of exchanges of vector mesons, this reduction would be induced by the larger mass of the charmed vector meson exchanged as compared to those of the vector mesons belonging to the ρ nonet, which are exchanged when there is no exchange of charm.

The symmetry-breaking pattern, with regards to flavor, follows the chain SU(8) $\supset$ SU(6) $\supset$ SU(3) $\supset$ SU(2), where the last group refers to isospin. To tag the resonances

with these quantum numbers, we start from the SU(8)-symmetric scenario, where hadrons in the same SU(8) multiplet share common properties (mass and decay constants). This produces a single resonance for the **120**-irrep and another for the **168**-irrep. Subsequently, the SU(8) $\supset$ SU(6) breaking is introduced by means of a deformation of the mass and decay constant parameters. Specifically, we use

$$\begin{aligned} m(x) &= (1-x)m_{\mathrm{SU(8)}} + x m_{\mathrm{SU(6)}}, \\ f(x) &= (1-x)f_{\mathrm{SU(8)}} + x f_{\mathrm{SU(6)}}. \end{aligned} \tag{12}$$

The parameter x runs from 0 [SU(8)-symmetric scenario] to 1 [SU(6) symmetric scenario]. The symmetric masses and decay constants are assigned by taking an average over the corresponding multiplet. The same procedure is applied to the other breakings, with

$$\begin{aligned} m(x') &= (1-x')m_{\mathrm{SU(6)}} + x' m_{\mathrm{SU(3)}}, \\ f(x') &= (1-x')f_{\mathrm{SU(6)}} + x' f_{\mathrm{SU(3)}}, \end{aligned} \tag{13}$$

and

$$\begin{aligned} m(x'') &= (1-x'')m_{\mathrm{SU(3)}} + x'' m_{\mathrm{SU(2)}}, \\ f(x'') &= (1-x'')f_{\mathrm{SU(3)}} + x'' f_{\mathrm{SU(2)}}. \end{aligned} \tag{14}$$

It should be noted that SU(6) and SU(3), as well as HQSS, are broken only kinematically, through masses and meson decay constants. On the other hand, the breaking of SU(8) comes also from the interaction matrix elements, since we have truncated the SU(8) multiplets by removing channels with $c\bar{c}$ pairs, in order to enforce HQSS. Nevertheless, to have SU(8) assignations is important in our scheme to be able to isolate the dominant **168** and **120** SU(8) irreps, and get rid of the subdominant and exotic **4752**. Therefore, instead of starting from an SU(6) $\times$ HQSS symmetric scenario, we find it preferable to start from a SU(8) symmetric world, and let the charmed quarks to get heavier. In this way the offending channels with $c\bar{c}$ pairs tend to decouple kinematically as we approach the physical point. At the end, we remove those channels and this introduces relatively small changes for the low-lying resonances that we are studying.

The procedure just described allows us to assign well-defined SU(8), SU(6) and SU(3) labels to the resonances. Conceivably the labels could depend on the precise choice of symmetric points or change if different paths in the parameter manifold were followed, but this seems unlikely. At the same time, the HQSS multiplets form themselves at the physical point, since this symmetry is present in the interaction, and also, very approximately, in the properties of the basic hadrons. In order to unambiguously identify those multiplets, one simply has to adiabatically move to the HQSS point, by imposing exact HQSS in the masses and decay constants of the basic hadrons. The members of a multiplet get exactly degenerated under this test.

Because light spin-flavor and HQSS are independent symmetries, the members of a HQSS multiplet always have equal SU(6), SU(3) and SU(2) labels. Quite often, the SU(8) label is also shared by the members of a HQSS multiplet, but not always, since this property is not ensured by construction.[5]

III. DYNAMICALLY-GENERATED CHARMED AND STRANGE BARYON STATES

In this section we show the dynamically-generated states obtained in the different charm and strangeness sectors. We have assigned to some of them a tentative identification with known states from the PDG [73]. This identification is made by comparing the data from the PDG on these states with the information we extract from the poles, namely, the mass, width and, most important, the couplings. The couplings give us valuable information on the structure of the state and on the possible decay channels and their relative strength. It should be stressed that there will be mixings between states with the same $CSIJ^P$ quantum numbers but belonging to different SU(8), SU(6) and/or SU(3) multiplets, since these symmetries are broken both within our approach and in nature. Additional breaking of SU(8) [and SU(6) and SU(3)] is expected to take place not only in the kinematics but also in the interaction amplitudes. This will occur when using more sophisticated models going beyond the (hopefully dominant) lowest order retained here.

Masses, widths and main couplings of the resonances found are displayed in Tables III, IV, V, VI, VII, VIII, and IX. The tables are collected by the quantum numbers CSI. States with equal CSI and spin $J = 1/2$ and $J = 3/2$ have been collected together in order to put HQSS multiplets members in consecutive rows. As a rule, two states with $J = 1/2$ and $J = 3/2$ and equal SU(8), SU(6) and SU(3) labels form a HQSS doublet [with some exceptions in the case of the SU(8) label]. The other states are HQSS singlets.

In what follows, we occasionally use an asterisk in the symbol of the states to emphasize that a resonance has spin $J = 3/2$, for instance Λ_c^* denotes a state with $CSIJ = (1, 0, 1/2, 3/2)$. The symbol without asterisk may refer to the generic case or to the $J = 1/2$ case.

A. Λ_c states ($C = 1$, $S = 0$, $I = 0$)

We present the poles obtained in the $C = 1$, $S = 0$ and $I = 0$ sector coming from the **120** and **168** SU(8) representations. Moreover, we determine the coupling constants to the various baryon-meson channels through the residues

[5]Note that if HQSS was an exact symmetry of the basic hadrons, we could move from the physical point to the SU(6) symmetric point while preserving HQSS all the way. However, to reach the SU(8) symmetric point would require to restore channels with $c\bar{c}$ pairs, breaking HQSS, and in the way members of a common HQSS can end up in different SU(8) irreps.

TABLE III. Λ_c ($J = 1/2$) and Λ_c^* ($J = 3/2$) resonances predicted by our model in the **168** and **120** SU(8) irreps. The first three columns contain the SU(8), SU(6) and SU(3) representations of the corresponding state. M_R and Γ_R stand for the mass and width of the state, in MeV. The next column displays the dominant couplings to the channels, ordered by their threshold energies. In boldface we indicate the channels which are open for decay. The last column shows the spin of the resonance. Pairs of states with $J = 1/2$ and $3/2$ and equal SU(8), SU(6) and SU(3) labels form HQSS doublets. They are displayed in consecutive rows. Tentative identifications with PDG resonances are shown when possible.

SU(8) irrep	SU(6) irrep	SU(3) irrep	M_R	Γ_R	Couplings to main channels	Status PDG	J
168	$\mathbf{15_{2,1}}$	$\mathbf{3_2^*}$	2617.3	89.8	$g_{\Sigma_c\pi} = \mathbf{2.3}$, $g_{ND} = 1.6$, $g_{ND^*} = 1.4$, $g_{\Sigma_c\rho} = 1.3$		1/2
168	$\mathbf{15_{2,1}}$	$\mathbf{3_4^*}$	2666.6	53.7	$g_{\Sigma_c^*\pi} = \mathbf{2.2}$, $g_{ND^*} = 2.0$, $g_{\Sigma_c\rho} = 0.8$, $g_{\Sigma_c^*\rho} = 1.3$	$\Lambda_c(2625)$ ***	3/2
168	$\mathbf{21_{2,1}}$	$\mathbf{3_2^*}$	2618.8	1.2	$g_{\Sigma_c\pi} = \mathbf{0.3}$, $g_{ND} = 3.5$, $g_{ND^*} = 5.6$, $g_{\Lambda D_s} = 1.4$, $g_{\Lambda D_s^*} = 2.9$, $g_{\Lambda_c\eta'} = 0.9$	$\Lambda_c(2595)$ ***	1/2
120	$\mathbf{21_{2,1}}$	$\mathbf{3_2^*}$	2828.4	0.8	$g_{ND} = \mathbf{0.3}$, $g_{\Lambda_c\eta} = 1.1$, $g_{\Xi_cK} = 1.6$, $g_{\Lambda D_s^*} = 1.1$, $g_{\Sigma_c\rho} = 1.1$, $g_{\Sigma_c^*\rho} = 1.0$, $g_{\Xi_c^*K^*} = 0.8$		1/2

TABLE IV. As in Table III, for Σ_c and Σ_c^* resonances.

SU(8) irrep	SU(6) irrep	SU(3) irrep	M_R	Γ_R	Couplings to main channels	J
168	$\mathbf{21_{2,1}}$	$\mathbf{6_2}$	2571.5	0.8	$g_{\Lambda_c\pi} = \mathbf{0.1}$, $g_{ND} = 2.2$, $g_{ND^*} = 1.2$, $g_{\Sigma D_s} = 1.5$, $g_{\Delta D^*} = 6.6$, $g_{\Sigma D_s^*} = 1.1$, $g_{\Sigma^* D_s^*} = 2.8$	1/2
168	$\mathbf{21_{2,1}}$	$\mathbf{6_4}$	2568.4	0.0	$g_{ND^*} = 2.5$, $g_{\Delta D} = 4.2$, $g_{\Delta D^*} = 5.3$, $g_{\Sigma D_s^*} = 2.2$, $g_{\Sigma^* D_s} = 1.5$, $g_{\Sigma^* D_s^*} = 2.3$	3/2
168	$\mathbf{15_{2,1}}$	$\mathbf{6_2}$	2622.7	188.0	$g_{\Lambda_c\pi} = \mathbf{1.9}$, $g_{\Sigma_c\pi} = \mathbf{0.2}$, $g_{ND} = 2.2$, $g_{ND^*} = 3.8$, $g_{\Xi_cK} = 0.8$, $g_{\Sigma_c\rho} = 1.3$, $g_{\Sigma_c^*\rho} = 1.5$	1/2
120	$\mathbf{21_{2,1}}$	$\mathbf{6_2}$	2643.4	87.0	$g_{\Lambda_c\pi} = \mathbf{0.2}$, $g_{\Sigma_c\pi} = \mathbf{2.0}$, $g_{ND} = 2.4$, $g_{ND^*} = 1.7$, $g_{\Lambda_c\rho} = 0.9$, $g_{\Delta D^*} = 1.1$, $g_{\Sigma_c\rho} = 0.9$, $g_{\Sigma^* D_s^*} = 1.3$	1/2
120	$\mathbf{21_{2,1}}$	$\mathbf{6_4}$	2692.9	67.0	$g_{\Sigma_c^*\pi} = \mathbf{1.9}$, $g_{ND^*} = 2.7$, $g_{\Lambda_c\rho} = 1.0$, $g_{\Sigma D_s^*} = 1.0$, $g_{\Sigma^* D_s^*} = 1.0$	3/2

of the corresponding amplitudes, as in Eq. (10). Results for $C = 1$ and $S = 0$ were reported previously in Ref. [53]. However, the analysis of the dynamically-generated states in terms of the attractive SU(8) ⊃ SU(6) ⊃ SU(3) ⊃ SU(2) multiplets was not done in this previous reference. Here we are able to assign SU(8), SU(6) and SU(3) labels to the resonances. Simultaneously, we also classify the resonances into HQSS multiplets, in practice doublets and singlets. This is of great interest as this symmetry is less broken than spin-flavor, being of a quality comparable to flavor SU(3).

1. Sector $J = 1/2$

In the sector $C = 1$, $S = 0$, $I = 0$, $J = 1/2$, there are 16 channels (the threshold energies, in MeV, are shown below each channel):

$\Sigma_c\pi$	ND	$\Lambda_c\eta$	ND^*	Ξ_cK	$\Lambda_c\omega$	$\Xi_c'K$	ΛD_s
2591.6,	2806.1,	2833.9,	2947.3,	2965.1,	3069.0,	3072.5,	3084.2,
ΛD_s^*	$\Sigma_c\rho$	$\Lambda_c\eta'$	$\Sigma_c^*\rho$	$\Lambda_c\phi$	Ξ_cK^*	$\Xi_c'K^*$	$\Xi_c^*K^*$
3228.0,	3229.0,	3244.2,	3293.5,	3305.9,	3363.3,	3470.7,	3540.2.

The dynamically-generated states are shown in Table III. We obtain the three lowest-lying states of Ref. [53] in this sector. We display in Fig. 4 the channel independent scattering amplitude defined in Eq. (11) in the SRS for this sector, where these three poles clearly show up. However, those states appear with slightly different masses as compared to Ref. [53]. The reason is that the subtraction point was slightly changed in this previous work in order to reproduce the position of the $\Lambda_c(2595)$ [14,15,21,73,77]. The same scaling factor of the subtraction point was introduced in all the sectors in [53]. Another difference with [53] is that there the value $f_{D_s^*} = f_{D^*} = 157.4$ MeV was

TABLE V. As in Table III, for the Ξ_c and Ξ_c^* resonances.

SU(8) irrep	SU(6) irrep	SU(3) irrep	M_R	Γ_R	Couplings to main channels	Status PDG	J
168	$\mathbf{15_{2,1}}$	$\mathbf{6_2}$	2702.8	177.8	$g_{\Xi_c\pi} = \mathbf{2.4}$, $g_{\Lambda D} = 1.2$, $g_{\Sigma D} = 1.1$, $g_{\Lambda D^*} = 2.1$, $g_{\Sigma D^*} = 1.7$, $g_{\Xi D_s^*} = 1.1$		1/2
168	$\mathbf{21_{2,1}}$	$\mathbf{3_2^*}$	2699.4	12.6	$g_{\Xi_c\pi} = \mathbf{0.8}$, $g_{\Lambda D} = 1.2$, $g_{\Sigma D} = 3.4$, $g_{\Lambda D^*} = 2.2$, $g_{\Sigma D^*} = 5.4$, $g_{\Xi D_s} = 1.9$, $g_{\Xi_c\eta'} = 1.0$, $g_{\Xi D_s^*} = 3.3$		1/2
168	$\mathbf{21_{2,1}}$	$\mathbf{6_2}$	2733.0	2.2	$g_{\Xi_c'\pi} = \mathbf{0.5}$, $g_{\Lambda D} = 1.9$, $g_{\Sigma D} = 1.8$, $g_{\Lambda D^*} = 0.9$, $g_{\Sigma D^*} = 1.2$, $g_{\Xi D_s} = 1.2$, $g_{\Sigma^* D^*} = 5.8$, $g_{\Xi_c'\eta'} = 0.9$, $g_{\Xi^* D_s^*} = 3.3$		1/2
168	$\mathbf{21_{2,1}}$	$\mathbf{6_4}$	2734.3	0.0	$g_{\Lambda D^*} = 2.2$, $g_{\Sigma D^*} = 2.1$, $g_{\Sigma^* D} = 3.6$, $g_{\Sigma^* D^*} = 4.6$, $g_{\Xi D_s^*} = 1.3$, $g_{\Xi^* D_s} = 2.1$, $g_{\Xi^* D_s^*} = 2.6$		3/2
120	$\mathbf{21_{2,1}}$	$\mathbf{3_2^*}$	2775.4	0.6	$g_{\Xi_c\pi} = \mathbf{0.1}$, $g_{\Xi_c'\pi} = \mathbf{0.1}$, $g_{\Lambda_c\bar{K}} = 1.4$, $g_{\Xi_c\eta} = 0.9$, $g_{\Lambda D^*} = 1.0$, $g_{\Sigma D^*} = 1.4$, $g_{\Sigma_c\bar{K}^*} = 1.0$, $g_{\Sigma_c^*\bar{K}^*} = 1.3$		1/2
168	$\mathbf{15_{2,1}}$	$\mathbf{3_2^*}$	2772.9	83.7	$g_{\Xi_c\pi} = \mathbf{0.1}$, $g_{\Xi_c'\pi} = \mathbf{2.3}$, $g_{\Sigma_c\bar{K}} = 1.2$, $g_{\Lambda D} = 2.1$, $g_{\Lambda D^*} = 1.5$, $g_{\Omega_c K} = 0.9$, $g_{\Sigma D^*} = 0.9$, $g_{\Xi_c\rho} = 1.0$, $g_{\Sigma_c\bar{K}^*} = 0.9$, $g_{\Xi_c'\rho} = 1.0$, $g_{\Sigma^* D^*} = 1.4$, $g_{\Xi^* D_s^*} = 1.1$		1/2
168	$\mathbf{15_{2,1}}$	$\mathbf{3_4^*}$	2819.7	32.4	$g_{\Xi_c^*\pi} = \mathbf{1.9}$, $g_{\Sigma_c^*\bar{K}} = 2.3$, $g_{\Lambda D^*} = 2.0$, $g_{\Lambda_c\bar{K}^*} = 1.0$, $g_{\Xi_c^*\eta} = 1.1$, $g_{\Sigma D^*} = 1.2$, $g_{\Xi_c\rho} = 1.1$, $g_{\Sigma_c\bar{K}^*} = 1.0$, $g_{\Sigma_c^*\bar{K}^*} = 2.0$		3/2
120	$\mathbf{21_{2,1}}$	$\mathbf{6_2}$	2804.8	20.7	$g_{\Xi_c'\pi} = \mathbf{1.1}$, $g_{\Sigma_c\bar{K}} = 2.4$, $g_{\Lambda D} = 1.5$, $g_{\Sigma D} = 1.2$, $g_{\Xi_c'\eta} = 1.3$, $g_{\Lambda_c\bar{K}^*} = 1.2$, $g_{\Sigma D^*} = 0.9$, $g_{\Sigma_c\bar{K}^*} = 1.8$, $g_{\Sigma^* D^*} = 1.1$, $g_{\Sigma_c^*\bar{K}^*} = 1.0$, $g_{\Xi^* D_s^*} = 1.2$	$\Xi_c(2790)$ ***	1/2
120	$\mathbf{21_{2,1}}$	$\mathbf{6_4}$	2845.2	44.0	$g_{\Xi_c^*\pi} = \mathbf{1.9}$, $g_{\Sigma_c^*\bar{K}} = 2.1$, $g_{\Lambda D^*} = 2.6$, $g_{\Lambda_c\bar{K}^*} = 1.4$, $g_{\Xi_c^*\eta} = 1.2$, $g_{\Sigma D^*} = 1.2$, $g_{\Xi_c\rho} = 0.9$, $g_{\Sigma_c\bar{K}^*} = 0.9$, $g_{\Sigma_c^*\bar{K}^*} = 1.7$, $g_{\Xi^* D_s} = 0.9$, $g_{\Xi^* D_s^*} = 1.1$	$\Xi_c(2815)$ ***	3/2

used, whereas here we use the more correct value $f_{D_s^*} = f_{D_s} = 193.7$ MeV. These two modifications will affect the comparison of other sectors too. A permutation on the order of the two first resonances as compared to Ref. [53] is also observed.

The experimental $\Lambda_c(2595)$ resonance can be identified with the $\mathbf{21_{2,1}}$ pole that we found around 2618.8 MeV, as similarly done in Ref. [53]. The width in our case is, however, bigger due to the increase of the phase space available for decay. As indicated in Ref. [53], we have not included the three-body decay channel $\Lambda_c\pi\pi$, which already represents almost one third of the decay events [73]. Therefore, the experimental value of $3.6^{+2.0}_{-1.3}$ MeV is still not reproduced. Our result for $\Lambda_c(2595)$ agrees with previous works on t-channel vector-meson-exchange models [39,42,44,45], but here as we first pointed out in

TABLE VI. Ω_c and Ω_c^* resonances.

SU(8) irrep	SU(6) irrep	SU(3) irrep	M_R	Γ_R	Couplings to main channels	J
168	$\mathbf{21_{2,1}}$	$\mathbf{6_2}$	2810.9	0.0	$g_{\Xi D} = 3.3$, $g_{\Xi D^*} = 1.7$, $g_{\Xi_c\bar{K}^*} = 0.9$, $g_{\Xi^* D^*} = 4.8$, $g_{\Omega_c\eta'} = 0.9$, $g_{\Omega D_s^*} = 4.2$	1/2
168	$\mathbf{21_{2,1}}$	$\mathbf{6_4}$	2814.3	0.0	$g_{\Xi D^*} = 3.7$, $g_{\Xi^* D} = 3.1$, $g_{\Xi^* D^*} = 3.8$, $g_{\Omega D_s} = 2.7$, $g_{\Omega_c^*\eta'} = 0.9$, $g_{\Omega D_s^*} = 3.4$	3/2
168	$\mathbf{15_{2,1}}$	$\mathbf{6_2}$	2884.5	0.0	$g_{\Xi_c\bar{K}} = 2.1$, $g_{\Xi D^*} = 1.7$, $g_{\Xi_c'\bar{K}^*} = 1.5$, $g_{\Xi_c^*\bar{K}^*} = 1.8$, $g_{\Omega_c\phi} = 0.9$, $g_{\Omega_c^*\phi} = 1.1$	1/2
120	$\mathbf{21_{2,1}}$	$\mathbf{6_2}$	2941.6	0.0	$g_{\Xi_c'\bar{K}} = 1.9$, $g_{\Xi D} = 1.5$, $g_{\Omega_c\eta} = 1.7$, $g_{\Xi_c\bar{K}^*} = 1.4$, $g_{\Xi_c'\bar{K}^*} = 1.1$, $g_{\Omega_c\phi} = 1.0$, $g_{\Omega D_s^*} = 0.9$	1/2
120	$\mathbf{21_{2,1}}$	$\mathbf{6_4}$	2980.0	0.0	$g_{\Xi_c^*\bar{K}} = 1.9$, $g_{\Omega_c^*\eta} = 1.6$, $g_{\Xi D^*} = 1.4$, $g_{\Xi_c\bar{K}^*} = 1.6$, $g_{\Xi_c^*\bar{K}^*} = 1.3$, $g_{\Omega_c^*\phi} = 1.2$	3/2

TABLE VII. Ξ_{cc} and Ξ^*_{cc} resonances. In this case, the HQSS classification differs from the SU(8) classification for the two HQSS doublets.

SU(8) irrep	SU(6) irrep	SU(3) irrep	M_R	Γ_R	Couplings to main channels	J
168	$\mathbf{6_{1,2}}$	$\mathbf{3_2}$	3698.1	1.3	$g_{\Xi_{cc}\pi} = \mathbf{0.3}$, $g_{\Lambda_c D^*} = 2.1$, $g_{\Sigma_c D} = 3.2$, $g_{\Sigma_c D^*} = 2.6$, $g_{\Sigma_c^* D^*} = 4.1$, $g_{\Xi_c' D_s} = 1.3$, $g_{\Xi_c D_s^*} = 1.4$, $g_{\Xi_c' D_s^*} = 1.1$, $g_{\Xi_c^* D_s^*} = 1.7$	1/2
120	$\mathbf{6_{3,2}}$	$\mathbf{3_2}$	3727.8	17.8	$g_{\Xi_{cc}\pi} = \mathbf{1.0}$, $g_{\Lambda_c D} = 2.0$, $g_{\Sigma_c D} = 1.1$, $g_{\Xi_c D_s} = 1.5$, $g_{\Sigma_c D^*} = 4.6$, $g_{\Xi_{cc}\eta'} = 1.4$, $g_{\Xi_{cc}^*\rho} = 0.9$, $g_{\Sigma_c^* D^*} = 3.6$, $g_{\Xi_c' D_s^*} = 2.0$, $g_{\Xi_c^* D_s^*} = 1.6$	1/2
168	$\mathbf{6_{3,2}}$	$\mathbf{3_4}$	3729.5	0.0	$g_{\Lambda_c D^*} = 1.2$, $g_{\Sigma_c^* D} = 2.9$, $g_{\Sigma_c D^*} = 1.8$, $g_{\Sigma_c^* D^*} = 3.7$, $g_{\Xi_c D_s^*} = 1.3$, $g_{\Xi_c^* D_s} = 1.2$, $g_{\Xi_{cc}^*\eta'} = 1.1$, $g_{\Xi_c^* D_s^*} = 1.5$	3/2
168	$\mathbf{6_{3,2}}$	$\mathbf{3_2}$	3727.4	120.2	$g_{\Xi_{cc}\pi} = \mathbf{2.4}$, $g_{\Lambda_c D} = 2.4$, $g_{\Lambda_c D^*} = 1.5$, $g_{\Sigma_c D^*} = 2.3$, $g_{\Sigma_c^* D^*} = 1.4$, $g_{\Xi_c' D_s^*} = 1.0$	1/2
120	$\mathbf{6_{3,2}}$	$\mathbf{3_4}$	3790.8	83.9	$g_{\Xi_{cc}^*\pi} = \mathbf{2.0}$, $g_{\Lambda_c D^*} = 2.9$, $g_{\Sigma_c^* D} = 0.8$, $g_{\Sigma_c^* D^*} = 1.1$, $g_{\Xi_c D_s^*} = 0.8$, $g_{\Xi_c^* D_s} = 0.8$, $g_{\Xi_{cc}^*\eta'} = 0.8$, $g_{\Xi_c^* D_s^*} = 1$	3/2

TABLE VIII. Ω_{cc} and Ω^*_{cc} resonances.

SU(8) irrep	SU(6) irrep	SU(3) irrep	M_R	Γ_R	Couplings to main channels	J
168	$\mathbf{6_{1,2}}$	$\mathbf{3_2}$	3761.8	0.0	$g_{\Xi_c D} = 1.2$, $g_{\Xi_c' D} = 2.7$, $g_{\Xi_c D^*} = 2.9$, $g_{\Xi_c' D^*} = 2.0$, $g_{\Xi_c^* D^*} = 3.6$, $g_{\Omega_c D_s} = 1.9$, $g_{\Omega_c D_s^*} = 1.4$, $g_{\Omega_c^* D_s^*} = 2.5$	1/2
168	$\mathbf{6_{3,2}}$	$\mathbf{3_2}$	3792.8	0.0	$g_{\Xi_{cc}\bar{K}} = 0.9$, $g_{\Xi_c D} = 2.3$, $g_{\Xi_c' D} = 0.9$, $g_{\Omega_{cc}\eta'} = 1.2$, $g_{\Xi_c' D^*} = 3.5$, $g_{\Xi_{cc}^*\bar{K}^*} = 1.1$, $g_{\Xi_c^* D^*} = 2.7$, $g_{\Omega_c D_s^*} = 2.6$, $g_{\Omega_c^* D_s^*} = 2.0$	1/2
168	$\mathbf{6_{3,2}}$	$\mathbf{3_4}$	3802.9	0.0	$g_{\Xi_c D^*} = 2.5$, $g_{\Xi_c^* D} = 2.6$, $g_{\Xi_c' D^*} = 1.6$, $g_{\Xi_{cc}^*\bar{K}^*} = 0.9$, $g_{\Xi_c^* D^*} = 3.3$, $g_{\Omega_c^* D_s} = 2.0$, $g_{\Omega_c D_s^*} = 1.2$, $g_{\Omega_{cc}^*\eta'} = 1.1$, $g_{\Omega_c^* D_s^*} = 2.5$	3/2
120	$\mathbf{6_{3,2}}$	$\mathbf{3_2}$	3900.2	0.0	$g_{\Xi_{cc}\bar{K}} = 2.1$, $g_{\Omega_{cc}\eta} = 1.1$, $g_{\Xi_c D} = 1.6$, $g_{\Xi_c D^*} = 0.9$, $g_{\Xi_{cc}^*\bar{K}^*} = 1.3$, $g_{\Omega_c D_s^*} = 1$	1/2
120	$\mathbf{6_{3,2}}$	$\mathbf{3_4}$	3936.3	0.0	$g_{\Xi_{cc}^*\bar{K}} = 2.1$, $g_{\Xi_{cc}\bar{K}^*} = 1.4$, $g_{\Omega_{cc}^*\eta} = 1$, $g_{\Xi_c D^*} = 1.6$, $g_{\Xi_{cc}^*\bar{K}^*} = 1.3$, $g_{\Omega_c^* D_s^*} = 0.9$	3/2

TABLE IX. Ω_{ccc} and Ω^*_{ccc} resonances. These two states are HQSS singlets.

SU(8) irrep	SU(6) irrep	SU(3) irrep	M_R	Γ_R	Couplings to main channels	J
168	$\mathbf{1_{2,3}}$	$\mathbf{1_2}$	4358.2	0.0	$g_{\Xi_{cc} D} = 2.9$, $g_{\Omega_{cc} D_s} = 1.3$, $g_{\Xi_{cc} D^*} = 1.9$, $g_{\Xi_{cc}^* D^*} = 4.6$, $g_{\Omega_{cc}^* D_s^*} = 2.1$	1/2
120	$\mathbf{1_{4,3}}$	$\mathbf{1_4}$	4501.4	0.0	$g_{\Xi_{cc} D^*} = 2.9$, $g_{\Xi_{cc}^* D} = 2.4$, $g_{\Omega_{cc} D_s^*} = 1.8$, $g_{\Xi_{cc}^* D^*} = 2.9$, $g_{\Omega_{cc}^* D_s} = 1.5$, $g_{\Omega_{ccc}\eta'} = 1.2$, $g_{\Omega_{cc}^* D_s^*} = 1.9$	3/2

Ref. [53], we claim a large (dominant) ND^* component in its structure. This is in sharp contrast with the findings of the former references, where it was generated mostly as one ND bound state.

In Fig. 4, we also observe a second broad resonance at 2617.3 MeV with a large coupling to the open channel $\Sigma_c\pi$, very close to $\Lambda_c(2595)$. This is precisely the same two-pole pattern found in the charmless $I = 0$, $S = -1$ sector for the $\Lambda(1405)$ [66,78,79].

As discussed in Ref. [53], the pole found at around 2828 MeV, and stemming from the **120** SU(8) irreducible representation, is mainly originated by a strong attraction in the $\Xi_c K$ channel, but it cannot be assigned to the $\Lambda_c(2880)$ [16–18,73] because of the spin parity determined by the Belle collaboration.

Some of the states found have coupling to channels with hadrons which are themselves resonances, like Δ, ρ or D^*. Their widths can be taken into account in the calculation by doing a convolution, as done for instance in [80]. In practice the effect of introducing this improvement is found to be negligible on the position of the dynamically-generated states. The reason is that in all cases the decay thresholds for these channels are far above the pole, as compared to the widths involved. In fact, the widths of the basic hadrons can be safely neglected in all sectors for the low-lying states we obtain.

2. Sector $J = 3/2$

For the $C = 1$, $S = 0$, $I = 0$, $J = 3/2$ sector, the 11 channels and thresholds (in MeV) are:

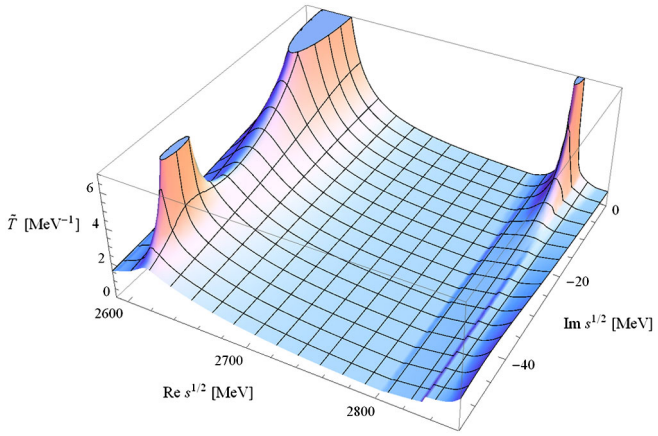

FIG. 4 (color online). $\tilde{T}^{I=0,J=(1/2),S=0,C=1}(s)$ amplitude (Λ_c resonances).

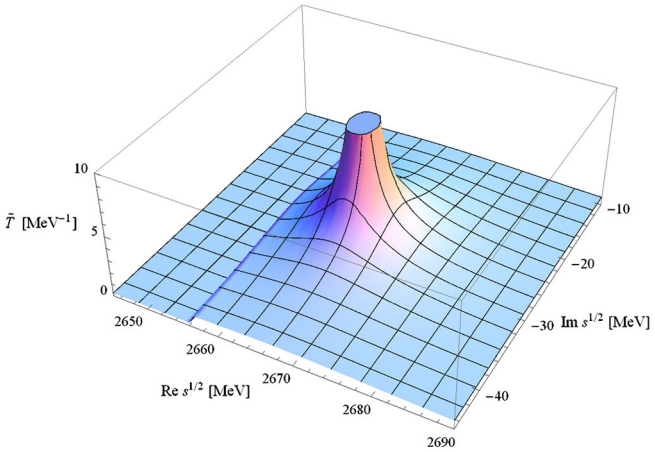

FIG. 5 (color online). $\tilde{T}^{I=0,J=(3/2),S=0,C=1}(s)$ (Λ_c^* resonance).

$\Sigma_c^*\pi$	ND^*	$\Lambda_c\omega$	Ξ_c^*K	ΛD_s^*	$\Sigma_c\rho$
2656.0,	2947.3,	3069.0,	3142.0,	3228.0,	3229.1,

$\Sigma_c^*\rho$	$\Lambda_c\phi$	Ξ_cK^*	$\Xi_c'K^*$	$\Xi_c^*K^*$
3293.5,	3305.9,	3363.3,	3470.7,	3540.2.

We find one pole in this sector (see Fig. 5 and Table III) located at ($2666.6 - i26.7$ MeV).

In Ref. [53], this structure had a Breit-Wigner shape with a width of 38 MeV and coupled most strongly to $\Sigma_c^*\pi$. It was assigned to the experimental $\Lambda_c(2625)$ [14,19–21,73]. The $\Lambda_c(2625)$ has a very narrow width, $\Gamma < 1.9$ MeV, and decays mostly to $\Lambda_c\pi\pi$. The reason for the assignment lies in the fact that changes in the subtraction point could move the resonance closer to the position of the experimental one, reducing its width significantly as it will stay below its dominant $\Sigma_c^*\pi$ channel. In our present calculation, we expect then a similar behavior.

A similar resonance was found at 2660 MeV in the t-channel vector-exchange model of Ref. [43]. The novelty of our calculation is that we obtain a non-negligible contribution from the baryon-vector meson channels to the generation of this resonance, as already observed in Ref. [53].

B. Σ_c states ($C = 1$, $S = 0$, $I = 1$)

1. Sector $J = 1/2$

The 22 channels and thresholds (in MeV) in this sector are:

$\Lambda_c\pi$	$\Sigma_c\pi$	ND	ND^*	Ξ_cK	$\Sigma_c\eta$	$\Lambda_c\rho$	$\Xi_c'K$
2424.5,	2591.6,	2806.1,	2947.3,	2965.1,	3001.0,	3062.0,	3072.5,

ΣD_s	ΔD^*	$\Sigma_c\rho$	$\Sigma_c\omega$	$\Sigma_c^*\rho$	$\Sigma_c^*\omega$	ΣD_s^*	Ξ_cK^*
3161.7,	3218.3,	3229.1,	3236.1,	3293.5,	3300.5,	3305.5,	3363.3,

$\Sigma_c\eta'$	$\Xi_c'K^*$	$\Sigma_c\phi$	$\Sigma^*D_s^*$	$\Sigma_c^*\phi$	$\Xi_c^*K^*$
3411.3,	3470.7,	3473.0,	3496.9,	3537.4,	3540.2.

The three resonances obtained for $J = 1/2$ (Table IV and Fig. 6) are predictions of our model, since no experimental data have been observed in this energy region. Our predictions here nicely agree with the three lowest-lying resonances found in Ref. [53].

The model of Ref. [45], based on the full t-channel vector exchange using baryon $1/2^+$ and pseudoscalar mesons as interacting channels, predicts the existence of two resonances with $I = 1$, $J = 1/2$, $S = 0$, $C = 1$. In this reference, the first one has a mass of 2551 MeV with a width 0.15 MeV. It couples strongly to the ΣD_s and ND channels and, therefore, might be associated with the resonance $\Sigma_c(2572)$ with $\Gamma = 0.8$ MeV of our model. Nevertheless, in our model this resonance couples most strongly to the other channels which incorporate vector mesons, such as $\Sigma^*D_s^*$ and ΔD^*, as it is shown in the Table IV and seen in Ref. [53].

The second resonance predicted in Ref. [45] has a mass of 2804 MeV and a width of 5 MeV, and it cannot be compared to any of our results because it is far from the energy region of our present calculations. This resonance, though, was identified with the state found in Ref. [42] at a substantially lower energy, 2680 MeV, and in Ref. [44] around 2750 MeV.

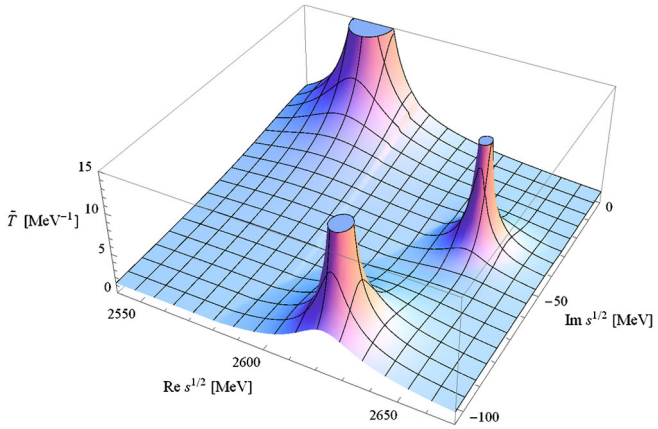

FIG. 6 (color online). $\tilde{T}^{I=1,J=(1/2),S=0,C=1}(s)$ amplitude (Σ_c resonances).

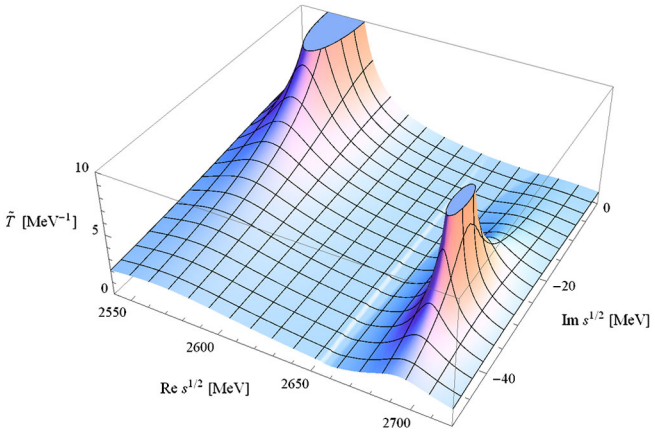

FIG. 7 (color online). $\tilde{T}^{I=1,J=(3/2),S=0,C=1}(s)$ amplitude (Σ_c^* resonances).

2. Sector $J = 3/2$

For the Σ_c^* case, the 20 channels and thresholds (in MeV) are:

$\Sigma_c^*\pi$	ND^*	$\Lambda_c\rho$	$\Sigma_c^*\eta$	ΔD	Ξ_c^*K	ΔD^*	$\Sigma_c\rho$
2656.0,	2947.3,	3062.0,	3065.4,	3077.2,	3142.0,	3218.3,	3229.1,
$\Sigma_c\omega$	$\Sigma_c^*\rho$	$\Sigma_c^*\omega$	ΣD_s^*	$\Sigma^* D_s$	$\Xi_c K^*$	$\Sigma_c^*\phi$	$\Xi_c^* K^*$
3236.1,	3293.5,	3300.5,	3305.5,	3353.1,	3363.3,	3470.7,	3473.0,
$\Xi_c' K^*$	$\Sigma_c\phi$	$\Sigma_c^*\eta'$	$\Sigma^* D_s^*$				
3475.8,	3496.9,	3537.4,	3540.2.				

The two predicted states are shown in Fig. 7 and their properties are collected in Table IV. A bound state at 2568.4 MeV (2550 MeV in Ref. [53]), whose main baryon-meson components contain a charmed meson, lies below the threshold of any possible decay channel. This state is thought to be the charmed counterpart of the hyperonic $\Sigma(1670)$ resonance. While the $\Sigma(1670)$ strongly couples to $\Delta\bar{K}$ channel, this resonance is mainly generated by the analogous ΔD and ΔD^* channels.

The second state at 2692.9 MeV has not a direct comparison with the available experimental data, as discussed in Ref. [53]. In fact, the experimental $\Sigma_c(2520)$ [22–24,73] cannot be assigned to any of these two states due to parity as well as because of the dominant decay channel, $\Lambda_c^+\pi$ (d-wave).

With regards to the experimental $\Sigma(2800)$ [25,26,73], there is also no correspondence with any of our states due to its high mass and also the empirically dominant $\Lambda_c\pi$ component. Heavier resonances were produced in [53] but they come from the SU(8) irrep **4752** which we have disregarded here.

C. Ξ_c states ($C = 1$, $S = -1$, $I = 1/2$)

We now study the $C = 1$, $S = -1$, $I = 1/2$ sector for different spin, $J = 1/2$ and $J = 3/2$. None of the strange sectors, and, in particular, this one, were studied in [53]. Those states are labeled by Ξ_c and our model predicts the existence of nine states stemming from the strongly attractive **120** and **168** SU(8) irreducible representations.

1. Sector $J = 1/2$

The 31 channels and thresholds (in MeV) for this sector are:

$\Xi_c\pi$	$\Xi_c'\pi$	$\Lambda_c\bar{K}$	$\Sigma_c\bar{K}$	ΛD	$\Xi_c\eta$	ΣD	ΛD^*
2607.5,	2714.9,	2782.1,	2949.2,	2982.9,	3016.9,	3060.4,	3124.0,
$\Xi_c'\eta$	$\Lambda_c\bar{K}^*$	$\Omega_c K$	ΣD^*	$\Xi_c\rho$	$\Xi_c\omega$	ΞD_s	$\Sigma_c\bar{K}^*$
3124.3,	3180.3,	3193.2,	3201.5,	3244.9,	3252.0,	3286.6,	3347.4,

$\Xi_c'\rho$	$\Xi_c'\omega$	Σ^*D^*	$\Sigma_c^*\bar{K}^*$	$\Xi_c^*\rho$	$\Xi_c\eta'$	$\Xi_c^*\omega$	ΞD_s^*
3352.3,	3359.4,	3392.9,	3411.9,	3421.8,	3427.2,	3428.9,	3430.4,

$\Xi_c\phi$	$\Xi_c'\eta'$	Ω_cK^*	$\Xi_c'\phi$	$\Xi^*D_s^*$	$\Omega_c^*K^*$	$\Xi_c^*\phi$
3488.9,	3534.6,	3591.4,	3596.3,	3645.7,	3662.2,	3665.8.

Six baryon resonances were expected (Table I) and found in this sector. The mass, width and couplings to the main channels are given in Table V and Fig. 8. In the energy range where these six states predicted by our model lie, three experimental resonances have been seen by the Belle, E687 and CLEO collaborations: $\Xi_c(2645)$ $J^P = 3/2^+$ [27–30,73], $\Xi_c(2790)$ $J^P = 1/2^-$ [31,73] and $\Xi_c(2815)$ $J^P = 3/2^-$ [27,32,73]. While $\Xi_c(2645)$ cannot be identified with any of our states for $J = 1/2$ and $J = 3/2$ due to parity, the $\Xi_c(2790)$ might be assigned with one of the six resonances in the $J = 1/2$ sector. The experimental $J^P = 3/2^-\Xi_c(2815)$ resonance will be analyzed in the $J = 3/2$ sector.

The state $\Xi_c(2790)$ has a width of $\Gamma < 12$–15 MeV and it decays to $\Xi_c'\pi$, with $\Xi_c' \to \Xi_c\gamma$. We might associate it to our 2733, 2775.4 or 2804.8 states. Because of the small coupling of 2775.4 to the $\Xi_c'\pi$ channel, it seems unlikely that it might correspond to the observed $\Xi_c(2790)$ state. In fact, the assignment to the 2804.8 state might be better since its larger $\Xi_c'\pi$ coupling and the fact that a slight modification of the subtraction point can lower its position to 2790 MeV and most probably reduce its width as it will get closer to the $\Xi_c'\pi$ channel, the only channel open at those energies that couples to this resonance. Moreover, this seems to be a reasonable assumption in view of the fact that, in this manner, this Ξ_c state is the HQSS partner of the 2845 Ξ_c^* state, which we will identify with the $\Xi_c(2815)$ resonance of the PDG. Nevertheless, it is also possible to identify our pole at 2733 MeV from the **168** irreducible representation with the experimental $\Xi_c(2790)$ state. In that case, one might expect that if the resonance position gets closer to the physical mass of 2790 MeV, its width will increase and it will easily reach values of the order of 10 MeV.

In Ref. [45] five baryon resonances were found in this sector for a wide range of energies up to 2977 MeV. As discussed in this reference, none of these five states seemed to fit the experimental $\Xi_c(2790)$ because of the small width observed. Higher-mass experimental states, such as the $\Xi_c(2980)$ [27,33,34,73], might correspond to one of the two higher-mass states in Ref. [45]. In our calculation, none of the states can be identified with such a heavy resonant state. In Ref. [42] three resonances appear below 3 GeV: 2691 MeV, 2793 MeV, and 2806 MeV, which mostly couple to $D\Sigma$, $\bar{K}\Sigma_c$, and $D\Lambda$, respectively. Those states are very similar in mass to some of those obtained in our calculations and we might identify the first two states, 2691 and 2793, to our 2699.4 and 2804.8 states because of the dominant decay channel.

2. Sector $J = 3/2$

The 26 channels (thresholds in MeV are also given) in the Ξ_c^* sector are:

$\Xi_c^*\pi$	$\Sigma_c^*\bar{K}$	ΛD^*	$\Lambda_c\bar{K}^*$	$\Xi_c^*\eta$	ΣD^*	$\Xi_c\rho$
2784.4,	3013.6,	3124.0,	3180.3,	3193.8,	3201.5,	3244.9,

Σ^*D	$\Xi_c\omega$	Ω_c^*K	$\Sigma_c\bar{K}^*$	$\Xi_c'\rho$	$\Xi_c'\omega$	Σ^*D^*
3251.8,	3252.0,	3264.0,	3347.4,	3352.3,	3359.4,	3392.9,

$\Sigma_c^*\bar{K}^*$	$\Xi_c^*\rho$	$\Xi_c^*\omega$	ΞD_s^*	$\Xi_c\phi$	Ξ^*D_s	Ω_cK^*
3411.8,	3421.8,	3428.9,	3430.4,	3488.9,	3501.9,	3591.4,

$\Xi_c'\phi$	$\Xi_c^*\eta'$	$\Xi^*D_s^*$	$\Omega_c^*K^*$	$\Xi_c^*\phi$
3596.3,	3604.1,	3645.7,	3662.2,	3665.8.

The resonances predicted by the model and generated from the **120** and **168** irreducible representations are compiled in Table V and Fig. 9.

The only experimental $J^P = 3/2^-$ baryon resonance with a mass in the energy region of interest is $\Xi_c(2815)$ [27,32,73]. The full width is expected to be less than 3.5 MeV for $\Xi_c^+(2815)$ and less than 6.5 MeV for $\Xi_c^0(2815)$, and the decay modes are $\Xi_{c+}\pi^+\pi^-$, $\Xi_{c0}\pi^+\pi^-$. We obtain two resonances at 2819.7 MeV and 2845.2 MeV, respectively, that couple strongly to $\Xi_c^*\pi$, with $\Xi_c^* \to \Xi_c\pi$. Allowing for this possible indirect three-body decay channel, we might identify one of them to the experimental result. This assignment is, indeed, possible for the state at 2845.2 MeV if we slightly change the subtraction point. In this way, we will lower its position and reduce its width as it gets closer to the open $\Xi_c^*\pi$ channel.

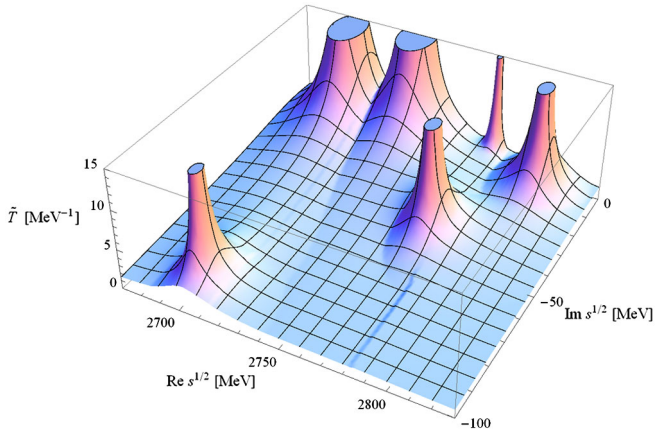

FIG. 8 (color online). $\tilde{T}^{I=(1/2),J=(1/2),S=-1,C=1}(s)$ amplitude (Ξ_c resonances).

In Refs. [42,43] a resonance with a similar energy of 2838 MeV and width of 16 MeV was identified with the $\Xi_c(2815)$. It was suggested that its small width reflected its small coupling strength to the $\Xi_c\pi$ channel.

D. Ω_c states ($C = 1$, $S = -2$, $I = 0$)

In this section we will discuss the $C = 1$, $S = -2$ and $I = 0$ resonant states with $J = 1/2$ and $J = 3/2$ coming from the **120** and **168** SU(8) representations. States with the $I = 1$ and the $J = 5/2$ belong to the **4752**-plet and are not discussed in this work.

1. Sector $J = 1/2$

The 15 physical baryon-meson pairs that are incorporated in the $I = 0$, $J = 1/2$ sector are as follows:

$\Xi_c\bar{K}$	$\Xi_c'\bar{K}$	ΞD	$\Omega_c\eta$	ΞD^*	$\Xi_c\bar{K}^*$
2965.1,	3072.5,	3185.3,	3245.0,	3326.5,	3363.3,
$\Xi_c'\bar{K}^*$	$\Omega_c\omega$	$\Xi_c^*\bar{K}^*$	$\Xi^* D^*$	$\Omega_c^*\omega$	$\Omega_c\eta'$
3470.7,	3480.1,	3540.2,	3541.8,	3550.9,	3655.3,

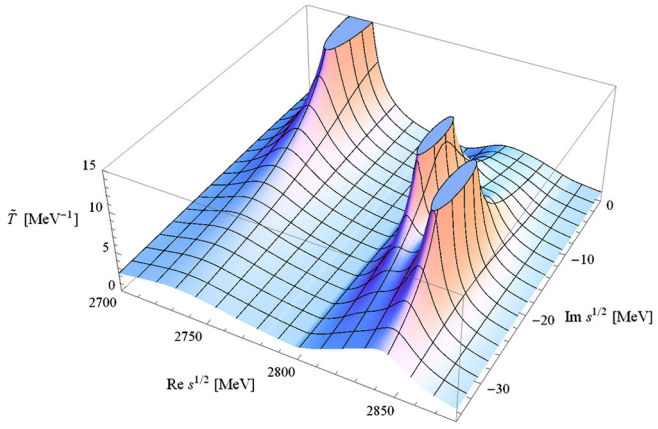

FIG. 9 (color online). $\tilde{T}^{I=(1/2),J=(3/2),S=-1,C=1}(s)$ amplitude (Ξ_c^* resonances).

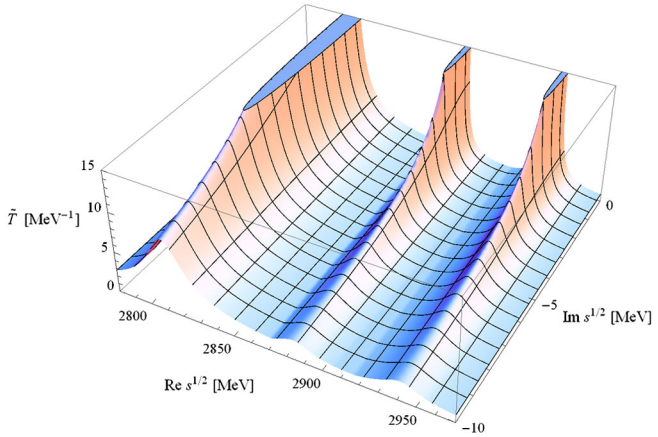

FIG. 10 (color online). $\tilde{T}^{I=0,J=(1/2),S=-2,C=1}(s)$ amplitude (Ω_c resonances).

$\Omega_c\phi$	ΩD_s^*	$\Omega_c^*\phi$
3717.0,	3784.8,	3787.8.

According to our analysis, there are three bound states which can be generated dynamically as baryon-meson molecular entities resulting from the strongly attractive representations of the SU(8) group. In Table VI and Fig. 10 we show the masses, widths, and the largest couplings of those poles to the scattering channels.

There is no experimental information on those excited states. However, our predictions can be compared to recent calculations of Refs. [42,45]. In Ref. [45] three resonances were found, one with mass $M_1 = 2959$ MeV and width $\Gamma_1 = 0$ MeV, a second one with $M_2 = 2966$ MeV and $\Gamma_2 = 1.1$ MeV, and the third one with $M_3 = 3117$ MeV and $\Gamma_3 = 16$ MeV. The dominant baryon-meson channels are $\bar{K}\Xi_c'$, $\bar{K}\Xi_c'$, and $D\Xi$, respectively. Three resonant states with lower masses were also observed in Ref. [42], but with slightly different dominant coupled channels.

In both previous references, vector baryon-meson channels were not considered, breaking in this manner HQSS. In fact, it is worth noticing that the coupling to vector baryon-meson states play an important role in the generation of the baryon resonances in this sector. Furthermore, we have checked that other states stemming from the **4752**-plet with the same quantum numbers might be seen in this energy region and, therefore, a straightforward identification of our states with the results of Refs. [42,45] might not be possible.

2. Sector $J = 3/2$

In the $C = 1$, $S = -2$, $I = 0$, $J = 3/2$ sector, there are 15 coupled channels:

$\Xi_c^*\bar{K}$	$\Omega_c^*\eta$	ΞD^*	$\Xi_c\bar{K}^*$	$\Xi^* D$	$\Xi_c'\bar{K}^*$
3142.0,	3315.8,	3326.5,	3363.3,	3400.6,	3470.7,
$\Omega_c\omega$	$\Xi_c^*\bar{K}^*$	$\Xi^* D^*$	$\Omega_c^*\omega$	ΩD_s	$\Omega_c\phi$
3480.1,	3540.2,	3541.8,	3550.9,	3641.0,	3717.0,

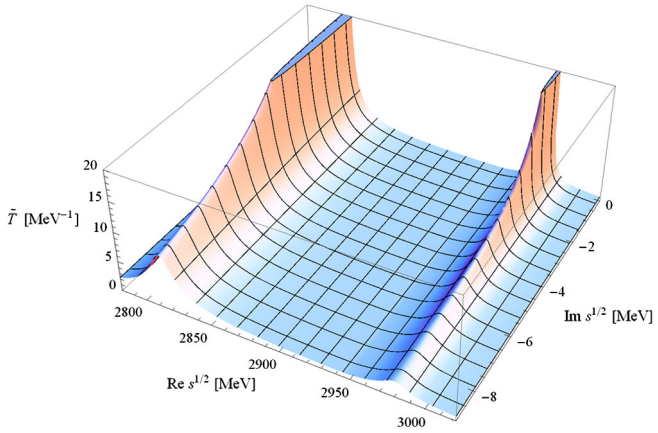

FIG. 11 (color online). $\tilde{T}^{I=0,J=(3/2),S=-2,C=1}(s)$ amplitude (Ω_c^* resonances).

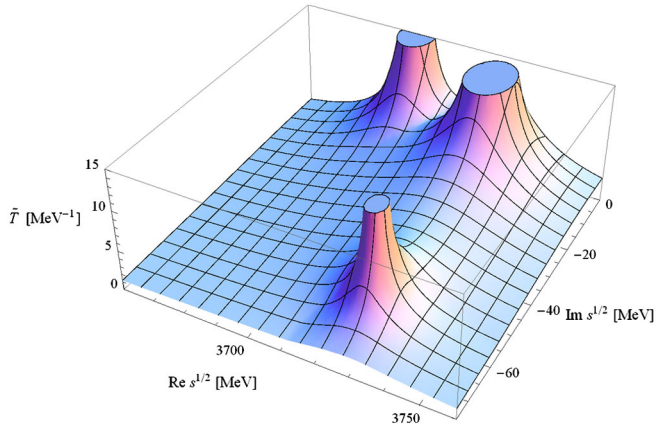

FIG. 12 (color online). $\tilde{T}^{I=(1/2),J=(1/2),S=0,C=2}(s)$ amplitude (Ξ_{cc} resonances).

$$\begin{array}{ccc} \Omega_c^*\eta' & \Omega D_s^* & \Omega_c^*\phi \\ 3726.1, & 3784.8, & 3787.8. \end{array}$$

We obtain two bound Ω_c^* states (Table VI and Fig. 11) with masses 2814.3, and 2980.0, which mainly couple to ΞD^* and $\Xi^* D^*$, and to $\Xi_c^* \bar{K}$, respectively. As seen in the $J = 1/2$ sector, no experimental information is available. In Ref. [43], two states at 2843 MeV and 3008 MeV with zero width were found. Those states couple most strongly to $D\Xi$ and $\bar{K}\Xi_c$, respectively, so an identification between the resonances in both models is not possible.

E. Ξ_{cc} states ($C = 2$, $S = 0$, $I = 1/2$)

In the $C = 2$ sector no experimental information is available yet. Therefore, all our results are predictions of the SU(8) WT model.

1. Sector $J = 1/2$

The 22 channels (thresholds are also given in MeV) for $C = 2$, $S = 0$, $I = 1/2$ and $J = 1/2$, are as follows:

$$\begin{array}{cccccc} \Xi_{cc}\pi & \Xi_{cc}\eta & \Lambda_c D & \Omega_{cc}K & \Xi_{cc}\rho & \Lambda_c D^* \\ 3657.0, & 4066.5, & 4153.7, & 4207.7, & 4294.5, & 4294.8, \end{array}$$

$$\begin{array}{cccccc} \Xi_{cc}\omega & \Sigma_c D & \Xi_{cc}^*\rho & \Xi_{cc}^*\omega & \Xi_c D_s & \Sigma_c D^* \\ 4301.6, & 4320.8, & 4375.5, & 4382.6, & 4438.0, & 4461.9, \end{array}$$

$$\begin{array}{ccccccc} \Xi_{cc}\eta' & \Sigma_c^* D^* & \Xi_{cc}\phi & \Xi_c' D_s & \Xi_c D_s^* & \Omega_{cc}K^* \\ 4476.8, & 4526.3, & 4538.5, & 4545.4, & 4581.8, & 4605.9, \end{array}$$

$$\begin{array}{cccc} \Xi_{cc}^*\phi & \Omega_{cc}^* K^* & \Xi_c' D_s^* & \Xi_c^* D_s^* \\ 4619.5, & 4688.9, & 4689.2, & 4758.7. \end{array}$$

The three predicted poles in the Ξ_{cc} sector can be seen in the Table VII and Fig. 12 together with the width and couplings to the main channels. Their masses are 3698.1, 3727.4 and 3727.8 MeV, with widths 1.3, 120.2 and 17.8 MeV, respectively. The dominant channels for the generation of those states are, in order, $\Sigma_c^* D^*$, $\Xi_{cc}\pi$ and $\Lambda_c D$, and $\Sigma_c D^*$. In Ref. [42] six states were found, two of them coming from the weak interaction of the open-charm mesons and open-charm baryons in the SU(4) antisextet and 15-plet. In this paper, we only consider those states coming from the strongly attractive SU(8) **120**- and **168**-plets. Therefore, only three states are expected in this sector. Moreover, an identification among resonances in both models is complicated because of the strong coupling of our states to channels with vector mesons, not considered in this previous reference.

2. Sector $J = 3/2$

In the Ξ_{cc}^* sector, the following 20 channels are coupled:

$$\begin{array}{ccccccc} \Xi_{cc}^*\pi & \Xi_{cc}^*\eta & \Omega_{cc}^* K & \Xi_{cc}\rho & \Lambda_c D^* & \Xi_{cc}\omega & \Xi_{cc}^*\rho \\ 3738.0, & 4147.5, & 4290.7, & 4294.5, & 4294.8, & 4301.6, & 4375.5, \end{array}$$

$$\begin{array}{ccccccc} \Xi_{cc}^*\omega & \Sigma_c^* D & \Sigma_c D^* & \Sigma_c^* D^* & \Xi_{cc}\phi & \Xi_{cc}^*\eta' & \Xi_c D_s^* \\ 4382.6, & 4385.2, & 4461.9, & 4526.3, & 4538.5, & 4557.8, & 4581.8, \end{array}$$

$$\begin{array}{cccccc} \Omega_{cc}K^* & \Xi_c^* D_s & \Xi_{cc}^*\phi & \Omega_{cc}^* K^* & \Xi_c' D_s^* & \Xi_c^* D_s^* \\ 4605.9, & 4614.9, & 4619.5, & 4688.9, & 4689.2, & 4758.7. \end{array}$$

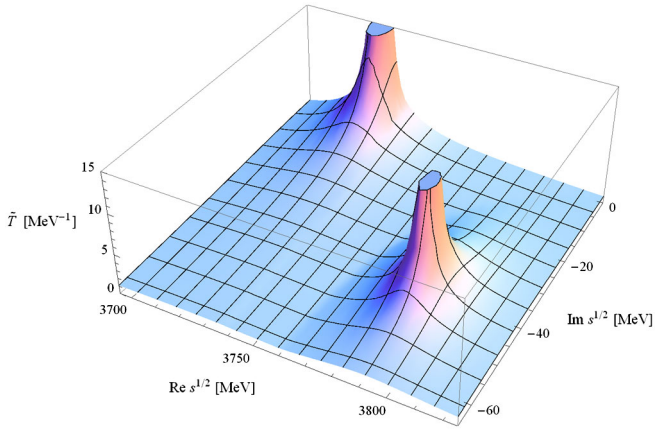

FIG. 13 (color online). $\tilde{T}^{I=(1/2),J=(3/2),S=0,C=2}(s)$ amplitude (Ξ_{cc}^{*} resonances).

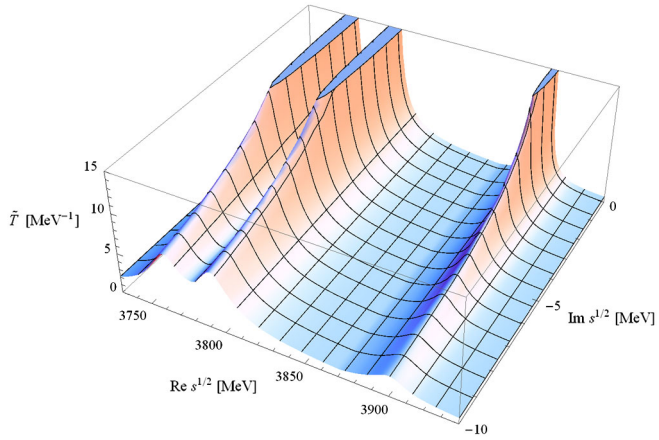

FIG. 14 (color online). $\tilde{T}^{I=0,J=(1/2),S=-1,C=2}(s)$ amplitude (Ω_{cc} resonances).

Two states, with masses 3729.5 and 3790.8 MeV have been obtained, which couple mainly to $\Sigma_c^{*}D$ and $\Sigma_c^{*}D^{*}$, and to $\Xi_{cc}^{*}\pi$ and $\Lambda_c D^{*}$, respectively (see Table VII and Fig. 13).

In Ref. [43], two states were obtained at 3671 MeV and 3723 MeV, with dominant coupling to the channels $\Sigma_c D$ and $\Xi_{cc}\pi$, respectively. However, the analysis there was done on the basis that the $\Xi_{cc}(3519)$ resonance is, in fact, a $J^P = 3/2^+$ state, whereas, in our calculation this resonance is the ground state, $J^P = 1/2^+$. It is argued in [43] that the second resonance should be more reliable in view of the dominant coupling to a baryon-Goldstone boson. Moreover, it was mentioned the necessity of implementing heavy-quark symmetry by incorporating 0^- and 1^- charmed mesons as well as $1/2^+$ and $3/2^+$ baryon in the coupled-channel basis. Therefore, in both models, the implementation of heavy-quark symmetry seems to move to higher energies the expected resonant states as well as to change their dominant molecular components.

F. Ω_{cc} states ($C = 2$, $S = -1$, $I = 0$)

1. Sector $J = 1/2$

The 17 channels in this Ω_{cc} sector are as follows:

$$\begin{array}{ccccccc} \Xi_{cc}\bar{K} & \Omega_{cc}\eta & \Xi_c D & \Xi_{cc}\bar{K}^{*} & \Xi_c' D & \Xi_c D^{*} & \Xi_{cc}^{*}\bar{K}^{*} \\ 4014.7, & 4259.5, & 4336.7, & 4412.9, & 4444.1, & 4477.8, & 4493.9, \end{array}$$

$$\begin{array}{ccccccc} \Omega_{cc}\omega & \Omega_{cc}^{*}\omega & \Xi_c' D^{*} & \Xi_c^{*} D^{*} & \Omega_c D_s & \Omega_{cc}\eta' & \Omega_{cc}\phi \\ 4494.6, & 4577.6, & 4585.2, & 4654.7, & 4666.0, & 4669.8, & 4731.5, \end{array}$$

$$\begin{array}{ccc} \Omega_c D_s^{*} & \Omega_{cc}^{*}\phi & \Omega_c^{*} D_s^{*} \\ 4809.8, & 4814.5, & 4880.6. \end{array}$$

The predicted bound states are three at 3761.8 MeV, 3792.8 MeV, and 3900.2 MeV, coupling strongly to $\Xi_c^{*}D^{*}$, $\Xi_c' D^{*}$ and $\Xi_{cc}\bar{K}$, respectively. They are shown in Table VIII and Fig. 14. In Ref. [42] four states were generated from the SU(4) 3-plet at 3.71 GeV, 3.74 GeV and 3.81 GeV and one coming from the SU(4) 15-plet at 4.57 GeV. We might be tempted to identify our three states with those coming from SU(4) 3-plet in Ref. [42] because the dominant channels are similar, if we do not consider those including vector mesons and $3/2^+$ baryons. However, the only clear identification that can be done is between our state at 3900.2 MeV and the one in Ref. [42] at 3.81 GeV because in this case the dominant channels coincide. For this state, channels with vector mesons and/or $3/2^+$ baryons do not play a significant role.

2. Sector $J = 3/2$

The 16 channels in the Ω_{cc}^* sector are:

$$\begin{array}{cccccccc} \Xi_{cc}^*\bar{K} & \Omega_{cc}^*\eta & \Xi_{cc}\bar{K}^* & \Xi_c D^* & \Xi_{cc}^*\bar{K}^* & \Omega_{cc}\omega & \Xi_c^* D \\ 4095.7, & 4342.5, & 4412.9, & 4477.8, & 4493.9, & 4494.6, & 4513.6, \end{array}$$

$$\begin{array}{cccccccc} \Omega_{cc}^*\omega & \Xi_c' D^* & \Xi_c^* D^* & \Omega_{cc}\phi & \Omega_c^* D_s & \Omega_{cc}^*\eta' & \Omega_c D_s^* \\ 4577.6, & 4585.2, & 4654.7, & 4731.5, & 4736.8, & 4752.8, & 4809.8, \end{array}$$

$$\begin{array}{cc} \Omega_{cc}^*\phi & \Omega_c^* D_s^* \\ 4814.5, & 4880.6. \end{array}$$

Two bound states at 3802.9 MeV and 3936.3 MeV are observed, which couple mostly to $\Xi_c^* D^*$ and $\Xi_{cc}^*\bar{K}$, respectively (see Table VIII and Fig. 15). Compared to Ref. [43], we see a similar pattern as observed in the $C = 2$, $S = 0$, $I = 1/2$, $J = 3/2$ sector. The two expected states are obtained with larger masses and the dominant molecular composition incorporates a vector meson, or a vector meson and $3/2^+$ baryon state when heavy-quark symmetry is implemented. As indicated also in Ref. [43], the second resonance should be more reliable as its main molecular contribution comes from the interaction of a baryon with a Goldstone boson.

G. Ω_{ccc} states ($C = 3$, $S = 0$, $I = 0$)

We finally study baryon resonances with charm $C = 3$ and strangeness $S = 0$.

1. Sector $J = 1/2$

The 8 coupled channels in the sector with $J = 1/2$, are (thresholds in MeV are also indicated):

$$\begin{array}{cccc} \Xi_{cc} D & \Xi_{cc} D^* & \Omega_{ccc}\omega & \Xi_{cc}^* D^* \\ 5386.2, & 5527.3, & 5581.6, & 5608.4, \end{array}$$

$$\begin{array}{cccc} \Omega_{cc} D_s & \Omega_{ccc}\phi & \Omega_{cc} D_s^* & \Omega_{cc}^* D_s^* \\ 5680.5, & 5818.5, & 5824.3, & 5907.3. \end{array}$$

There is only one baryon state generated by the model in this sector. The mass (4358.2 MeV), width (0 MeV) and the couplings are shown in the Table IX and Fig. 16. In Ref. [42], a resonance at 4.31–4.33 GeV was also obtained. In both schemes, the Ω_{ccc} resonance couples strongly to $\Xi_{cc} D$ and $\Omega_{cc} D_s$ but in our SU(8) model, the dominant contribution comes from channels with vector mesons and/or $3/2^+$ baryons. Therefore, this result points to the necessity of extending the coupled-channel basis to incorporate channels with charmed vector mesons and $3/2^+$ baryons as required by heavy-quark symmetry.

2. Sector $J = 3/2$

The 10 channels and thresholds (in MeV) in the sector Ω_{ccc}^* are as follows:

$$\begin{array}{ccccc} \Omega_{ccc}\eta & \Xi_{cc}^* D & \Xi_{cc} D^* & \Omega_{ccc}\omega & \Xi_{cc}^* D^* \\ 5346.5, & 5467.2, & 5527.3, & 5581.6, & 5608.4, \end{array}$$

$$\begin{array}{ccccc} \Omega_{ccc}\eta' & \Omega_{cc}^* D_s & \Omega_{ccc}\phi & \Omega_{cc} D_s^* & \Omega_{cc}^* D_s^* \\ 5756.8, & 5763.5, & 5818.5, & 5824.3, & 5907.3. \end{array}$$

The Ω_{ccc}^* resonance with $J = 3/2$ has a mass approximately 1 GeV below the lowest baryon-meson threshold. This resonance stems from the **120** irrep of SU(8) and it is shown in Table IX and Fig. 17. One resonance was also seen in Ref. [43], much below the first open threshold, coupling dominantly to $\Xi_{cc} D$. Our results show that this bound state mainly couples to $\Xi_{cc} D^*$, $\Xi_{cc}^* D^*$ and $\Xi_{cc}^* D$

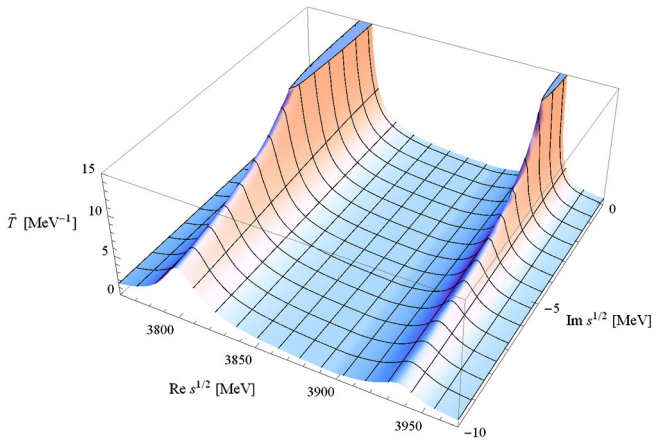

FIG. 15 (color online). $\tilde{T}^{I=0,J=(3/2),S=-1,C=2}(s)$ amplitude (Ω_{cc}^* resonances).

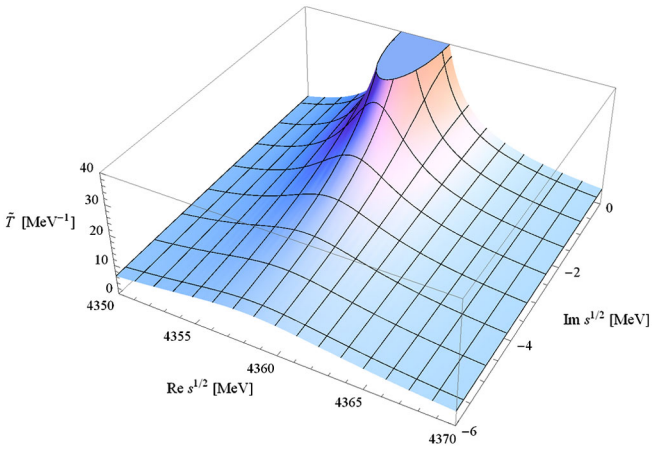

FIG. 16 (color online). $\tilde{T}^{I=0,J=(1/2),S=0,C=3}(s)$ amplitude (Ω_{ccc} resonance).

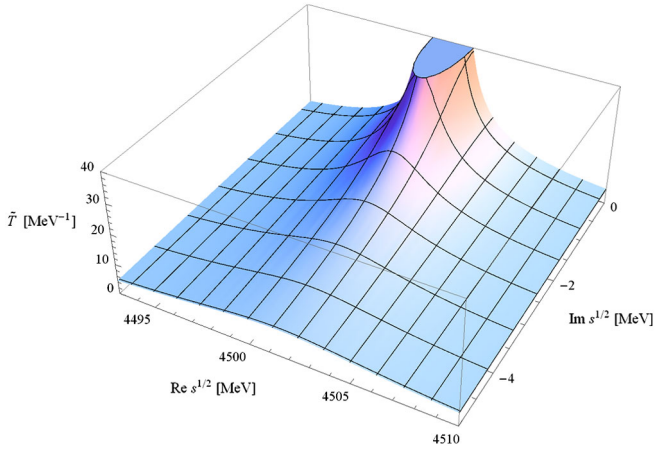

FIG. 17 (color online). $\tilde{T}^{I=0,J=(3/2),S=0,C=3}(s)$ amplitude (Ω^*_{ccc} resonance).

states as we incorporate charmed vector mesons and $3/2^+$ baryons according to heavy-quark symmetry. The large separation from the closest threshold suggests that interaction mechanisms involving d-wave could be relevant for this resonance. This remark applies also to the Ω_{ccc} dynamically-generated resonance with $J = 1/2$.

H. HQSS in the results

The factor $\mathrm{SU}_C(2) \times \mathrm{U}_C(1)$ in Eq. (4) implements HQSS for the sectors studied in this work. The HQSS group acts by changing the coupling of spin of the charmed quarks, relative to the spin of the block formed by light quarks. At the level of basic hadrons, it reflects in the nearly degeneracy of D and D^* mesons, which form a HQSS doublet.[6] Other doublets are $(\bar{D}_s, \bar{D}^*_s)$, and $(\eta_c, J/\psi)$ in mesons, and (Σ_c, Σ^*_c), (Ξ'_c, Ξ^*_c), (Ω_c, Ω^*_c), (Ξ_{cc}, Ξ^*_{cc}), $(\Omega_{cc}, \Omega^*_{cc})$, in baryons. On the other hand, Λ_c, Ξ_c and Ω_{ccc} are singlets, as are all the other basic hadrons not containing charmed quarks. This information is collected in Table II.[7]

HQSS multiplets form also in the baryon-meson states. Specifically, in the reduction in Eq. (6) and Figs. 1, 2 and 3, the pair $(\mathbf{6_2}, \mathbf{6_4})$ forms a HQSS doublet in the reduction of $\mathbf{21_{2,1}}$, while $\mathbf{3^*_2}$ is a singlet. Similarly, $(\mathbf{3^*_2}, \mathbf{3^*_4})$ in $\mathbf{15_{2,1}}$, and $(\mathbf{3_2}, \mathbf{3_4})$ in $\mathbf{6_{3,2}}$, are doublets, whereas all other $\mathrm{SU}(3) \times \mathrm{SU}(2)$ representations are HQSS singlets.

HQSS is much less broken than spin-flavor of light quarks, implemented by SU(6), so HQSS is more visible in the results. If we imposed strict HQSS, by setting equal masses and decay constants as required by the symmetry, exactly degenerated HQSS multiplet would form, regardless of the amount of breaking of SU(6). We break HQSS only through the use of physical masses and decay constants,[8] but not in the interaction. Therefore we estimate that our breaking is no larger than that present in full QCD. This suggests that the amount of breaking we find is not an overestimation due to the model, on the contrary, we expect to find more degeneracy than actually exists.

The approximate HQSS doublets can be observed in the results by comparing states with equal SU(8) and $\mathrm{SU}(6) \times \mathrm{SU}_C(2) \times \mathrm{U}_C(1)$ labels with $J = 1/2$ and $J = 3/2$. The only exception is for the Ξ_{cc} states in Table VII where the SU(8) labels are mixed in the two doublets. As noted in Sec. II B this reflects that exact SU(8) symmetry is broken in the interaction after dropping the channels with extra $c\bar{c}$ pairs.

For convenience we have arranged the tables so that HQSS partners are in consecutive rows. So, in Table III, the Λ_c state 2617.3 MeV with labels $(\mathbf{168}, \mathbf{15_{21,}}, \mathbf{3^*_2})$, matches the Λ^*_c state 2666.6 MeV with labels $(\mathbf{168}, \mathbf{15_{21,}}, \mathbf{3^*_4})$. The matching refers not only to the mass but also the width and the couplings, taking into account that, e.g., Σ_c in one state corresponds to Σ^*_c in the other. (Note that HQSS also implies relations between couplings in the same resonance.) If the identifications in Table III are correct, it would imply that $\Lambda_c(2595)$ is a HQSS singlet whereas $\Lambda_c(2625)$ belongs to a doublet. Similarly, in Table IV, the Σ_c state 2571.5 MeV is the HQSS partner of the Σ^*_c state 2568.4 MeV [both in $(\mathbf{168}, \mathbf{21_{2,1}})$], whereas the states 2643.4 MeV and 2692.9 MeV are partners in $(\mathbf{120}, \mathbf{21_{2,1}})$. Of special interest is the case of Ξ_c states. Here we find that the two three-star resonances $\Xi_c(2790)$ and $\Xi_c(2815)$ are candidates to form a HQSS doublet. Further doublets are predicted for Ω_c and for the $C = 2$ resonances, Ξ_{cc} and Ω_{cc}. On the other hand, no doublet is present in the Ω_{ccc} sector. All these considerations follow unambiguously from the SU(8) structure if the **168** and **120** irreps are dominant, as predicted by the extended WT scheme.

IV. SUMMARY

In the present work, we have studied odd-parity charmed baryon resonances within a coupled-channel unitary approach that implements the characteristic features of HQSS. This implies, for instance, that D and D^* mesons have to be treated on an equal footing and that channels containing a different number of c or $\bar{c}$ quarks cannot be coupled. This is accomplished by extending the SU(3) WT

[6]We use "doublet" to indicate that only two multiplets with well-defined *CSIJ* get mixed by the HQSS group. The space spanned by the eight D or D^* states reduces into two dimension four irreducible subspaces under HQSS, corresponding to the four spin states of D and D^* with given charge.

[7]The classification of basic hadrons into HQSS multiplets can be obtained from the hadron wavefunctions in the Appendix A of [53]. For instance, for Σ_c and Σ^*_c the two light quarks are coupled to spin triplet (since they form an isospin triplet and color is antisymmetric) and this can give $J = 1/2$ or $J = 3/2$ when coupled to the spin of the charmed quark. A systematic classification can be found in [81].

[8]Most of the values in Table II are obtained from the experiment while some of them are guesses from models or from lattice calculations.

chiral interaction to SU(8) spin-flavor symmetry and implementing a strong flavor symmetry breaking. Thus, our tree-level s-wave WT amplitudes are obtained not only by adopting the physical hadron masses, but also by introducing the physical weak decay constants of the mesons involved in the transitions. Besides, and to deal with the UV divergences that appear after summing the bubble chain implicit in the Bethe-Salpeter equation, here we adopt the prescription of Ref. [42]. It amounts to force the renormalized loop function to vanish at certain scale that depends only on CSI. In this manner, we have no free parameters. We have not refitted the subtraction points to achieve better agreement in masses and widths of the few known states.

This scheme was first derived in Ref. [53], where results for all non strange sectors with $C = 1$ were already analyzed. Here, we have discuss the predictions of the model for all $C = 1$ strange sectors and have also looked at the $C = 2$ and 3 predicted states. The SU(8) model generates a great number of states, most of them stemming from the **4752** representation. The interaction in this subspace, though attractive, is much weaker than in the **168** and **120** ones (-2 vs -22 and -16). Indeed, in the large N_C limit, we expect the **4752** states will disappear and only those related to the **168** representation will remain [64]. Besides, being so weak, the interaction in the **4752** subspace, small corrections (higher orders in the expansion, d-wave terms, etc.) could strongly modify the properties of the states that arise from this representation. For all this, we have restricted our study in this work to the 288 states (counting multiplicities in spin and isospin) that stem from the **168** and **120** representations, for which we believe the predictions of the model are more robust.

A similar study for the light SU(6) spin-flavor sector was carried out in Ref. [62]. There, it was found that most of the low-lying three- and four-star odd-parity baryon resonances with spin $1/2$ and $3/2$ can be related to the **56** and **70** multiplets of the spin-flavor symmetry group SU(6). These are precisely the charmless multiplets that appear in the decomposition in Eq. (5) of the **120** and **168** SU(8) representations. Thus, out of the 288 states mentioned above, we are left with only 162 charmed states.[9]

To identify these states, we have adiabatically followed the trajectories of the **168** and **120** poles, generated in a symmetric SU(8) world, when the symmetry is broken down to SU(6) $\times$ SU$_C$(2) and later SU(6) is broken down to SU(3) $\times$ SU(2). In this way, we have been able to assign well-defined SU(8), SU(6) and SU(3) labels to the resonances. A first result of this work is that we have been able to identify the **168** and **120** resonances among the plethora of resonances predicted in Ref. [53] for the different strangeness $C = 1$ sectors. As expected, they turn out to be the lowest-lying ones, and we are pretty confident about their existence. This appreciation is being reinforced by our previous study of Ref. [62] in the light SU(6) sector. Thus, we interpret the $\Lambda_c(2595)$ and $\Lambda_c(2625)$ as a members of the SU(8) **168**-plet, and in both cases with a dynamics strongly influenced by the ND^* channel, in sharp contrast with previous studies inconsistent with HQSS. Moreover, the changes induced by a suppression factor in the interaction when charm is exchanged do not modify the conclusions (see Appendix A). Second, we have identified the HQSS multiplets in which the resonances are arranged. Specifically, the Λ_c, Λ_c^* sector arranges into two singlets, the $\Lambda_c(2595)$ being one of them, and one doublet, which contains the $\Lambda_c(2625)$. Similarly the Σ_c, Σ_c^* sector contains one singlet and two doublets. For the Ξ_c, Ξ_c^* sector, there are three doublets and three singlets. According to our tentative identification, $\Xi_c(2790)$ and $\Xi_c(2815)$ form a HQSS doublet. Finally, Ω_c, Ω_c^* states form two doublets and one singlet. Third, we have worked out the predictions of the model of Ref. [53] for strange charmed and $C = 2$ and $C = 3$ resonances linked to the strongly attractive **168** and **120** subspaces. To our knowledge, these are the first predictions in these sectors deduced from a model fulfilling HQSS. The organization into HQSS multiplets is also given in this case. There is scarce experimental information in these sectors, and we have only identified the three-star $\Xi_c(2790)$ and $\Xi_c(2815)$ resonances, but we believe that the rest of our predictions are robust, and will find experimental confirmation in the future. Of particular relevance to this respect will be the program of PANDA at the future facility FAIR.

[9]All exotic states, this is to say, those that cannot be accommodated within a simple qqq picture of the baryon, lie in the **4752** space, and thus they have not been discussed here. Some of them ($C = -1$) were discussed in Ref. [54].

ACKNOWLEDGMENTS

We thank Michael Döring for the fruitful discussion and introducing the excellent method of calculating the couplings. This research was supported by DGI and FEDER funds, under Contract Nos. FIS2011-28853-C02-02, FIS2008-01143, FIS2011-24149, FPA2010-16963 and the Spanish Consolider-Ingenio 2010 Programme CPAN (CSD2007-00042), by Junta de Andalucía Grant No. FQM-225, by Generalitat Valenciana under Contract No. PROMETEO/2009/0090 and by the EU HadronPhysics2 project, Grant Agreement No. 227431. O. R. and L. T. wish to acknowledge support from the Rosalind Franklin Programme. L. T. acknowledges support from Ramon y Cajal Research Programme, and from FP7-PEOPLE-2011-CIG under Contract No. PCIG09-GA-2011-291679.

APPENDIX A: CHARM-EXCHANGE SUPPRESSION

In this section we discuss the effect of the inclusion of a suppression factor in the interaction when charm-exchange is present.

TABLE X. Λ_c and Λ_c^* resonances with inclusion of the suppression factor κ_c.

SU(8) irrep	SU(6) irrep	SU(3) irrep	M_R	Γ_R	Couplings to main channels	Status PDG	J
168	$\mathbf{15_{2,1}}$	$\mathbf{3_2}$	2624.6	103.9	$g_{\Sigma_c\pi} = \mathbf{2.3}$, $g_{ND} = 0.4$, $g_{ND^*} = 0.4$, $g_{\Sigma_c\rho} = 1.6$		1/2
168	$\mathbf{15_{2,1}}$	$\mathbf{3_4}$	2675.1	65.7	$g_{\Sigma_c^*\pi} = \mathbf{2.1}$, $g_{ND^*} = 0.5$, $g_{\Sigma_c\rho} = 0.9$, $g_{\Sigma_c^*\rho} = 1.6$	$\Lambda_c(2625)$ ***	3/2
168	$\mathbf{21_{2,1}}$	$\mathbf{3_2}$	2624.1	0.1	$g_{\Sigma_c\pi} = \mathbf{0.1}$, $g_{ND} = 3.4$, $g_{ND^*} = 5.7$, $g_{\Lambda D_s} = 1.4$, $g_{\Lambda D_s^*} = 3.0$, $g_{\Lambda_c\eta'} = 0.2$	$\Lambda_c(2595)$ ***	1/2
120	$\mathbf{21_{2,1}}$	$\mathbf{3_2}$	2824.9	0.4	$\mathbf{g}_{ND} = \mathbf{0.1}$, $g_{\Lambda_c\eta} = 1.1$, $g_{\Xi_cK} = 1.9$, $g_{\Lambda D_s^*} = 1.1$, $g_{\Sigma_c\rho} = 1.1$, $g_{\Sigma_c^*\rho} = 1.4$, $g_{\Xi_c^*K^*} = 1.0$		1/2

TABLE XI. Σ_c and Σ_c^* resonances with inclusion of the suppression factor κ_c.

SU(8) irrep	SU(6) irrep	SU(3) irrep	M_R	Γ_R	Couplings to main channels	Status PDG	J
168	$\mathbf{21_{2,1}}$	$\mathbf{6_2}$	2583.4	0.0	$g_{\Lambda_c\pi} = \mathbf{0.03}$, $g_{ND} = 2.4$, $g_{ND^*} = 1.3$, $g_{\Sigma D_s} = 1.7$, $g_{\Delta D^*} = 6.8$, $g_{\Sigma D_s^*} = 1.2$, $g_{\Sigma^* D_s^*} = 3.1$		1/2
168	$\mathbf{21_{2,1}}$	$\mathbf{6_4}$	2577.8	0.0	$g_{ND^*} = 2.7$, $g_{\Delta D} = 4.3$, $g_{\Delta D^*} = 5.4$, $g_{\Sigma D_s^*} = 2.4$, $g_{\Sigma^* D_s} = 1.6$, $g_{\Sigma^* D_s^*} = 2.4$		3/2
168	$\mathbf{15_{2,1}}$	$\mathbf{6_2}$	2691.3	137.6	$g_{\Lambda_c\pi} = \mathbf{1.6}$, $g_{\Sigma_c\pi} = \mathbf{0.3}$, $g_{ND} = 0.5$, $g_{ND^*} = 0.7$, $g_{\Xi_cK} = 1.1$, $g_{\Sigma_c\rho} = 1.8$, $g_{\Sigma_c^*\rho} = 2.5$, $g_{\Xi_c^*K^*} = 0.9$		1/2
120	$\mathbf{21_{2,1}}$	$\mathbf{6_2}$	2653.9	95.0	$g_{\Lambda_c\pi} = \mathbf{0.2}$, $g_{\Sigma_c\pi} = \mathbf{2.0}$, $g_{ND} = 0.6$, $g_{ND^*} = 0.4$, $g_{\Lambda_c\rho} = 1.7$, $g_{\Delta D^*} = 0.4$, $g_{\Sigma_c\rho} = 1.3$, $g_{\Sigma^* D_s^*} = 0.4$		1/2
120	$\mathbf{21_{2,1}}$	$\mathbf{6_4}$	2697.2	65.8	$g_{\Sigma_c^*\pi} = \mathbf{1.9}$, $g_{ND^*} = 0.6$, $g_{\Lambda_c\rho} = 1.7$, $g_{\Sigma_c^*\rho} = 1.1$, $g_{\Sigma D_s^*} = 0.3$, $g_{\Sigma^* D_s^*} = 0.3$		3/2

In our approach, the interactions are implemented by a contact term, and each matrix element is affected by the decay constants of the mesons in the external legs of the interaction vertex. In particular, the charm-exchange terms always involve a $D \leftrightarrow \pi$-like transition, and thus they carry a factor $1/(f_\pi f_D)$. This source of flavor symmetry breaking turns out to enhance (suppress) these transitions with respect to some others like $ND \to ND$ ($\Sigma_c\pi \to \Sigma_c\pi$) where there is no charm exchange, and that scale instead like $1/f_D^2$ ($1/f_\pi^2$).

On the other hand, only decay constants of light mesons are involved in the t-channel vector-meson exchange models, as the one used in [42–44]. Nevertheless, there is another source of quenching for charm-exchange interactions, coming from the larger mass of the charmed meson exchanged, as compared to those of the vector mesons belonging to the ρ nonet. Qualitatively, a factor $\kappa_c = 1/4 \simeq m_\rho^2/m_{D^*}^2$ is applied in the matrix elements involving charm exchange, whereas $\kappa_c = 1$ is kept in the remaining matrix elements [44]. The introduction of these quenching factors does not spoil HQSS (note however, that neither the scheme of Ref. [42,43] nor that of Ref. [44] are consistent with HQSS) but it is a new source of flavor breaking. In this appendix, we study the effects of including this suppression factor κ_c within our scheme. In this case, the potential looks as follows:

$$V_{ij}(s) = \kappa_c D_{ij} \frac{2\sqrt{s} - M_i - M_j}{4 f_i f_j} \sqrt{\frac{E_i + M_i}{2M_i}} \sqrt{\frac{E_j + M_j}{2M_j}}. \tag{A1}$$

In Tables X and XI we show the results including the κ_c factor for the sectors with $C = 1$, $S = 0$. As it can be seen, there are some small changes in the masses and the widths of the resonances in comparison with the values shown in Tables III and IV, while the values of the couplings also change in some cases. However, in general, the changes induced by the inclusion of this new source of flavor breaking are not dramatic, and they do not modify the main conclusions of this work.

APPENDIX B: BARYON-MESON MATRIX ELEMENTS

In this appendix the coefficients D_{ij} appearing in Eq. (7) are shown for the various $CSIJ$ sectors studied in this work (Tables XII, XIII, XIV, XV, XVI, XVII, XVIII, XIX, XX, XXI, XXII, XXIII, XXIV, and XXV). The D-matrices for the channels with $C = 1$, $S = 0$ can be found in an Appendix B of Ref. [53]. The tables for Ξ_c and Ξ_c^* states have been divided in three blocks.

TABLE XII. $C = 1$, $S = -1$, $I = 1/2$, $J = 1/2$.

	$\Xi_c\pi$	$\Xi_c'\pi$	$\Lambda_c\bar{K}$	$\Sigma_c\bar{K}$	ΛD	$\Xi_c\eta$	ΣD	ΛD^*	$\Xi_c'\eta$	$\Lambda_c\bar{K}^*$	$\Omega_c K$	ΣD^*	$\Xi_c\rho$	$\Xi_c\omega$	ΞD_s	$\Sigma_c\bar{K}^*$
$\Xi_c\pi$	-2	0	$\sqrt{\frac{3}{2}}$	0	$\sqrt{\frac{3}{8}}$	0	$\sqrt{\frac{3}{8}}$	$\sqrt{\frac{9}{8}}$	0	0	0	$\sqrt{\frac{9}{8}}$	0	0	0	$\sqrt{\frac{1}{2}}$
$\Xi_c'\pi$	0	-2	0	$\sqrt{\frac{1}{2}}$	$\sqrt{\frac{9}{8}}$	0	$-\sqrt{\frac{1}{8}}$	$-\sqrt{\frac{3}{8}}$	0	$\sqrt{\frac{3}{2}}$	$-\sqrt{3}$	$\sqrt{\frac{1}{24}}$	2	0	0	$\sqrt{\frac{2}{3}}$
$\Lambda_c\bar{K}$	$\sqrt{\frac{3}{2}}$	0	-1	0	1	$-\sqrt{\frac{3}{2}}$	0	$\sqrt{3}$	0	0	0	0	0	0	0	$\sqrt{3}$
$\Sigma_c\bar{K}$	0	$\sqrt{\frac{1}{2}}$	0	-3	0	0	1	0	$\sqrt{\frac{9}{2}}$	$\sqrt{3}$	0	$-\sqrt{\frac{1}{3}}$	$\sqrt{\frac{1}{2}}$	$\sqrt{\frac{3}{2}}$	0	$-\sqrt{12}$
ΛD	$\sqrt{\frac{3}{8}}$	$\sqrt{\frac{9}{8}}$	1	0	-1	$-\sqrt{\frac{1}{24}}$	0	0	$-\sqrt{\frac{1}{8}}$	$\sqrt{3}$	0	$\sqrt{3}$	$\sqrt{\frac{9}{8}}$	$-\sqrt{\frac{3}{8}}$	$\sqrt{\frac{3}{2}}$	0
$\Xi_c\eta$	0	0	$-\sqrt{\frac{3}{2}}$	0	$-\sqrt{\frac{1}{24}}$	0	$\sqrt{\frac{3}{8}}$	$-\sqrt{\frac{1}{8}}$	0	0	0	$\sqrt{\frac{9}{8}}$	0	0	-1	$\sqrt{\frac{9}{2}}$
ΣD	$\sqrt{\frac{3}{8}}$	$-\sqrt{\frac{1}{8}}$	0	1	0	$\sqrt{\frac{3}{8}}$	-3	$\sqrt{3}$	$-\sqrt{\frac{1}{8}}$	0	0	$-\sqrt{12}$	$\sqrt{\frac{9}{8}}$	$\sqrt{\frac{27}{8}}$	$-\sqrt{\frac{3}{2}}$	$-\sqrt{\frac{1}{3}}$
ΛD^*	$\sqrt{\frac{9}{8}}$	$-\sqrt{\frac{3}{8}}$	$\sqrt{3}$	0	0	$-\sqrt{\frac{1}{8}}$	$\sqrt{3}$	-1	$\sqrt{\frac{1}{24}}$	-1	0	2	$-\sqrt{\frac{3}{8}}$	$\sqrt{\frac{1}{8}}$	$\sqrt{\frac{1}{2}}$	0
$\Xi_c'\eta$	0	0	0	$\sqrt{\frac{9}{2}}$	$-\sqrt{\frac{1}{8}}$	0	$-\sqrt{\frac{1}{8}}$	$\sqrt{\frac{1}{24}}$	0	$-\sqrt{\frac{3}{2}}$	$-\sqrt{3}$	$\sqrt{\frac{1}{24}}$	0	0	$-\sqrt{\frac{1}{3}}$	$\sqrt{6}$
$\Lambda_c\bar{K}^*$	0	$\sqrt{\frac{3}{2}}$	0	$\sqrt{3}$	$\sqrt{3}$	0	0	-1	$-\sqrt{\frac{3}{2}}$	-1	0	0	$\sqrt{\frac{3}{2}}$	$-\sqrt{\frac{1}{2}}$	0	2
$\Omega_c K$	0	$-\sqrt{3}$	0	0	0	0	0	0	$-\sqrt{3}$	0	-2	0	$\sqrt{3}$	1	-1	0
ΣD^*	$\sqrt{\frac{9}{8}}$	$\sqrt{\frac{1}{24}}$	0	$-\sqrt{\frac{1}{3}}$	$\sqrt{3}$	$\sqrt{\frac{9}{8}}$	$-\sqrt{12}$	2	$\sqrt{\frac{1}{24}}$	0	0	-7	$-\sqrt{\frac{3}{8}}$	$-\sqrt{\frac{9}{8}}$	$-\sqrt{\frac{25}{2}}$	$\frac{5}{3}$
$\Xi_c\rho$	0	2	0	$\sqrt{\frac{1}{2}}$	$\sqrt{\frac{9}{8}}$	0	$\sqrt{\frac{9}{8}}$	$-\sqrt{\frac{3}{8}}$	0	$\sqrt{\frac{3}{2}}$	$\sqrt{3}$	$-\sqrt{\frac{3}{8}}$	-2	0	0	$-\sqrt{\frac{2}{3}}$
$\Xi_c\omega$	0	0	0	$\sqrt{\frac{3}{2}}$	$-\sqrt{\frac{3}{8}}$	0	$\sqrt{\frac{27}{8}}$	$\sqrt{\frac{1}{8}}$	0	$-\sqrt{\frac{1}{2}}$	1	$-\sqrt{\frac{9}{8}}$	0	0	0	$-\sqrt{2}$
ΞD_s	0	0	0	0	$\sqrt{\frac{3}{2}}$	-1	$-\sqrt{\frac{3}{2}}$	$\sqrt{\frac{1}{2}}$	$-\sqrt{\frac{1}{3}}$	0	-1	$-\sqrt{\frac{25}{2}}$	0	0	-2	0
$\Sigma_c\bar{K}^*$	$\sqrt{\frac{1}{2}}$	$\sqrt{\frac{2}{3}}$	$\sqrt{3}$	$-\sqrt{12}$	0	$\sqrt{\frac{9}{2}}$	$-\sqrt{\frac{1}{3}}$	0	$\sqrt{6}$	2	0	$\frac{5}{3}$	$-\sqrt{\frac{2}{3}}$	$-\sqrt{2}$	0	-7

TABLE XIII. $C = 1$, $S = -1$, $I = 1/2$, $J = 1/2$ (continued).

	$\Xi_c'\rho$	$\Xi_c'\omega$	$\Sigma^* D^*$	$\Sigma_c^*\bar{K}^*$	$\Xi_c^*\rho$	$\Xi_c\eta'$	$\Xi_c^*\omega$	ΞD_s^*	$\Xi_c\phi$	$\Xi_c'\eta'$	$\Omega_c K^*$	$\Xi_c'\phi$	$\Xi^* D_s^*$	$\Omega_c^* K^*$	$\Xi_c^*\phi$
$\Xi_c\pi$	2	0	0	1	$\sqrt{8}$	0	0	0	0	0	$\sqrt{3}$	0	0	$\sqrt{6}$	0
$\Xi_c'\pi$	$-\sqrt{\frac{16}{3}}$	0	$\sqrt{\frac{4}{3}}$	$-\sqrt{\frac{1}{3}}$	$\sqrt{\frac{8}{3}}$	0	0	0	0	0	-2	0	0	$\sqrt{2}$	0
$\Lambda_c\bar{K}$	$\sqrt{\frac{3}{2}}$	$-\sqrt{\frac{1}{2}}$	0	$\sqrt{6}$	$\sqrt{3}$	0	-1	0	0	0	0	-1	0	0	$-\sqrt{2}$
$\Sigma_c\bar{K}$	$\sqrt{\frac{2}{3}}$	$\sqrt{2}$	$\sqrt{\frac{8}{3}}$	$\sqrt{6}$	$-\sqrt{\frac{1}{3}}$	0	-1	0	$\sqrt{3}$	0	0	2	0	0	$-\sqrt{2}$
ΛD	$-\sqrt{\frac{3}{8}}$	$\sqrt{\frac{1}{8}}$	$\sqrt{6}$	0	$\sqrt{3}$	$-\sqrt{\frac{1}{12}}$	-1	$\sqrt{\frac{1}{2}}$	0	$-\frac{1}{2}$	0	0	2	0	0
$\Xi_c\eta$	0	0	0	3	0	0	0	$-\sqrt{3}$	0	0	$\sqrt{3}$	0	0	$\sqrt{6}$	0
ΣD	$\sqrt{\frac{1}{24}}$	$\sqrt{\frac{1}{8}}$	$\sqrt{6}$	$\sqrt{\frac{8}{3}}$	$-\sqrt{\frac{1}{3}}$	$\sqrt{\frac{3}{4}}$	-1	$-\sqrt{\frac{25}{2}}$	0	$-\frac{1}{2}$	0	0	2	0	0
ΛD^*	$\sqrt{\frac{25}{8}}$	$-\sqrt{\frac{25}{24}}$	$-\sqrt{2}$	0	1	$-\frac{1}{2}$	$-\sqrt{\frac{1}{3}}$	$\sqrt{\frac{25}{6}}$	0	$\sqrt{\frac{1}{12}}$	0	0	$-\sqrt{\frac{4}{3}}$	0	0
$\Xi_c'\eta$	0	0	$\sqrt{\frac{4}{3}}$	$-\sqrt{3}$	0	0	0	$\frac{1}{3}$	0	0	-2	0	$-\sqrt{\frac{32}{9}}$	$\sqrt{2}$	0
$\Lambda_c\bar{K}^*$	$-\sqrt{2}$	$\sqrt{\frac{2}{3}}$	0	$-\sqrt{2}$	1	0	$-\sqrt{\frac{1}{3}}$	0	-1	0	0	$-\sqrt{\frac{4}{3}}$	0	0	$\sqrt{\frac{2}{3}}$
$\Omega_c K$	-2	$-\sqrt{\frac{4}{3}}$	0	0	$\sqrt{2}$	0	$\sqrt{\frac{2}{3}}$	$\sqrt{\frac{1}{3}}$	$\sqrt{2}$	0	$-\sqrt{\frac{16}{3}}$	$-\sqrt{\frac{8}{3}}$	$\sqrt{\frac{8}{3}}$	$\sqrt{\frac{8}{3}}$	$\sqrt{\frac{4}{3}}$
ΣD^*	$-\sqrt{\frac{25}{72}}$	$-\sqrt{\frac{25}{24}}$	$-\sqrt{2}$	$\sqrt{\frac{8}{9}}$	$-\frac{1}{3}$	$\frac{3}{2}$	$-\sqrt{\frac{1}{3}}$	$-\sqrt{\frac{169}{6}}$	0	$\sqrt{\frac{1}{12}}$	0	0	$-\sqrt{\frac{4}{3}}$	0	0
$\Xi_c\rho$	$\sqrt{\frac{4}{3}}$	2	0	$\sqrt{\frac{1}{3}}$	$-\sqrt{\frac{2}{3}}$	0	$-\sqrt{2}$	0	0	0	2	0	0	$-\sqrt{2}$	0
$\Xi_c\omega$	2	$\sqrt{\frac{4}{3}}$	0	1	$-\sqrt{2}$	0	$-\sqrt{\frac{2}{3}}$	0	0	0	$\sqrt{\frac{4}{3}}$	0	0	$-\sqrt{\frac{2}{3}}$	0
ΞD_s	0	0	-2	0	0	$\sqrt{\frac{1}{2}}$	0	$-\sqrt{\frac{16}{3}}$	$-\sqrt{\frac{9}{2}}$	$\sqrt{\frac{1}{6}}$	$\sqrt{\frac{1}{3}}$	$\sqrt{\frac{1}{6}}$	$-\sqrt{\frac{8}{3}}$	$-\sqrt{\frac{8}{3}}$	$-\sqrt{\frac{4}{3}}$
$\Sigma_c\bar{K}^*$	$-\sqrt{\frac{1}{18}}$	$-\sqrt{\frac{1}{6}}$	$\sqrt{\frac{8}{9}}$	$-\sqrt{2}$	$-\frac{1}{3}$	0	$-\sqrt{\frac{1}{3}}$	0	2	0	0	$\sqrt{\frac{49}{3}}$	0	0	$\sqrt{\frac{2}{3}}$

TABLE XIV. $C = 1$, $S = -1$, $I = 1/2$, $J = 1/2$ (continued).

	$\Xi_c'\rho$	$\Xi_c'\omega$	$\Sigma^* D^*$	$\Sigma_c^*\bar{K}^*$	$\Xi_c^*\rho$	$\Xi_c\eta'$	$\Xi_c^*\omega$	ΞD_s^*	$\Xi_c\phi$	$\Xi_c'\eta'$	$\Omega_c K^*$	$\Xi_c'\phi$	$\Xi^* D_s^*$	$\Omega_c^* K^*$	$\Xi_c^*\phi$
$\Xi_c'\rho$	$-\frac{10}{3}$	$-\sqrt{\frac{16}{3}}$	$\frac{2}{3}$	$-\frac{1}{3}$	$-\sqrt{\frac{2}{9}}$	0	$-\sqrt{\frac{2}{3}}$	0	0	0	$-\sqrt{\frac{49}{3}}$	0	0	$-\sqrt{\frac{2}{3}}$	0
$\Xi_c'\omega$	$-\sqrt{\frac{16}{3}}$	$-\frac{4}{3}$	$\sqrt{\frac{4}{3}}$	$-\sqrt{\frac{1}{3}}$	$-\sqrt{\frac{2}{3}}$	0	$-\sqrt{\frac{2}{9}}$	0	0	0	$-\frac{7}{3}$	0	0	$-\sqrt{\frac{2}{9}}$	0
$\Sigma^* D^*$	$\frac{2}{3}$	$\sqrt{\frac{4}{3}}$	-8	$-\frac{2}{3}$	$-\sqrt{\frac{2}{9}}$	0	$-\sqrt{\frac{2}{3}}$	$\sqrt{\frac{4}{3}}$	0	$\sqrt{\frac{8}{3}}$	0	0	$-\sqrt{\frac{128}{3}}$	0	0
$\Sigma_c^*\bar{K}^*$	$-\frac{1}{3}$	$-\sqrt{\frac{1}{3}}$	$-\frac{2}{3}$	-8	$-\sqrt{\frac{2}{9}}$	0	$-\sqrt{\frac{2}{3}}$	0	$-\sqrt{2}$	0	0	$\sqrt{\frac{2}{3}}$	0	0	$\sqrt{\frac{64}{3}}$
$\Xi_c^*\rho$	$-\sqrt{\frac{2}{9}}$	$-\sqrt{\frac{2}{3}}$	$-\sqrt{\frac{2}{9}}$	$-\sqrt{\frac{2}{9}}$	$-\frac{11}{3}$	0	$-\sqrt{\frac{25}{3}}$	0	0	0	$-\sqrt{\frac{2}{3}}$	0	0	$-\sqrt{\frac{64}{3}}$	0
$\Xi_c\eta'$	0	0	0	0	0	0	0	$\sqrt{\frac{3}{2}}$	0	0	0	0	0	0	0
$\Xi_c^*\omega$	$-\sqrt{\frac{2}{3}}$	$-\sqrt{\frac{2}{9}}$	$-\sqrt{\frac{2}{3}}$	$-\sqrt{\frac{2}{3}}$	$-\sqrt{\frac{25}{3}}$	0	$-\frac{5}{3}$	0	0	0	$-\sqrt{\frac{2}{9}}$	0	0	$-\frac{8}{3}$	0
ΞD_s^*	0	0	$\sqrt{\frac{4}{3}}$	0	0	$\sqrt{\frac{3}{2}}$	0	$-\frac{14}{3}$	$\sqrt{\frac{3}{2}}$	$-\sqrt{\frac{1}{18}}$	$-\frac{5}{3}$	$-\sqrt{\frac{25}{18}}$	$\sqrt{\frac{8}{9}}$	$-\sqrt{\frac{8}{9}}$	$-\frac{2}{3}$
$\Xi_c\phi$	0	0	0	$-\sqrt{2}$	0	0	0	$\sqrt{\frac{3}{2}}$	0	0	$-\sqrt{\frac{8}{3}}$	$-\sqrt{\frac{16}{3}}$	0	$\sqrt{\frac{4}{3}}$	$\sqrt{\frac{8}{3}}$
$\Xi_c'\eta'$	0	0	$\sqrt{\frac{8}{3}}$	0	0	0	0	$-\sqrt{\frac{1}{18}}$	0	0	0	0	$\frac{4}{3}$	0	0
$\Omega_c K^*$	$-\sqrt{\frac{49}{3}}$	$-\frac{7}{3}$	0	0	$-\sqrt{\frac{2}{3}}$	0	$-\sqrt{\frac{2}{9}}$	$-\frac{5}{3}$	$-\sqrt{\frac{8}{3}}$	0	$-\frac{14}{3}$	$\sqrt{\frac{2}{9}}$	$\sqrt{\frac{8}{9}}$	$-\sqrt{\frac{8}{9}}$	$\frac{2}{3}$
$\Xi_c'\phi$	0	0	0	$\sqrt{\frac{2}{3}}$	0	0	0	$-\sqrt{\frac{25}{18}}$	$-\sqrt{\frac{16}{3}}$	0	$\sqrt{\frac{2}{9}}$	$-\frac{8}{3}$	$-\frac{4}{3}$	$\frac{2}{3}$	$-\sqrt{\frac{8}{9}}$
$\Xi^* D_s^*$	0	0	$-\sqrt{\frac{128}{3}}$	0	0	0	0	$\sqrt{\frac{8}{9}}$	0	$\frac{4}{3}$	$\sqrt{\frac{8}{9}}$	$-\frac{4}{3}$	$-\frac{16}{3}$	$-\frac{2}{3}$	$\sqrt{\frac{8}{9}}$
$\Omega_c^* K^*$	$-\sqrt{\frac{2}{3}}$	$-\sqrt{\frac{2}{9}}$	0	0	$-\sqrt{\frac{64}{3}}$	0	$-\frac{8}{3}$	$-\sqrt{\frac{8}{9}}$	$\sqrt{\frac{4}{3}}$	0	$-\sqrt{\frac{8}{9}}$	$\frac{2}{3}$	$-\frac{2}{3}$	$-\frac{16}{3}$	$\sqrt{\frac{8}{9}}$
$\Xi_c^*\phi$	0	0	0	$\sqrt{\frac{64}{3}}$	0	0	0	$-\frac{2}{3}$	$\sqrt{\frac{8}{3}}$	0	$\frac{2}{3}$	$-\sqrt{\frac{8}{9}}$	$\sqrt{\frac{8}{9}}$	$\sqrt{\frac{8}{9}}$	$-\frac{10}{3}$

TABLE XV. $C = 1$, $S = -1$, $I = 1/2$, $J = 3/2$.

	$\Xi_c^*\pi$	$\Sigma_c^*\bar{K}$	ΛD^*	$\Lambda_c\bar{K}^*$	$\Xi_c^*\eta$	ΣD^*	$\Xi_c\rho$	$\Sigma^* D$	$\Xi_c\omega$	$\Omega_c^* K$	$\Sigma_c\bar{K}^*$	$\Xi_c'\rho$	$\Xi_c'\omega$
$\Xi_c^*\pi$	-2	$\sqrt{\frac{1}{2}}$	$-\sqrt{\frac{3}{2}}$	$-\sqrt{\frac{3}{2}}$	0	$\sqrt{\frac{1}{6}}$	-2	$\sqrt{\frac{1}{2}}$	0	$-\sqrt{3}$	$\sqrt{\frac{1}{6}}$	$-\sqrt{\frac{4}{3}}$	0
$\Sigma_c^*\bar{K}$	$\sqrt{\frac{1}{2}}$	-3	0	$-\sqrt{3}$	$\sqrt{\frac{9}{2}}$	$-\sqrt{\frac{4}{3}}$	$-\sqrt{\frac{1}{2}}$	1	$-\sqrt{\frac{3}{2}}$	0	$-\sqrt{3}$	$\sqrt{\frac{1}{6}}$	$\sqrt{\frac{1}{2}}$
ΛD^*	$-\sqrt{\frac{3}{2}}$	0	-1	2	$\sqrt{\frac{1}{6}}$	-1	$\sqrt{\frac{3}{2}}$	$-\sqrt{3}$	$-\sqrt{\frac{1}{2}}$	0	0	$\sqrt{\frac{1}{2}}$	$-\sqrt{\frac{1}{6}}$
$\Lambda_c\bar{K}^*$	$-\sqrt{\frac{3}{2}}$	$-\sqrt{3}$	2	-1	$\sqrt{\frac{3}{2}}$	0	$\sqrt{\frac{3}{2}}$	0	$-\sqrt{\frac{1}{2}}$	0	-1	$\sqrt{\frac{1}{2}}$	$-\sqrt{\frac{1}{6}}$
$\Xi_c^*\eta$	0	$\sqrt{\frac{9}{2}}$	$\sqrt{\frac{1}{6}}$	$\sqrt{\frac{3}{2}}$	0	$\sqrt{\frac{1}{6}}$	0	$\sqrt{\frac{1}{2}}$	0	$-\sqrt{3}$	$\sqrt{\frac{3}{2}}$	0	0
ΣD^*	$\sqrt{\frac{1}{6}}$	$-\sqrt{\frac{4}{3}}$	-1	0	$\sqrt{\frac{1}{6}}$	-1	$\sqrt{\frac{3}{2}}$	$-\sqrt{3}$	$\sqrt{\frac{9}{2}}$	0	$\frac{2}{3}$	$-\sqrt{\frac{1}{18}}$	$-\sqrt{\frac{1}{6}}$
$\Xi_c\rho$	-2	$-\sqrt{\frac{1}{2}}$	$\sqrt{\frac{3}{2}}$	$\sqrt{\frac{3}{2}}$	0	$\sqrt{\frac{3}{2}}$	-2	0	0	$-\sqrt{3}$	$\sqrt{\frac{1}{6}}$	$-\sqrt{\frac{1}{3}}$	-1
$\Sigma^* D$	$\sqrt{\frac{1}{2}}$	1	$-\sqrt{3}$	0	$\sqrt{\frac{1}{2}}$	$-\sqrt{3}$	0	-3	0	0	$-\sqrt{\frac{4}{3}}$	$-\sqrt{\frac{2}{3}}$	$-\sqrt{2}$
$\Xi_c\omega$	0	$-\sqrt{\frac{3}{2}}$	$-\sqrt{\frac{1}{2}}$	$-\sqrt{\frac{1}{2}}$	0	$\sqrt{\frac{9}{2}}$	0	0	0	-1	$\sqrt{\frac{1}{2}}$	-1	$-\sqrt{\frac{1}{3}}$
$\Omega_c^* K$	$-\sqrt{3}$	0	0	0	$-\sqrt{3}$	0	$-\sqrt{3}$	0	-1	-2	0	-1	$-\sqrt{\frac{1}{3}}$
$\Sigma_c\bar{K}^*$	$\sqrt{\frac{1}{6}}$	$-\sqrt{3}$	0	-1	$\sqrt{\frac{3}{2}}$	$\frac{2}{3}$	$\sqrt{\frac{1}{6}}$	$-\sqrt{\frac{4}{3}}$	$\sqrt{\frac{1}{2}}$	0	-1	$\sqrt{\frac{25}{18}}$	$\sqrt{\frac{25}{6}}$
$\Xi_c'\rho$	$-\sqrt{\frac{4}{3}}$	$\sqrt{\frac{1}{6}}$	$\sqrt{\frac{1}{2}}$	$\sqrt{\frac{1}{2}}$	0	$-\sqrt{\frac{1}{18}}$	$-\sqrt{\frac{1}{3}}$	$-\sqrt{\frac{2}{3}}$	-1	-1	$\sqrt{\frac{25}{18}}$	$-\frac{4}{3}$	$\sqrt{\frac{4}{3}}$
$\Xi_c'\omega$	0	$\sqrt{\frac{1}{2}}$	$-\sqrt{\frac{1}{6}}$	$-\sqrt{\frac{1}{6}}$	0	$-\sqrt{\frac{1}{6}}$	-1	$-\sqrt{2}$	$-\sqrt{\frac{1}{3}}$	$-\sqrt{\frac{1}{3}}$	$\sqrt{\frac{25}{6}}$	$\sqrt{\frac{4}{3}}$	$\frac{2}{3}$

TABLE XVI. $C = 1$, $S = -1$, $I = 1/2$, $J = 3/2$ (continued).

	$\Sigma^* D^*$	$\Sigma_c^* \bar{K}^*$	$\Xi_c^* \rho$	$\Xi_c^* \omega$	ΞD_s^*	$\Xi_c \phi$	$\Xi^* D_s$	$\Omega_c K^*$	$\Xi_c' \phi$	$\Xi_c^* \eta'$	$\Xi^* D_s^*$	$\Omega_c^* K^*$	$\Xi_c^* \phi$
$\Xi_c^* \pi$	$\sqrt{\frac{5}{6}}$	$\sqrt{\frac{5}{6}}$	$-\sqrt{\frac{20}{3}}$	0	0	0	0	-1	0	0	0	$-\sqrt{5}$	0
$\Sigma_c^* \bar{K}$	$\sqrt{\frac{5}{3}}$	$-\sqrt{15}$	$\sqrt{\frac{5}{6}}$	$\sqrt{\frac{5}{2}}$	0	$-\sqrt{3}$	0	0	1	0	0	0	$\sqrt{5}$
ΛD^*	$-\sqrt{5}$	0	$\sqrt{\frac{5}{2}}$	$-\sqrt{\frac{5}{6}}$	$\sqrt{\frac{2}{3}}$	0	$-\sqrt{2}$	0	0	$\sqrt{\frac{1}{3}}$	$-\sqrt{\frac{10}{3}}$	0	0
$\Lambda_c \bar{K}^*$	0	$-\sqrt{5}$	$\sqrt{\frac{5}{2}}$	$-\sqrt{\frac{5}{6}}$	0	-1	0	0	$\sqrt{\frac{1}{3}}$	0	0	0	$\sqrt{\frac{5}{3}}$
$\Xi_c^* \eta$	$\sqrt{\frac{5}{6}}$	$\sqrt{\frac{15}{2}}$	0	0	$\frac{2}{3}$	0	$-\sqrt{\frac{4}{3}}$	-1	0	0	$-\sqrt{\frac{20}{9}}$	$-\sqrt{5}$	0
ΣD^*	$-\sqrt{5}$	$\sqrt{\frac{20}{9}}$	$-\sqrt{\frac{5}{18}}$	$-\sqrt{\frac{5}{6}}$	$\sqrt{\frac{2}{3}}$	0	$-\sqrt{2}$	0	0	$\sqrt{\frac{1}{3}}$	$-\sqrt{\frac{10}{3}}$	0	0
$\Xi_c \rho$	0	$\sqrt{\frac{5}{6}}$	$-\sqrt{\frac{5}{3}}$	$-\sqrt{5}$	0	0	0	-1	0	0	0	$-\sqrt{5}$	0
$\Sigma^* D$	$-\sqrt{15}$	$\sqrt{\frac{5}{3}}$	$\sqrt{\frac{5}{6}}$	$\sqrt{\frac{5}{2}}$	$\sqrt{2}$	0	$-\sqrt{6}$	0	0	1	$-\sqrt{10}$	0	0
$\Xi_c \omega$	0	$\sqrt{\frac{5}{2}}$	$-\sqrt{5}$	$-\sqrt{\frac{5}{3}}$	0	0	0	$-\sqrt{\frac{1}{3}}$	0	0	0	$-\sqrt{\frac{5}{3}}$	0
$\Omega_c^* K$	0	0	$-\sqrt{5}$	$-\sqrt{\frac{5}{3}}$	$\sqrt{\frac{4}{3}}$	$-\sqrt{2}$	1	$-\sqrt{\frac{4}{3}}$	$-\sqrt{\frac{2}{3}}$	0	$\sqrt{\frac{5}{3}}$	$-\sqrt{\frac{20}{3}}$	$-\sqrt{\frac{10}{3}}$
$\Sigma_c \bar{K}^*$	$\sqrt{\frac{20}{9}}$	$-\sqrt{5}$	$-\sqrt{\frac{5}{18}}$	$-\sqrt{\frac{5}{6}}$	0	-1	0	0	$\sqrt{\frac{1}{3}}$	0	0	0	$\sqrt{\frac{5}{3}}$
$\Xi_c' \rho$	$\sqrt{\frac{10}{9}}$	$-\sqrt{\frac{5}{18}}$	$-\sqrt{\frac{5}{9}}$	$-\sqrt{\frac{5}{3}}$	0	0	0	$-\sqrt{\frac{1}{3}}$	0	0	0	$-\sqrt{\frac{5}{3}}$	0
$\Xi_c' \omega$	$\sqrt{\frac{10}{3}}$	$-\sqrt{\frac{5}{6}}$	$-\sqrt{\frac{5}{3}}$	$-\sqrt{\frac{5}{9}}$	0	0	0	$-\frac{1}{3}$	0	0	0	$-\sqrt{\frac{5}{9}}$	0

TABLE XVII. $C = 1$, $S = -1$, $I = 1/2$, $J = 3/2$. (continued).

	$\Sigma^* D^*$	$\Sigma_c^* \bar{K}^*$	$\Xi_c^* \rho$	$\Xi_c^* \omega$	ΞD_s^*	$\Xi_c \phi$	$\Xi^* D_s$	$\Omega_c K^*$	$\Xi_c' \phi$	$\Xi_c^* \eta'$	$\Xi^* D_s^*$	$\Omega_c^* K^*$	$\Xi_c^* \phi$
$\Sigma^* D^*$	-5	$\frac{1}{3}$	$\sqrt{\frac{1}{18}}$	$\sqrt{\frac{1}{6}}$	$\sqrt{\frac{10}{3}}$	0	$-\sqrt{10}$	0	0	$\sqrt{\frac{5}{3}}$	$-\sqrt{\frac{50}{3}}$	0	0
$\Sigma_c^* \bar{K}^*$	$\frac{1}{3}$	-5	$\sqrt{\frac{1}{18}}$	$\sqrt{\frac{1}{6}}$	0	$-\sqrt{5}$	0	0	$\sqrt{\frac{5}{3}}$	0	0	0	$\sqrt{\frac{25}{3}}$
$\Xi_c^* \rho$	$\sqrt{\frac{1}{18}}$	$\sqrt{\frac{1}{18}}$	$-\frac{8}{3}$	$-\sqrt{\frac{4}{3}}$	0	0	0	$-\sqrt{\frac{5}{3}}$	0	0	0	$-\sqrt{\frac{25}{3}}$	0
$\Xi_c^* \omega$	$\sqrt{\frac{1}{6}}$	$\sqrt{\frac{1}{6}}$	$-\sqrt{\frac{4}{3}}$	$-\frac{2}{3}$	0	0	0	$-\sqrt{\frac{5}{9}}$	0	0	0	$-\frac{5}{3}$	0
ΞD_s^*	$\sqrt{\frac{10}{3}}$	0	0	0	$-\frac{2}{3}$	$-\sqrt{6}$	$\sqrt{\frac{4}{3}}$	$-\frac{2}{3}$	$-\sqrt{\frac{2}{9}}$	$-\sqrt{\frac{2}{9}}$	$\sqrt{\frac{20}{9}}$	$-\sqrt{\frac{20}{9}}$	$-\sqrt{\frac{10}{9}}$
$\Xi_c \phi$	0	$-\sqrt{5}$	0	0	$-\sqrt{6}$	0	0	$\sqrt{\frac{2}{3}}$	$\sqrt{\frac{4}{3}}$	0	0	$\sqrt{\frac{10}{3}}$	$\sqrt{\frac{20}{3}}$
$\Xi^* D_s$	$-\sqrt{10}$	0	0	0	$\sqrt{\frac{4}{3}}$	0	-2	$-\sqrt{\frac{4}{3}}$	$\sqrt{\frac{8}{3}}$	$\sqrt{\frac{2}{3}}$	$-\sqrt{\frac{20}{3}}$	$\sqrt{5}$	$-\sqrt{\frac{10}{3}}$
$\Omega_c K^*$	0	0	$-\sqrt{\frac{5}{3}}$	$-\sqrt{\frac{5}{9}}$	$-\frac{2}{3}$	$\sqrt{\frac{2}{3}}$	$-\sqrt{\frac{4}{3}}$	$-\frac{2}{3}$	$-\sqrt{\frac{50}{9}}$	0	$\sqrt{\frac{20}{9}}$	$-\sqrt{\frac{20}{9}}$	$\sqrt{\frac{10}{9}}$
$\Xi_c' \phi$	0	$\sqrt{\frac{5}{3}}$	0	0	$-\sqrt{\frac{2}{9}}$	$\sqrt{\frac{4}{3}}$	$\sqrt{\frac{8}{3}}$	$-\sqrt{\frac{50}{9}}$	$\frac{4}{3}$	0	$-\sqrt{\frac{40}{9}}$	$\sqrt{\frac{10}{9}}$	$-\sqrt{\frac{20}{9}}$
$\Xi_c^* \eta'$	$\sqrt{\frac{5}{3}}$	0	0	0	$-\sqrt{\frac{2}{9}}$	0	$\sqrt{\frac{2}{3}}$	0	0	0	$\sqrt{\frac{10}{9}}$	0	0
$\Xi^* D_s^*$	$-\sqrt{\frac{50}{3}}$	0	0	0	$\sqrt{\frac{20}{9}}$	0	$-\sqrt{\frac{20}{3}}$	$\sqrt{\frac{20}{9}}$	$-\sqrt{\frac{40}{9}}$	$\sqrt{\frac{10}{9}}$	$-\frac{10}{3}$	$\frac{1}{3}$	$-\sqrt{\frac{2}{9}}$
$\Omega_c^* K^*$	0	0	$-\sqrt{\frac{25}{3}}$	$-\frac{5}{3}$	$-\sqrt{\frac{20}{9}}$	$\sqrt{\frac{10}{3}}$	$\sqrt{\frac{5}{3}}$	$-\sqrt{\frac{20}{9}}$	$\sqrt{\frac{10}{9}}$	0	$\frac{1}{3}$	$-\frac{10}{3}$	$-\sqrt{\frac{2}{9}}$
$\Xi_c^* \phi$	0	$\sqrt{\frac{25}{3}}$	0	0	$-\sqrt{\frac{10}{9}}$	$\sqrt{\frac{20}{3}}$	$-\sqrt{\frac{10}{3}}$	$\sqrt{\frac{10}{9}}$	$-\sqrt{\frac{20}{9}}$	0	$-\sqrt{\frac{2}{9}}$	$-\sqrt{\frac{2}{9}}$	$-\frac{4}{3}$

TABLE XVIII. $C = 1$, $S = -2$, $I = 0$, $J = 1/2$.

	$\Xi_c\bar{K}$	$\Xi_c'\bar{K}$	ΞD	$\Omega_c\eta$	ΞD^*	$\Xi_c\bar{K}^*$	$\Xi_c'\bar{K}^*$	$\Omega_c\omega$	$\Xi_c^*\bar{K}^*$	$\Xi^* D^*$	$\Omega_c^*\omega$	$\Omega_c\eta'$	$\Omega_c\phi$	ΩD_s^*	$\Omega_c^*\phi$
$\Xi_c\bar{K}$	-1	0	$\sqrt{\frac{3}{2}}$	0	$\sqrt{\frac{9}{2}}$	0	3	$-\sqrt{2}$	$\sqrt{18}$	0	-2	0	-2	0	$-\sqrt{8}$
$\Xi_c'\bar{K}$	0	-1	$\sqrt{\frac{1}{2}}$	$\sqrt{6}$	$-\sqrt{\frac{1}{6}}$	3	$-\sqrt{\frac{4}{3}}$	$\sqrt{\frac{8}{3}}$	$\sqrt{\frac{2}{3}}$	$\sqrt{\frac{16}{3}}$	$-\sqrt{\frac{4}{3}}$	0	$\sqrt{\frac{16}{3}}$	0	$-\sqrt{\frac{8}{3}}$
ΞD	$\sqrt{\frac{3}{2}}$	$\sqrt{\frac{1}{2}}$	-2	$-\sqrt{\frac{1}{3}}$	$\sqrt{\frac{4}{3}}$	$\sqrt{\frac{9}{2}}$	$-\sqrt{\frac{1}{6}}$	$\sqrt{\frac{1}{3}}$	$\sqrt{\frac{4}{3}}$	$\sqrt{\frac{32}{3}}$	$-\sqrt{\frac{8}{3}}$	$-\sqrt{\frac{2}{3}}$	0	4	0
$\Omega_c\eta$	0	$\sqrt{6}$	$-\sqrt{\frac{1}{3}}$	0	$\frac{1}{3}$	$-\sqrt{6}$	$\sqrt{8}$	0	-2	$\sqrt{\frac{8}{9}}$	0	0	0	$-\sqrt{\frac{16}{3}}$	0
ΞD^*	$\sqrt{\frac{9}{2}}$	$-\sqrt{\frac{1}{6}}$	$\sqrt{\frac{4}{3}}$	$\frac{1}{3}$	$-\frac{2}{3}$	$-\sqrt{\frac{3}{2}}$	$\sqrt{\frac{25}{18}}$	$-\frac{5}{3}$	$\frac{2}{3}$	$-\sqrt{\frac{32}{9}}$	$-\sqrt{\frac{8}{9}}$	$\sqrt{\frac{2}{9}}$	0	$-\sqrt{\frac{16}{3}}$	0
$\Xi_c\bar{K}^*$	0	3	$\sqrt{\frac{9}{2}}$	$-\sqrt{6}$	$-\sqrt{\frac{3}{2}}$	-1	$\sqrt{\frac{4}{3}}$	$\sqrt{\frac{8}{3}}$	$-\sqrt{\frac{2}{3}}$	0	$-\sqrt{\frac{4}{3}}$	0	$-\sqrt{\frac{16}{3}}$	0	$\sqrt{\frac{8}{3}}$
$\Xi_c'\bar{K}^*$	3	$-\sqrt{\frac{4}{3}}$	$-\sqrt{\frac{1}{6}}$	$\sqrt{8}$	$\sqrt{\frac{25}{18}}$	$\sqrt{\frac{4}{3}}$	-5	$-\sqrt{\frac{2}{9}}$	$-\sqrt{2}$	$\frac{4}{3}$	$-\frac{2}{3}$	0	$\frac{14}{3}$	0	$\sqrt{\frac{8}{9}}$
$\Omega_c\omega$	$-\sqrt{2}$	$\sqrt{\frac{8}{3}}$	$\sqrt{\frac{1}{3}}$	0	$-\frac{5}{3}$	$\sqrt{\frac{8}{3}}$	$-\sqrt{\frac{2}{9}}$	0	$-\frac{2}{3}$	$\sqrt{\frac{8}{9}}$	0	0	0	0	0
$\Xi_c^*\bar{K}^*$	$\sqrt{18}$	$\sqrt{\frac{2}{3}}$	$\sqrt{\frac{4}{3}}$	-2	$\frac{2}{3}$	$-\sqrt{\frac{2}{3}}$	$-\sqrt{2}$	$-\frac{2}{3}$	-6	$-\sqrt{\frac{8}{9}}$	$-\sqrt{\frac{8}{9}}$	0	$\sqrt{\frac{8}{9}}$	0	$\frac{16}{3}$
$\Xi^* D^*$	0	$\sqrt{\frac{16}{3}}$	$\sqrt{\frac{32}{3}}$	$\sqrt{\frac{8}{9}}$	$-\sqrt{\frac{32}{9}}$	0	$\frac{4}{3}$	$\sqrt{\frac{8}{9}}$	$-\sqrt{\frac{8}{9}}$	$-\frac{16}{3}$	$-\frac{2}{3}$	$\frac{4}{3}$	0	$-\sqrt{\frac{128}{3}}$	0
$\Omega_c^*\omega$	-2	$-\sqrt{\frac{4}{3}}$	$-\sqrt{\frac{8}{3}}$	0	$-\sqrt{\frac{8}{9}}$	$-\sqrt{\frac{4}{3}}$	$-\frac{2}{3}$	0	$-\sqrt{\frac{8}{9}}$	$-\frac{2}{3}$	0	0	0	0	0
$\Omega_c\eta'$	0	0	$-\sqrt{\frac{2}{3}}$	0	$\sqrt{\frac{2}{9}}$	0	0	0	0	$\frac{4}{3}$	0	0	0	$\sqrt{\frac{8}{3}}$	0
$\Omega_c\phi$	-2	$\sqrt{\frac{16}{3}}$	0	0	0	$-\sqrt{\frac{16}{3}}$	$\frac{14}{3}$	0	$\sqrt{\frac{8}{9}}$	0	0	0	$-\frac{16}{3}$	$-\sqrt{\frac{8}{3}}$	$-\sqrt{\frac{32}{9}}$
ΩD_s^*	0	0	4	$-\sqrt{\frac{16}{3}}$	$-\sqrt{\frac{16}{3}}$	0	0	0	0	$-\sqrt{\frac{128}{3}}$	0	$\sqrt{\frac{8}{3}}$	$-\sqrt{\frac{8}{3}}$	-8	$\sqrt{\frac{4}{3}}$
$\Omega_c^*\phi$	$-\sqrt{8}$	$-\sqrt{\frac{8}{3}}$	0	0	0	$\sqrt{\frac{8}{3}}$	$\sqrt{\frac{8}{9}}$	0	$\frac{16}{3}$	0	0	0	$-\sqrt{\frac{32}{9}}$	$\sqrt{\frac{4}{3}}$	$-\frac{20}{3}$

TABLE XIX. $C = 1$, $S = -2$, $I = 0$, $J = 3/2$.

	$\Xi_c^*\bar{K}$	$\Omega_c^*\eta$	ΞD^*	$\Xi_c\bar{K}^*$	$\Xi^* D$	$\Xi_c'\bar{K}^*$	$\Omega_c\omega$	$\Xi_c^*\bar{K}^*$	$\Xi^* D^*$	$\Omega_c^*\omega$	ΩD_s	$\Omega_c\phi$	$\Omega_c^*\eta'$	ΩD_s^*	$\Omega_c^*\phi$
$\Xi_c^*\bar{K}$	-1	$\sqrt{6}$	$-\sqrt{\frac{2}{3}}$	-3	$\sqrt{2}$	$-\sqrt{\frac{1}{3}}$	$\sqrt{\frac{2}{3}}$	$-\sqrt{\frac{5}{3}}$	$\sqrt{\frac{10}{3}}$	$\sqrt{\frac{10}{3}}$	0	$\sqrt{\frac{4}{3}}$	0	0	$\sqrt{\frac{20}{3}}$
$\Omega_c^*\eta$	$\sqrt{6}$	0	$\frac{2}{3}$	$\sqrt{6}$	$\sqrt{\frac{1}{3}}$	$\sqrt{2}$	0	$\sqrt{10}$	$\sqrt{\frac{5}{9}}$	0	$-\sqrt{2}$	0	0	$-\sqrt{\frac{10}{3}}$	0
ΞD^*	$-\sqrt{\frac{2}{3}}$	$\frac{2}{3}$	$-\frac{8}{3}$	$\sqrt{6}$	$-\sqrt{\frac{16}{3}}$	$\sqrt{\frac{2}{9}}$	$-\frac{2}{3}$	$\sqrt{\frac{10}{9}}$	$-\sqrt{\frac{80}{9}}$	$-\sqrt{\frac{20}{9}}$	$-\sqrt{8}$	0	$\sqrt{\frac{8}{9}}$	$-\sqrt{\frac{40}{3}}$	0
$\Xi_c\bar{K}^*$	-3	$\sqrt{6}$	$\sqrt{6}$	-1	0	$-\sqrt{\frac{1}{3}}$	$-\sqrt{\frac{2}{3}}$	$-\sqrt{\frac{5}{3}}$	0	$-\sqrt{\frac{10}{3}}$	0	$\sqrt{\frac{4}{3}}$	0	0	$\sqrt{\frac{20}{3}}$
$\Xi^* D$	$\sqrt{2}$	$\sqrt{\frac{1}{3}}$	$-\sqrt{\frac{16}{3}}$	0	-2	$-\sqrt{\frac{8}{3}}$	$-\sqrt{\frac{4}{3}}$	$\sqrt{\frac{10}{3}}$	$-\sqrt{\frac{20}{3}}$	$\sqrt{\frac{5}{3}}$	$-\sqrt{6}$	0	$\sqrt{\frac{2}{3}}$	$-\sqrt{10}$	0
$\Xi_c'\bar{K}^*$	$-\sqrt{\frac{1}{3}}$	$\sqrt{2}$	$\sqrt{\frac{2}{9}}$	$-\sqrt{\frac{1}{3}}$	$-\sqrt{\frac{8}{3}}$	1	$\sqrt{\frac{50}{9}}$	$-\sqrt{5}$	$\sqrt{\frac{40}{9}}$	$-\sqrt{\frac{10}{9}}$	0	$\frac{2}{3}$	0	0	$\sqrt{\frac{20}{9}}$
$\Omega_c\omega$	$\sqrt{\frac{2}{3}}$	0	$-\frac{2}{3}$	$-\sqrt{\frac{2}{3}}$	$-\sqrt{\frac{4}{3}}$	$\sqrt{\frac{50}{9}}$	0	$-\sqrt{\frac{10}{9}}$	$\sqrt{\frac{20}{9}}$	0	0	0	0	0	0
$\Xi_c^*\bar{K}^*$	$-\sqrt{\frac{5}{3}}$	$\sqrt{10}$	$\sqrt{\frac{10}{9}}$	$-\sqrt{\frac{5}{3}}$	$\sqrt{\frac{10}{3}}$	$-\sqrt{5}$	$-\sqrt{\frac{10}{9}}$	-3	$\sqrt{\frac{2}{9}}$	$\sqrt{\frac{2}{9}}$	0	$\sqrt{\frac{20}{9}}$	0	0	$\frac{10}{3}$
$\Xi^* D^*$	$\sqrt{\frac{10}{3}}$	$\sqrt{\frac{5}{9}}$	$-\sqrt{\frac{80}{9}}$	0	$-\sqrt{\frac{20}{3}}$	$\sqrt{\frac{40}{9}}$	$\sqrt{\frac{20}{9}}$	$\sqrt{\frac{2}{9}}$	$-\frac{10}{3}$	$\frac{1}{3}$	$-\sqrt{10}$	0	$\sqrt{\frac{10}{9}}$	$-\sqrt{\frac{50}{3}}$	0
$\Omega_c^*\omega$	$\sqrt{\frac{10}{3}}$	0	$-\sqrt{\frac{20}{9}}$	$-\sqrt{\frac{10}{3}}$	$\sqrt{\frac{5}{3}}$	$-\sqrt{\frac{10}{9}}$	0	$\sqrt{\frac{2}{9}}$	$\frac{1}{3}$	0	0	0	0	0	0
ΩD_s	0	$-\sqrt{2}$	$-\sqrt{8}$	0	$-\sqrt{6}$	0	0	0	$-\sqrt{10}$	0	-3	2	1	$-\sqrt{15}$	$-\sqrt{5}$
$\Omega_c\phi$	$\sqrt{\frac{4}{3}}$	0	0	$\sqrt{\frac{4}{3}}$	0	$\frac{2}{3}$	0	$\sqrt{\frac{20}{9}}$	0	0	2	$\frac{8}{3}$	0	$-\sqrt{\frac{20}{3}}$	$-\sqrt{\frac{80}{9}}$
$\Omega_c^*\eta'$	0	0	$\sqrt{\frac{8}{9}}$	0	$\sqrt{\frac{2}{3}}$	0	0	0	$\sqrt{\frac{10}{9}}$	0	1	0	0	$\sqrt{\frac{5}{3}}$	0
ΩD_s^*	0	$-\sqrt{\frac{10}{3}}$	$-\sqrt{\frac{40}{3}}$	0	$-\sqrt{10}$	0	0	0	$-\sqrt{\frac{50}{3}}$	0	$-\sqrt{15}$	$-\sqrt{\frac{20}{3}}$	$\sqrt{\frac{5}{3}}$	-5	$-\sqrt{\frac{1}{3}}$
$\Omega_c^*\phi$	$\sqrt{\frac{20}{3}}$	0	0	$\sqrt{\frac{20}{3}}$	0	$\sqrt{\frac{20}{9}}$	0	$\frac{10}{3}$	0	0	$-\sqrt{5}$	$-\sqrt{\frac{80}{9}}$	0	$-\sqrt{\frac{1}{3}}$	$-\frac{8}{3}$

TABLE XX. $C = 2$, $S = 0$, $I = 1/2$, $J = 1/2$.

	$\Xi_{cc}\pi$	$\Omega_{cc}K$	$\Xi_{cc}\eta$	$\Lambda_c D$	$\Xi_{cc}\rho$	$\Lambda_c D^*$	$\Xi_{cc}\omega$	$\Sigma_c D$	$\Xi_c D_s$	$\Omega_{cc}K^*$	$\Sigma_c D^*$	$\Xi_{cc}\eta'$	$\Xi^*_{cc}\rho$	$\Sigma^*_c D^*$	$\Xi^*_{cc}\omega$	$\Xi_{cc}\phi$	$\Xi'_c D_s$	$\Xi_c D^*_s$	$\Xi'_c D^*_s$	$\Xi^*_c D^*_s$	$\Xi^*_{cc}\phi$	$\Omega^*_{cc}K^*$
$\Xi_{cc}\pi$	-2	$-\sqrt{\frac{3}{2}}$	0	$\frac{3}{2}$	$\sqrt{\frac{4}{3}}$	$\sqrt{\frac{3}{4}}$	0	$\frac{1}{2}$	0	$\sqrt{\frac{1}{2}}$	$\sqrt{\frac{25}{12}}$	0	$\sqrt{\frac{32}{3}}$	$\sqrt{\frac{2}{3}}$	0	0	0	0	0	0	0	2
$\Omega_{cc}K$	$-\sqrt{\frac{3}{2}}$	-1	$-\sqrt{\frac{3}{2}}$	0	$\sqrt{\frac{1}{2}}$	0	$\sqrt{\frac{1}{6}}$	0	$-\sqrt{\frac{3}{2}}$	$\sqrt{\frac{1}{3}}$	0	0	2	0	$\sqrt{\frac{4}{3}}$	$\sqrt{\frac{1}{3}}$	$\sqrt{\frac{1}{2}}$	$-\sqrt{\frac{1}{2}}$	$\sqrt{\frac{25}{6}}$	$\sqrt{\frac{4}{3}}$	$\sqrt{\frac{8}{3}}$	$\sqrt{\frac{8}{3}}$
$\Xi_{cc}\eta$	0	$-\sqrt{\frac{3}{2}}$	0	$-\frac{1}{2}$	0	$-\sqrt{\frac{1}{12}}$	0	$\frac{1}{2}$	-1	$\sqrt{\frac{1}{2}}$	$\sqrt{\frac{25}{12}}$	0	0	$\sqrt{\frac{2}{3}}$	0	0	$-\sqrt{\frac{1}{3}}$	$-\sqrt{\frac{1}{3}}$	$-\frac{5}{3}$	$-\sqrt{\frac{8}{9}}$	0	2
$\Lambda_c D$	$\frac{3}{2}$	0	$-\frac{1}{2}$	0	$\sqrt{\frac{3}{4}}$	$\sqrt{3}$	$-\frac{1}{2}$	0	1	0	$\sqrt{3}$	$-\sqrt{\frac{1}{2}}$	$\sqrt{6}$	$\sqrt{6}$	$-\sqrt{2}$	0	0	0	1	$\sqrt{2}$	0	0
$\Xi_{cc}\rho$	$\sqrt{\frac{4}{3}}$	$\sqrt{\frac{1}{2}}$	0	$\sqrt{\frac{3}{4}}$	$-\frac{4}{3}$	$\frac{1}{2}$	$\sqrt{\frac{4}{3}}$	$\sqrt{\frac{25}{12}}$	0	$-\sqrt{\frac{1}{6}}$	$-\frac{7}{6}$	0	$-\sqrt{\frac{8}{9}}$	$\sqrt{\frac{2}{9}}$	$-\sqrt{\frac{8}{3}}$	0	0	0	0	0	0	$-\sqrt{\frac{4}{3}}$
$\Lambda_c D^*$	$\sqrt{\frac{3}{4}}$	0	$-\sqrt{\frac{1}{12}}$	$\sqrt{3}$	$\frac{1}{2}$	-2	$-\sqrt{\frac{1}{12}}$	$\sqrt{3}$	0	0	2	$-\sqrt{\frac{1}{6}}$	$\sqrt{2}$	$-\sqrt{2}$	$-\sqrt{\frac{2}{3}}$	0	1	1	$\sqrt{\frac{4}{3}}$	$-\sqrt{\frac{2}{3}}$	0	0
$\Xi_{cc}\omega$	0	$\sqrt{\frac{1}{6}}$	0	$-\frac{1}{2}$	$\sqrt{\frac{4}{3}}$	$-\sqrt{\frac{1}{12}}$	$\frac{2}{3}$	$\frac{5}{2}$	0	$-\sqrt{\frac{1}{18}}$	$-\sqrt{\frac{49}{12}}$	0	$-\sqrt{\frac{8}{3}}$	$\sqrt{\frac{2}{3}}$	$-\sqrt{\frac{8}{9}}$	0	0	0	0	0	0	$-\frac{2}{3}$
$\Sigma_c D$	$\frac{1}{2}$	0	$\frac{1}{2}$	0	$\sqrt{\frac{25}{12}}$	$\sqrt{3}$	$\frac{5}{2}$	-2	0	0	$-\sqrt{\frac{49}{3}}$	$\sqrt{\frac{1}{2}}$	$-\sqrt{\frac{2}{3}}$	$\sqrt{\frac{50}{3}}$	$-\sqrt{2}$	0	$-\sqrt{3}$	$-\sqrt{3}$	-2	$\sqrt{2}$	0	0
$\Xi_c D_s$	0	$-\sqrt{\frac{3}{2}}$	-1	1	0	0	0	0	0	$-\sqrt{\frac{1}{2}}$	$-\sqrt{3}$	$\sqrt{\frac{1}{2}}$	0	$-\sqrt{6}$	0	$-\sqrt{\frac{1}{2}}$	0	$\sqrt{3}$	-1	$-\sqrt{2}$	-2	-2
$\Omega_{cc}K^*$	$\sqrt{\frac{1}{2}}$	$\sqrt{\frac{1}{3}}$	$\sqrt{\frac{1}{2}}$	0	$-\sqrt{\frac{1}{6}}$	0	$-\sqrt{\frac{1}{18}}$	0	$-\sqrt{\frac{1}{2}}$	$-\frac{1}{3}$	0	0	$-\sqrt{\frac{4}{3}}$	0	$-\frac{2}{3}$	$-\frac{5}{3}$	$\sqrt{\frac{25}{6}}$	$-\sqrt{\frac{1}{6}}$	$-\sqrt{\frac{49}{18}}$	$\frac{2}{3}$	$\sqrt{\frac{8}{9}}$	$-\sqrt{\frac{8}{9}}$
$\Sigma_c D^*$	$\sqrt{\frac{25}{12}}$	0	$\sqrt{\frac{25}{12}}$	$\sqrt{3}$	$-\frac{7}{6}$	2	$-\sqrt{\frac{49}{12}}$	$-\sqrt{\frac{49}{3}}$	$-\sqrt{3}$	0	$-\frac{16}{3}$	$\sqrt{\frac{25}{6}}$	$-\sqrt{\frac{2}{9}}$	$-\sqrt{\frac{2}{9}}$	$-\sqrt{\frac{2}{3}}$	0	-2	-2	$-\sqrt{\frac{49}{3}}$	$-\sqrt{\frac{2}{3}}$	0	0
$\Xi_{cc}\eta'$	0	0	0	$-\sqrt{\frac{1}{2}}$	0	$-\sqrt{\frac{1}{6}}$	0	$\sqrt{\frac{1}{2}}$	$\sqrt{\frac{1}{2}}$	0	$\sqrt{\frac{25}{6}}$	0	0	$\sqrt{\frac{4}{3}}$	0	0	$\sqrt{\frac{1}{6}}$	$\sqrt{\frac{1}{6}}$	$\sqrt{\frac{25}{18}}$	$\frac{2}{3}$	0	0
$\Xi^*_{cc}\rho$	$\sqrt{\frac{32}{3}}$	2	0	$\sqrt{6}$	$-\sqrt{\frac{8}{9}}$	$\sqrt{2}$	$-\sqrt{\frac{8}{3}}$	$-\sqrt{\frac{2}{3}}$	0	$-\sqrt{\frac{4}{3}}$	$-\sqrt{\frac{2}{9}}$	0	$-\frac{11}{3}$	$-\frac{2}{3}$	$-\sqrt{\frac{25}{3}}$	0	0	0	0	0	0	$-\sqrt{\frac{32}{3}}$
$\Sigma^*_c D^*$	$\sqrt{\frac{2}{3}}$	0	$\sqrt{\frac{2}{3}}$	$\sqrt{6}$	$\sqrt{\frac{2}{9}}$	$-\sqrt{2}$	$\sqrt{\frac{2}{3}}$	$\sqrt{\frac{50}{3}}$	$-\sqrt{6}$	0	$-\sqrt{\frac{2}{9}}$	$\sqrt{\frac{4}{3}}$	$-\frac{2}{3}$	$-\frac{26}{3}$	$-\sqrt{\frac{4}{3}}$	0	$\sqrt{2}$	$\sqrt{2}$	$-\sqrt{\frac{2}{3}}$	$-\sqrt{\frac{64}{3}}$	0	
$\Xi^*_{cc}\omega$	0	$\sqrt{\frac{4}{3}}$	0	$-\sqrt{2}$	$-\sqrt{\frac{8}{3}}$	$-\sqrt{\frac{2}{3}}$	$-\sqrt{\frac{8}{9}}$	$-\sqrt{2}$	0	$-\frac{2}{3}$	$-\sqrt{\frac{2}{3}}$	0	$-\sqrt{\frac{25}{3}}$	$-\sqrt{\frac{4}{3}}$	$-\frac{5}{3}$	0	0	0	0	0	0	$-\sqrt{\frac{32}{9}}$
$\Xi_{cc}\phi$	0	$\sqrt{\frac{1}{3}}$	0	0	0	0	0	0	$-\sqrt{\frac{1}{2}}$	$-\frac{5}{3}$	0	0	0	0	0	0	$-\sqrt{\frac{25}{6}}$	$-\sqrt{\frac{1}{6}}$	$\sqrt{\frac{49}{18}}$	$-\frac{2}{3}$	0	$\sqrt{\frac{8}{9}}$
$\Xi'_c D_s$	0	$\sqrt{\frac{1}{2}}$	$-\sqrt{\frac{1}{3}}$	0	0	1	0	$-\sqrt{3}$	0	$\sqrt{\frac{25}{6}}$	-2	$\sqrt{\frac{1}{6}}$	0	$\sqrt{2}$	0	$-\sqrt{\frac{25}{6}}$	0	-1	$-\sqrt{3}$	$\sqrt{6}$	$\sqrt{\frac{4}{3}}$	$-\sqrt{\frac{4}{3}}$
$\Xi_c D^*_s$	0	$-\sqrt{\frac{1}{2}}$	$-\sqrt{\frac{1}{3}}$	0	0	1	0	$-\sqrt{3}$	$\sqrt{3}$	$-\sqrt{\frac{1}{6}}$	-2	$\sqrt{\frac{1}{6}}$	0	$\sqrt{2}$	0	$-\sqrt{\frac{1}{6}}$	-1	-2	$-\sqrt{\frac{4}{3}}$	$\sqrt{\frac{2}{3}}$	$-\sqrt{\frac{4}{3}}$	$-\sqrt{\frac{4}{3}}$
$\Xi'_c D^*_s$	0	$\sqrt{\frac{25}{6}}$	$-\frac{5}{3}$	1	0	$\sqrt{\frac{4}{3}}$	0	-2	-1	$-\sqrt{\frac{49}{18}}$	$-\sqrt{\frac{49}{3}}$	$\sqrt{\frac{25}{18}}$	0	$-\sqrt{\frac{2}{3}}$	0	$\sqrt{\frac{49}{18}}$	$-\sqrt{3}$	$-\sqrt{\frac{4}{3}}$	$-\frac{2}{3}$	$\sqrt{\frac{2}{9}}$	$\frac{2}{3}$	$-\frac{2}{3}$
$\Xi^*_c D^*_s$	0	$\sqrt{\frac{4}{3}}$	$-\sqrt{\frac{8}{9}}$	$\sqrt{2}$	0	$-\sqrt{\frac{2}{3}}$	0	$\sqrt{2}$	$-\sqrt{2}$	$\frac{2}{3}$	$-\sqrt{\frac{2}{3}}$	$\frac{2}{3}$	0	$-\sqrt{\frac{64}{3}}$	0	$-\frac{2}{3}$	$\sqrt{6}$	$\sqrt{\frac{2}{3}}$	$\sqrt{\frac{2}{9}}$	$-\frac{10}{3}$	$\sqrt{\frac{8}{9}}$	$-\sqrt{\frac{8}{9}}$
$\Xi^*_{cc}\phi$	0	$\sqrt{\frac{8}{3}}$	0	0	0	0	0	0	-2	$\sqrt{\frac{8}{9}}$	0	0	0	0	0	0	$\sqrt{\frac{4}{3}}$	$-\sqrt{\frac{4}{3}}$	$\frac{2}{3}$	$\sqrt{\frac{8}{9}}$	0	$\frac{2}{3}$
$\Omega^*_{cc}K^*$	2	$\sqrt{\frac{8}{3}}$	2	0	$-\sqrt{\frac{4}{3}}$	0	$-\frac{2}{3}$	0	-2	$-\sqrt{\frac{8}{9}}$	0	0	$-\sqrt{\frac{32}{3}}$	0	$-\sqrt{\frac{32}{9}}$	$\sqrt{\frac{8}{9}}$	$-\sqrt{\frac{4}{3}}$	$-\sqrt{\frac{4}{3}}$	$-\frac{2}{3}$	$-\sqrt{\frac{8}{9}}$	$\frac{2}{3}$	$-\frac{8}{3}$

TABLE XXI. $C = 2$, $S = 0$, $I = 1/2$, $J = 3/2$.

	$\Xi_{cc}^{*}\pi$	$\Xi_{cc}^{*}\eta$	$\Xi_{cc}\rho$	$\Lambda_c D^{*}$	$\Xi_{cc}\omega$	$\Sigma_c^{*} D$	$\Omega_{cc}^{*} K$	$\Omega_{cc} K^{*}$	$\Sigma_c D^{*}$	$\Xi_{cc}^{*}\rho$	$\Sigma_c^{*} D^{*}$	$\Xi_{cc}^{*}\omega$	$\Xi_{cc}\phi$	$\Xi_c D_s^{*}$	$\Xi_c^{*} D_s$	$\Xi_c' D_s^{*}$	$\Xi_{cc}^{*}\eta'$	$\Xi_c^{*} D_s^{*}$	$\Xi_{cc}^{*}\phi$	$\Omega_{cc}^{*} K^{*}$
$\Xi_{cc}^{*}\pi$	-2	0	$-\sqrt{\frac{16}{3}}$	$-\sqrt{3}$	0	1	$-\sqrt{\frac{3}{2}}$	$-\sqrt{2}$	$\sqrt{\frac{1}{3}}$	$-\sqrt{\frac{20}{3}}$	$\sqrt{\frac{5}{3}}$	0	0	0	0	0	0	0	0	$-\sqrt{\frac{5}{2}}$
$\Xi_{cc}^{*}\eta$	0	0	0	$\sqrt{\frac{1}{3}}$	0	1	$-\sqrt{\frac{3}{2}}$	$-\sqrt{2}$	$\sqrt{\frac{1}{3}}$	0	$\sqrt{\frac{5}{3}}$	0	0	$\sqrt{\frac{4}{3}}$	$-\sqrt{\frac{4}{3}}$	$-\frac{2}{3}$	0	$-\sqrt{\frac{20}{9}}$	0	$-\sqrt{\frac{5}{2}}$
$\Xi_{cc}\rho$	$-\sqrt{\frac{16}{3}}$	0	$-\frac{7}{3}$	2	$-\sqrt{\frac{1}{3}}$	$-\sqrt{\frac{1}{3}}$	$-\sqrt{2}$	$-\sqrt{\frac{8}{3}}$	$\frac{4}{3}$	$-\sqrt{\frac{20}{9}}$	$\sqrt{\frac{5}{9}}$	$-\sqrt{\frac{20}{3}}$	0	0	0	0	0	0	0	$-\sqrt{\frac{10}{3}}$
$\Lambda_c D^{*}$	$-\sqrt{3}$	$\sqrt{\frac{1}{3}}$	2	1	$-\sqrt{\frac{4}{3}}$	$-\sqrt{3}$	0	0	-1	$\sqrt{5}$	$-\sqrt{5}$	$-\sqrt{\frac{5}{3}}$	0	1	-1	$-\sqrt{\frac{1}{3}}$	$\sqrt{\frac{2}{3}}$	$-\sqrt{\frac{5}{3}}$	0	0
$\Xi_{cc}\omega$	0	0	$-\sqrt{\frac{1}{3}}$	$-\sqrt{\frac{4}{3}}$	$-\frac{1}{3}$	-1	$-\sqrt{\frac{2}{3}}$	$-\sqrt{\frac{8}{9}}$	$\sqrt{\frac{16}{3}}$	$-\sqrt{\frac{20}{3}}$	$\sqrt{\frac{5}{3}}$	$-\sqrt{\frac{20}{9}}$	0	0	0	0	0	0	0	$-\sqrt{\frac{10}{9}}$
$\Sigma_c^{*} D$	1	1	$-\sqrt{\frac{1}{3}}$	$-\sqrt{3}$	-1	-2	0	0	$-\sqrt{\frac{25}{3}}$	$\sqrt{\frac{5}{3}}$	$-\sqrt{\frac{20}{3}}$	$\sqrt{5}$	0	$\sqrt{3}$	$-\sqrt{3}$	-1	$\sqrt{2}$	$-\sqrt{5}$	0	0
$\Omega_{cc}^{*} K$	$-\sqrt{\frac{3}{2}}$	$-\sqrt{\frac{3}{2}}$	$-\sqrt{2}$	0	$-\sqrt{\frac{2}{3}}$	0	-1	$-\sqrt{\frac{4}{3}}$	0	$-\sqrt{\frac{5}{2}}$	0	$-\sqrt{\frac{5}{6}}$	$-\sqrt{\frac{4}{3}}$	$\sqrt{2}$	$\sqrt{2}$	$\sqrt{\frac{2}{3}}$	0	$\sqrt{\frac{10}{3}}$	$-\sqrt{\frac{5}{3}}$	$-\sqrt{\frac{5}{3}}$
$\Omega_{cc} K^{*}$	$-\sqrt{2}$	$-\sqrt{2}$	$-\sqrt{\frac{8}{3}}$	0	$-\sqrt{\frac{8}{9}}$	0	$-\sqrt{\frac{4}{3}}$	$-\frac{4}{3}$	0	$-\sqrt{\frac{10}{3}}$	0	$-\sqrt{\frac{10}{9}}$	$-\frac{2}{3}$	$-\sqrt{\frac{8}{3}}$	$-\sqrt{\frac{2}{3}}$	$\sqrt{\frac{32}{9}}$	0	$\sqrt{\frac{10}{9}}$	$\sqrt{\frac{20}{9}}$	$-\sqrt{\frac{20}{9}}$
$\Sigma_c D^{*}$	$\sqrt{\frac{1}{3}}$	$\sqrt{\frac{1}{3}}$	$\frac{4}{3}$	-1	$\sqrt{\frac{16}{3}}$	$-\sqrt{\frac{25}{3}}$	0	0	$-\frac{1}{3}$	$-\sqrt{\frac{5}{9}}$	$-\sqrt{\frac{5}{9}}$	$-\sqrt{\frac{5}{3}}$	0	1	-1	$-\sqrt{\frac{1}{3}}$	$\sqrt{\frac{2}{3}}$	$-\sqrt{\frac{5}{3}}$	0	0
$\Xi_{cc}^{*}\rho$	$-\sqrt{\frac{20}{3}}$	0	$-\sqrt{\frac{20}{9}}$	$\sqrt{5}$	$-\sqrt{\frac{20}{3}}$	$\sqrt{\frac{5}{3}}$	$-\sqrt{\frac{5}{2}}$	$-\sqrt{\frac{10}{3}}$	$-\sqrt{\frac{5}{9}}$	$-\frac{8}{3}$	$\frac{1}{3}$	$-\sqrt{\frac{4}{3}}$	0	0	0	0	0	0	0	$-\sqrt{\frac{25}{6}}$
$\Sigma_c^{*} D^{*}$	$\sqrt{\frac{5}{3}}$	$\sqrt{\frac{5}{3}}$	$\sqrt{\frac{5}{9}}$	$-\sqrt{5}$	$\sqrt{\frac{5}{3}}$	$-\sqrt{\frac{20}{3}}$	0	0	$-\sqrt{\frac{5}{9}}$	$\frac{1}{3}$	$-\frac{14}{3}$	$\sqrt{\frac{1}{3}}$	0	$\sqrt{5}$	$-\sqrt{5}$	$-\sqrt{\frac{5}{3}}$	$\sqrt{\frac{10}{3}}$	$-\sqrt{\frac{25}{3}}$	0	0
$\Xi_{cc}^{*}\omega$	0	0	$-\sqrt{\frac{20}{3}}$	$-\sqrt{\frac{5}{3}}$	$-\sqrt{\frac{20}{9}}$	$\sqrt{5}$	$-\sqrt{\frac{5}{6}}$	$-\sqrt{\frac{10}{9}}$	$-\sqrt{\frac{5}{3}}$	$-\sqrt{\frac{4}{3}}$	$\sqrt{\frac{1}{3}}$	$-\frac{2}{3}$	0	0	0	0	0	0	0	$-\sqrt{\frac{25}{18}}$
$\Xi_{cc}\phi$	0	0	0	0	0	0	$-\sqrt{\frac{4}{3}}$	$-\frac{2}{3}$	0	0	0	0	0	$-\sqrt{\frac{8}{3}}$	$\sqrt{\frac{2}{3}}$	$-\sqrt{\frac{32}{9}}$	0	$-\sqrt{\frac{10}{9}}$	0	$\sqrt{\frac{20}{9}}$
$\Xi_c D_s^{*}$	0	$\sqrt{\frac{4}{3}}$	0	1	0	$\sqrt{3}$	$\sqrt{2}$	$-\sqrt{\frac{8}{3}}$	1	0	$\sqrt{5}$	0	$-\sqrt{\frac{8}{3}}$	1	1	$\sqrt{\frac{1}{3}}$	$-\sqrt{\frac{2}{3}}$	$\sqrt{\frac{5}{3}}$	$-\sqrt{\frac{10}{3}}$	$-\sqrt{\frac{10}{3}}$
$\Xi_c^{*} D_s$	0	$-\sqrt{\frac{4}{3}}$	0	-1	0	$-\sqrt{3}$	$\sqrt{2}$	$-\sqrt{\frac{2}{3}}$	-1	0	$-\sqrt{5}$	0	$\sqrt{\frac{2}{3}}$	1	0	$-\sqrt{3}$	$\sqrt{\frac{2}{3}}$	0	$-\sqrt{\frac{10}{3}}$	$\sqrt{\frac{10}{3}}$
$\Xi_c' D_s^{*}$	0	$-\frac{2}{3}$	0	$-\sqrt{\frac{1}{3}}$	0	-1	$\sqrt{\frac{2}{3}}$	$\sqrt{\frac{32}{9}}$	$-\sqrt{\frac{1}{3}}$	0	$-\sqrt{\frac{5}{3}}$	0	$-\sqrt{\frac{32}{9}}$	$\sqrt{\frac{1}{3}}$	$-\sqrt{3}$	$\frac{1}{3}$	$\sqrt{\frac{2}{9}}$	$\sqrt{\frac{5}{9}}$	$\sqrt{\frac{10}{9}}$	$-\sqrt{\frac{10}{9}}$
$\Xi_{cc}^{*}\eta'$	0	0	0	$\sqrt{\frac{2}{3}}$	0	$\sqrt{2}$	0	0	$\sqrt{\frac{2}{3}}$	0	$\sqrt{\frac{10}{3}}$	0	0	$-\sqrt{\frac{2}{3}}$	$\sqrt{\frac{2}{3}}$	$\sqrt{\frac{2}{9}}$	0	$\sqrt{\frac{10}{9}}$	0	0
$\Xi_c^{*} D_s^{*}$	0	$-\sqrt{\frac{20}{9}}$	0	$-\sqrt{\frac{5}{3}}$	0	$-\sqrt{5}$	$\sqrt{\frac{10}{3}}$	$\sqrt{\frac{10}{9}}$	$-\sqrt{\frac{5}{3}}$	0	$-\sqrt{\frac{25}{3}}$	0	$-\sqrt{\frac{10}{9}}$	$\sqrt{\frac{5}{3}}$	0	$\sqrt{\frac{5}{9}}$	$\sqrt{\frac{10}{9}}$	$-\frac{4}{3}$	$-\sqrt{\frac{2}{9}}$	$\sqrt{\frac{2}{9}}$
$\Xi_{cc}^{*}\phi$	0	0	0	0	0	0	$-\sqrt{\frac{5}{3}}$	$\sqrt{\frac{20}{9}}$	0	0	0	0	0	$-\sqrt{\frac{10}{3}}$	$-\sqrt{\frac{10}{3}}$	$\sqrt{\frac{10}{9}}$	0	$-\sqrt{\frac{2}{9}}$	0	$-\frac{1}{3}$
$\Omega_{cc}^{*} K^{*}$	$-\sqrt{\frac{5}{2}}$	$-\sqrt{\frac{5}{2}}$	$-\sqrt{\frac{10}{3}}$	0	$-\sqrt{\frac{10}{9}}$	0	$-\sqrt{\frac{5}{3}}$	$-\sqrt{\frac{20}{9}}$	0	$-\sqrt{\frac{25}{6}}$	0	$-\sqrt{\frac{25}{18}}$	$\sqrt{\frac{20}{9}}$	$-\sqrt{\frac{10}{3}}$	$\sqrt{\frac{10}{3}}$	$-\sqrt{\frac{10}{9}}$	0	$\sqrt{\frac{2}{9}}$	$-\frac{1}{3}$	$-\frac{5}{3}$

TABLE XXII. $C = 2$, $S = -1$, $I = 0$, $J = 1/2$.

	$\Xi_{cc}\bar{K}$	$\Omega_{cc}\eta$	$\Omega_{cc}\omega$	$\Xi_c D$	$\Xi_{cc}\bar{K}^*$	$\Xi_c' D$	$\Xi_c D^*$	$\Omega_{cc}\eta'$	$\Omega_{cc}\phi$	$\Xi_c' D^*$	$\Xi_{cc}^*\bar{K}^*$	$\Xi_c^* D^*$	$\Omega_c D_s$	$\Omega_{cc}^*\omega$	$\Omega_c D_s^*$	$\Omega_c^* D_s^*$	$\Omega_{cc}^*\phi$
$\Xi_{cc}\bar{K}$	-2	$\sqrt{3}$	$-\sqrt{\frac{1}{3}}$	$\sqrt{\frac{3}{2}}$	$\sqrt{\frac{4}{3}}$	$\sqrt{\frac{1}{2}}$	$\sqrt{\frac{1}{2}}$	0	$-\sqrt{\frac{2}{3}}$	$\sqrt{\frac{25}{6}}$	$\sqrt{\frac{32}{3}}$	$\sqrt{\frac{4}{3}}$	0	$-\sqrt{\frac{8}{3}}$	0	0	$-\sqrt{\frac{16}{3}}$
$\Omega_{cc}\eta$	$\sqrt{3}$	0	0	$-\sqrt{\frac{1}{2}}$	-1	$\sqrt{\frac{1}{6}}$	$-\sqrt{\frac{1}{6}}$	0	0	$\sqrt{\frac{25}{18}}$	$-\sqrt{8}$	$\frac{2}{3}$	$-\sqrt{\frac{2}{3}}$	0	$-\sqrt{\frac{50}{9}}$	$-\frac{4}{3}$	0
$\Omega_{cc}\omega$	$-\sqrt{\frac{1}{3}}$	0	0	$-\sqrt{\frac{1}{2}}$	$\frac{5}{3}$	$\sqrt{\frac{25}{6}}$	$-\sqrt{\frac{1}{6}}$	0	0	$-\sqrt{\frac{49}{18}}$	$-\sqrt{\frac{8}{9}}$	$\frac{2}{3}$	0	0	0	0	0
$\Xi_c D$	$\sqrt{\frac{3}{2}}$	$-\sqrt{\frac{1}{2}}$	$-\sqrt{\frac{1}{2}}$	-1	$\sqrt{\frac{1}{2}}$	0	$\sqrt{3}$	-1	0	2	2	$\sqrt{8}$	0	-2	2	$\sqrt{8}$	0
$\Xi_{cc}\bar{K}^*$	$\sqrt{\frac{4}{3}}$	-1	$\frac{5}{3}$	$\sqrt{\frac{1}{2}}$	$-\frac{2}{3}$	$\sqrt{\frac{25}{6}}$	$\sqrt{\frac{1}{6}}$	0	$\sqrt{\frac{2}{9}}$	$-\sqrt{\frac{49}{18}}$	$-\sqrt{\frac{32}{9}}$	$\frac{2}{3}$	0	$-\sqrt{\frac{8}{9}}$	0	0	$\frac{4}{3}$
$\Xi_c' D$	$\sqrt{\frac{1}{2}}$	$\sqrt{\frac{1}{6}}$	$\sqrt{\frac{25}{6}}$	0	$\sqrt{\frac{25}{6}}$	-1	2	$\sqrt{\frac{1}{3}}$	0	$-\sqrt{\frac{25}{3}}$	$-\sqrt{\frac{4}{3}}$	$\sqrt{\frac{32}{3}}$	-2	$-\sqrt{\frac{4}{3}}$	$-\sqrt{\frac{16}{3}}$	$\sqrt{\frac{8}{3}}$	0
$\Xi_c D^*$	$\sqrt{\frac{1}{2}}$	$-\sqrt{\frac{1}{6}}$	$-\sqrt{\frac{1}{6}}$	$\sqrt{3}$	$\sqrt{\frac{1}{6}}$	2	-3	$-\sqrt{\frac{1}{3}}$	0	$\sqrt{\frac{16}{3}}$	$\sqrt{\frac{4}{3}}$	$-\sqrt{\frac{8}{3}}$	2	$-\sqrt{\frac{4}{3}}$	$\sqrt{\frac{16}{3}}$	$-\sqrt{\frac{8}{3}}$	0
$\Omega_{cc}\eta'$	0	0	0	-1	0	$\sqrt{\frac{1}{3}}$	$-\sqrt{\frac{1}{3}}$	0	0	$\frac{5}{3}$	0	$\sqrt{\frac{8}{9}}$	$\sqrt{\frac{1}{3}}$	0	$\frac{5}{3}$	$\sqrt{\frac{8}{9}}$	0
$\Omega_{cc}\phi$	$-\sqrt{\frac{2}{3}}$	0	0	0	$\sqrt{\frac{2}{9}}$	0	0	0	$\frac{4}{3}$	0	$\frac{4}{3}$	0	$-\sqrt{\frac{25}{3}}$	0	$\frac{7}{3}$	$-\sqrt{\frac{8}{9}}$	$-\sqrt{\frac{32}{9}}$
$\Xi_c' D^*$	$\sqrt{\frac{25}{6}}$	$\sqrt{\frac{25}{18}}$	$-\sqrt{\frac{49}{18}}$	2	$-\sqrt{\frac{49}{18}}$	$-\sqrt{\frac{25}{3}}$	$\sqrt{\frac{16}{3}}$	$\frac{5}{3}$	0	-3	$-\frac{2}{3}$	0	$-\sqrt{\frac{16}{3}}$	$-\frac{2}{3}$	$-\frac{14}{3}$	$-\sqrt{\frac{8}{9}}$	0
$\Xi_{cc}^*\bar{K}^*$	$\sqrt{\frac{32}{3}}$	$-\sqrt{8}$	$-\sqrt{\frac{8}{9}}$	2	$-\sqrt{\frac{32}{9}}$	$-\sqrt{\frac{4}{3}}$	$\sqrt{\frac{4}{3}}$	0	$\frac{4}{3}$	$-\frac{2}{3}$	$-\frac{16}{3}$	$-\sqrt{\frac{8}{9}}$	0	$-\frac{2}{3}$	0	0	$\sqrt{\frac{128}{9}}$
$\Xi_c^* D^*$	$\sqrt{\frac{4}{3}}$	$\frac{2}{3}$	$\frac{2}{3}$	$\sqrt{8}$	$\frac{2}{3}$	$\sqrt{\frac{32}{3}}$	$-\sqrt{\frac{8}{3}}$	$\sqrt{\frac{8}{9}}$	0	0	$-\sqrt{\frac{8}{9}}$	-6	$\sqrt{\frac{8}{3}}$	$-\sqrt{\frac{8}{9}}$	$-\sqrt{\frac{8}{9}}$	$-\frac{16}{3}$	0
$\Omega_c D_s$	0	$-\sqrt{\frac{2}{3}}$	0	0	0	-2	2	$\sqrt{\frac{1}{3}}$	$-\sqrt{\frac{25}{3}}$	$-\sqrt{\frac{16}{3}}$	0	$\sqrt{\frac{8}{3}}$	-1	0	$-\sqrt{\frac{25}{3}}$	$\sqrt{\frac{32}{3}}$	$\sqrt{\frac{8}{3}}$
$\Omega_{cc}^*\omega$	$-\sqrt{\frac{8}{3}}$	0	0	-2	$-\sqrt{\frac{8}{9}}$	$-\sqrt{\frac{4}{3}}$	$-\sqrt{\frac{4}{3}}$	0	0	$-\frac{2}{3}$	$-\frac{2}{3}$	$-\sqrt{\frac{8}{9}}$	0	0	0	0	0
$\Omega_c D_s^*$	0	$-\sqrt{\frac{50}{9}}$	0	2	0	$-\sqrt{\frac{16}{3}}$	$\sqrt{\frac{16}{3}}$	$\frac{5}{3}$	$\frac{7}{3}$	$-\frac{14}{3}$	0	$-\sqrt{\frac{8}{9}}$	$-\sqrt{\frac{25}{3}}$	0	-3	0	$\sqrt{\frac{8}{9}}$
$\Omega_c^* D_s^*$	0	$-\frac{4}{3}$	0	$\sqrt{8}$	0	$\sqrt{\frac{8}{3}}$	$-\sqrt{\frac{8}{3}}$	$\sqrt{\frac{8}{9}}$	$-\sqrt{\frac{8}{9}}$	$-\sqrt{\frac{8}{9}}$	0	$-\frac{16}{3}$	$\sqrt{\frac{32}{3}}$	0	0	-6	$\frac{4}{3}$
$\Omega_{cc}^*\phi$	$-\sqrt{\frac{16}{3}}$	0	0	0	$\frac{4}{3}$	0	0	0	$-\sqrt{\frac{32}{9}}$	0	$\sqrt{\frac{128}{9}}$	0	$\sqrt{\frac{8}{3}}$	0	$\sqrt{\frac{8}{9}}$	$\frac{4}{3}$	$-\frac{10}{3}$

TABLE XXIII. $C = 2$, $S = -1$, $I = 0$, $J = 3/2$.

	$\Xi_{cc}^*\bar{K}$	$\Omega_{cc}\omega$	$\Xi_{cc}\bar{K}^*$	$\Omega_{cc}^*\eta$	$\Xi_c D^*$	$\Xi_c^* D$	$\Omega_{cc}\phi$	$\Xi_c' D^*$	$\Xi_{cc}^*\bar{K}^*$	$\Xi_c^* D^*$	$\Omega_{cc}^*\omega$	$\Omega_c^* D_s$	$\Omega_c D_s^*$	$\Omega_{cc}^*\eta'$	$\Omega_c^* D_s^*$	$\Omega_{cc}^*\phi$
$\Xi_{cc}^*\bar{K}$	-2	$\sqrt{\frac{4}{3}}$	$-\sqrt{\frac{16}{3}}$	$\sqrt{3}$	$-\sqrt{2}$	$\sqrt{2}$	$\sqrt{\frac{8}{3}}$	$\sqrt{\frac{2}{3}}$	$-\sqrt{\frac{20}{3}}$	$\sqrt{\frac{10}{3}}$	$\sqrt{\frac{5}{3}}$	0	0	0	0	$\sqrt{\frac{10}{3}}$
$\Omega_{cc}\omega$	$\sqrt{\frac{4}{3}}$	0	$\frac{2}{3}$	0	$-\sqrt{\frac{8}{3}}$	$-\sqrt{\frac{2}{3}}$	0	$\sqrt{\frac{32}{9}}$	$-\sqrt{\frac{20}{9}}$	$\sqrt{\frac{10}{9}}$	0	0	0	0	0	0
$\Xi_{cc}\bar{K}^*$	$-\sqrt{\frac{16}{3}}$	$\frac{2}{3}$	$-\frac{8}{3}$	2	$\sqrt{\frac{8}{3}}$	$-\sqrt{\frac{2}{3}}$	$\sqrt{\frac{32}{9}}$	$\sqrt{\frac{32}{9}}$	$-\sqrt{\frac{80}{9}}$	$\sqrt{\frac{10}{9}}$	$-\sqrt{\frac{20}{9}}$	0	0	0	0	$\sqrt{\frac{40}{9}}$
$\Omega_{cc}^*\eta$	$\sqrt{3}$	0	2	0	$\sqrt{\frac{2}{3}}$	$\sqrt{\frac{2}{3}}$	0	$\sqrt{\frac{2}{9}}$	$\sqrt{5}$	$\sqrt{\frac{10}{9}}$	0	$-\sqrt{\frac{8}{3}}$	$-\sqrt{\frac{8}{9}}$	0	$-\sqrt{\frac{40}{9}}$	0
$\Xi_c D^*$	$-\sqrt{2}$	$-\sqrt{\frac{8}{3}}$	$\sqrt{\frac{8}{3}}$	$\sqrt{\frac{2}{3}}$	0	-2	0	$-\sqrt{\frac{4}{3}}$	$\sqrt{\frac{10}{3}}$	$-\sqrt{\frac{20}{3}}$	$-\sqrt{\frac{10}{3}}$	-2	$-\sqrt{\frac{4}{3}}$	$\sqrt{\frac{4}{3}}$	$-\sqrt{\frac{20}{3}}$	0
$\Xi_c^* D$	$\sqrt{2}$	$-\sqrt{\frac{2}{3}}$	$-\sqrt{\frac{2}{3}}$	$\sqrt{\frac{2}{3}}$	-2	-1	0	$-\sqrt{\frac{16}{3}}$	$\sqrt{\frac{10}{3}}$	$-\sqrt{\frac{5}{3}}$	$\sqrt{\frac{10}{3}}$	-2	$-\sqrt{\frac{4}{3}}$	$\sqrt{\frac{4}{3}}$	$-\sqrt{\frac{20}{3}}$	0
$\Omega_{cc}\phi$	$\sqrt{\frac{8}{3}}$	0	$\sqrt{\frac{32}{9}}$	0	0	0	$-\frac{2}{3}$	0	$\sqrt{\frac{40}{9}}$	0	0	$\sqrt{\frac{4}{3}}$	$-\frac{8}{3}$	0	$-\sqrt{\frac{20}{9}}$	$-\sqrt{\frac{80}{9}}$
$\Xi_c' D^*$	$\sqrt{\frac{2}{3}}$	$\sqrt{\frac{32}{9}}$	$\sqrt{\frac{32}{9}}$	$\sqrt{\frac{2}{9}}$	$-\sqrt{\frac{4}{3}}$	$-\sqrt{\frac{16}{3}}$	0	0	$-\sqrt{\frac{10}{9}}$	0	$-\sqrt{\frac{10}{9}}$	$-\sqrt{\frac{4}{3}}$	$-\frac{2}{3}$	$\frac{2}{3}$	$-\sqrt{\frac{20}{9}}$	0
$\Xi_{cc}^*\bar{K}^*$	$-\sqrt{\frac{20}{3}}$	$-\sqrt{\frac{20}{9}}$	$-\sqrt{\frac{80}{9}}$	$\sqrt{5}$	$\sqrt{\frac{10}{3}}$	$\sqrt{\frac{10}{3}}$	$\sqrt{\frac{40}{9}}$	$-\sqrt{\frac{10}{9}}$	$-\frac{10}{3}$	$\sqrt{\frac{2}{9}}$	$\frac{1}{3}$	0	0	0	0	$\sqrt{\frac{50}{9}}$
$\Xi_c^* D^*$	$\sqrt{\frac{10}{3}}$	$\sqrt{\frac{10}{9}}$	$\sqrt{\frac{10}{9}}$	$\sqrt{\frac{10}{9}}$	$-\sqrt{\frac{20}{3}}$	$-\sqrt{\frac{5}{3}}$	0	0	$\sqrt{\frac{2}{9}}$	-3	$\sqrt{\frac{2}{9}}$	$-\sqrt{\frac{20}{3}}$	$-\sqrt{\frac{20}{9}}$	$\sqrt{\frac{20}{9}}$	$-\frac{10}{3}$	0
$\Omega_{cc}^*\omega$	$\sqrt{\frac{5}{3}}$	0	$-\sqrt{\frac{20}{9}}$	0	$-\sqrt{\frac{10}{3}}$	$\sqrt{\frac{10}{3}}$	0	$-\sqrt{\frac{10}{9}}$	$\frac{1}{3}$	$\sqrt{\frac{2}{9}}$	0	0	0	0	0	0
$\Omega_c^* D_s$	0	0	0	$-\sqrt{\frac{8}{3}}$	-2	-2	$\sqrt{\frac{4}{3}}$	$-\sqrt{\frac{4}{3}}$	0	$-\sqrt{\frac{20}{3}}$	0	-1	$-\sqrt{\frac{16}{3}}$	$\sqrt{\frac{4}{3}}$	$-\sqrt{\frac{5}{3}}$	$-\sqrt{\frac{20}{3}}$
$\Omega_c D_s^*$	0	0	0	$-\sqrt{\frac{8}{9}}$	$-\sqrt{\frac{4}{3}}$	$-\sqrt{\frac{4}{3}}$	$-\frac{8}{3}$	$-\frac{2}{3}$	0	$-\sqrt{\frac{20}{9}}$	0	$-\sqrt{\frac{16}{3}}$	0	$\frac{2}{3}$	0	$\sqrt{\frac{20}{9}}$
$\Omega_{cc}^*\eta'$	0	0	0	0	$\sqrt{\frac{4}{3}}$	$\sqrt{\frac{4}{3}}$	0	$\frac{2}{3}$	0	$\sqrt{\frac{20}{9}}$	0	$\sqrt{\frac{4}{3}}$	$\frac{2}{3}$	0	$\sqrt{\frac{20}{9}}$	0
$\Omega_c^* D_s^*$	0	0	0	$-\sqrt{\frac{40}{9}}$	$-\sqrt{\frac{20}{3}}$	$-\sqrt{\frac{20}{3}}$	$-\sqrt{\frac{20}{9}}$	$-\sqrt{\frac{20}{9}}$	0	$-\frac{10}{3}$	0	$-\sqrt{\frac{5}{3}}$	0	$\sqrt{\frac{20}{9}}$	-3	$-\frac{2}{3}$
$\Omega_{cc}^*\phi$	$\sqrt{\frac{10}{3}}$	0	$\sqrt{\frac{40}{9}}$	0	0	0	$-\sqrt{\frac{80}{9}}$	0	$\sqrt{\frac{50}{9}}$	0	0	$-\sqrt{\frac{20}{3}}$	$\sqrt{\frac{20}{9}}$	0	$-\frac{2}{3}$	$-\frac{4}{3}$

TABLE XXIV. $C = 3$, $S = 0$, $I = 0$, $J = 1/2$.

	$\Xi_{cc}D$	$\Omega_{cc}D_s$	$\Xi_{cc}D^*$	$\Omega_{cc}D_s^*$	$\Xi_{cc}^*D^*$	$\Omega_{ccc}\omega$	$\Omega_{cc}^*D_s^*$	$\Omega_{ccc}\phi$
$\Xi_{cc}D$	0	$-\sqrt{2}$	$\sqrt{12}$	$\sqrt{\frac{2}{3}}$	$\sqrt{24}$	$-\sqrt{8}$	$\sqrt{\frac{16}{3}}$	0
$\Omega_{cc}D_s$	$-\sqrt{2}$	1	$\sqrt{\frac{2}{3}}$	$\sqrt{\frac{25}{3}}$	$\sqrt{\frac{16}{3}}$	0	$\sqrt{\frac{32}{3}}$	$\sqrt{8}$
$\Xi_{cc}D^*$	$\sqrt{12}$	$\sqrt{\frac{2}{3}}$	$-\frac{4}{3}$	$-\sqrt{\frac{2}{9}}$	$-\sqrt{\frac{8}{9}}$	$-\sqrt{\frac{8}{3}}$	$-\frac{4}{3}$	0
$\Omega_{cc}D_s^*$	$\sqrt{\frac{2}{3}}$	$\sqrt{\frac{25}{3}}$	$-\sqrt{\frac{2}{9}}$	-1	$-\frac{4}{3}$	0	0	$\sqrt{\frac{8}{3}}$
$\Xi_{cc}^*D^*$	$\sqrt{24}$	$\sqrt{\frac{16}{3}}$	$-\sqrt{\frac{8}{9}}$	$-\frac{4}{3}$	$-\frac{20}{3}$	$-\sqrt{\frac{4}{3}}$	$-\sqrt{\frac{128}{9}}$	0
$\Omega_{ccc}\omega$	$-\sqrt{8}$	0	$-\sqrt{\frac{8}{3}}$	0	$-\sqrt{\frac{4}{3}}$	0	0	0
$\Omega_{cc}^*D_s^*$	$\sqrt{\frac{16}{3}}$	$\sqrt{\frac{32}{3}}$	$-\frac{4}{3}$	0	$-\sqrt{\frac{128}{9}}$	0	-4	$\sqrt{\frac{4}{3}}$
$\Omega_{ccc}\phi$	0	$\sqrt{8}$	0	$\sqrt{\frac{8}{3}}$	0	0	$\sqrt{\frac{4}{3}}$	0

TABLE XXV. $C = 3$, $S = 0$, $I = 0$, $J = 3/2$.

	$\Xi_{cc}D^*$	$\Omega_{ccc}\eta$	Ξ_{cc}^*D	$\Omega_{cc}D_s^*$	$\Xi_{cc}^*D^*$	$\Omega_{ccc}\omega$	$\Omega_{cc}^*D_s$	$\Omega_{ccc}\eta'$	$\Omega_{cc}^*D_s^*$	$\Omega_{ccc}\phi$
$\Xi_{cc}D^*$	$\frac{2}{3}$	$\sqrt{\frac{4}{3}}$	$-\sqrt{12}$	$-\sqrt{\frac{32}{9}}$	$-\sqrt{\frac{20}{9}}$	$-\sqrt{\frac{20}{3}}$	$-\sqrt{\frac{8}{3}}$	$\sqrt{\frac{8}{3}}$	$-\sqrt{\frac{40}{9}}$	0
$\Omega_{ccc}\eta$	$\sqrt{\frac{4}{3}}$	0	1	$-\sqrt{\frac{8}{3}}$	$\sqrt{\frac{5}{3}}$	0	$-\sqrt{2}$	0	$-\sqrt{\frac{10}{3}}$	0
Ξ_{cc}^*D	$-\sqrt{12}$	1	0	$-\sqrt{\frac{8}{3}}$	0	$\sqrt{5}$	$-\sqrt{2}$	$\sqrt{2}$	$-\sqrt{\frac{10}{3}}$	0
$\Omega_{cc}D_s^*$	$-\sqrt{\frac{32}{9}}$	$-\sqrt{\frac{8}{3}}$	$-\sqrt{\frac{8}{3}}$	2	$-\sqrt{\frac{40}{9}}$	0	$-\sqrt{\frac{16}{3}}$	$\sqrt{\frac{4}{3}}$	0	$\sqrt{\frac{20}{3}}$
$\Xi_{cc}^*D^*$	$-\sqrt{\frac{20}{9}}$	$\sqrt{\frac{5}{3}}$	0	$-\sqrt{\frac{40}{9}}$	$-\frac{8}{3}$	$\sqrt{\frac{1}{3}}$	$-\sqrt{\frac{10}{3}}$	$\sqrt{\frac{10}{3}}$	$-\sqrt{\frac{50}{9}}$	0
$\Omega_{ccc}\omega$	$-\sqrt{\frac{20}{3}}$	0	$\sqrt{5}$	0	$\sqrt{\frac{1}{3}}$	0	0	0	0	0
$\Omega_{cc}^*D_s$	$-\sqrt{\frac{8}{3}}$	$-\sqrt{2}$	$-\sqrt{2}$	$-\sqrt{\frac{16}{3}}$	$-\sqrt{\frac{10}{3}}$	0	1	1	$\sqrt{\frac{5}{3}}$	$-\sqrt{5}$
$\Omega_{ccc}\eta'$	$\sqrt{\frac{8}{3}}$	0	$\sqrt{2}$	$\sqrt{\frac{4}{3}}$	$\sqrt{\frac{10}{3}}$	0	1	0	$\sqrt{\frac{5}{3}}$	0
$\Omega_{cc}^*D_s^*$	$-\sqrt{\frac{40}{9}}$	$-\sqrt{\frac{10}{3}}$	$-\sqrt{\frac{10}{3}}$	0	$-\sqrt{\frac{50}{9}}$	0	$\sqrt{\frac{5}{3}}$	$\sqrt{\frac{5}{3}}$	-1	$-\sqrt{\frac{1}{3}}$
$\Omega_{ccc}\phi$	0	0	0	$\sqrt{\frac{20}{3}}$	0	0	$-\sqrt{5}$	0	$-\sqrt{\frac{1}{3}}$	0

[1] B. Aubert *et al.* (*BABAR* Collaboration), Phys. Rev. Lett. **90**, 242001 (2003).

[2] R. A. Briere *et al.* (CLEO Collaboration), Phys. Rev. D **74**, 031106 (2006).

[3] P. Krokovny *et al.* (Belle Collaboration), Phys. Rev. Lett. **91**, 262002 (2003).

[4] K. Abe *et al.* (Belle Collaboration), Phys. Rev. Lett. **92**, 012002 (2004).

[5] S. K. Choi *et al.* (Belle Collaboration), Phys. Rev. Lett. **91**, 262001 (2003).

[6] D. E. Acosta *et al.* (CDF II Collaboration), Phys. Rev. Lett. **93**, 072001 (2004).

[7] V. M. Abazov *et al.* (D0 Collaboration), Phys. Rev. Lett. **93**, 162002 (2004).

[8] B. Aubert *et al.* (*BABAR* Collaboration), Phys. Rev. D **71**, 071103 (2005).

[9] K. Abe *et al.* (Belle Collaboration), Phys. Rev. Lett. **98**, 082001 (2007).

[10] P. Pakhlov *et al.* (Belle Collaboration), Phys. Rev. Lett. **100**, 202001 (2008).

[11] S.-K. Choi *et al.* (Belle Collaboration), Phys. Rev. Lett. **94**, 182002 (2005).
[12] B. Aubert *et al.* (*BABAR* Collaboration), Phys. Rev. Lett. **101**, 082001 (2008).
[13] S. Uehara *et al.* (Belle Collaboration), Phys. Rev. Lett. **96**, 082003 (2006).
[14] H. Albrecht *et al.* (ARGUS Collaboration), Phys. Lett. B **402**, 207 (1997).
[15] P. L. Frabetti *et al.* (E687 Collaboration), Phys. Lett. B **365**, 461 (1996).
[16] B. Aubert *et al.* (*BABAR* Collaboration), Phys. Rev. Lett. **98**, 012001 (2007).
[17] K. Abe *et al.* (Belle Collaboration), Phys. Rev. Lett. **98**, 262001 (2007).
[18] M. Artuso *et al.* (CLEO Collaboration), Phys. Rev. Lett. **86**, 4479 (2001).
[19] H. Albrecht *et al.* (ARGUS Collaboration), Phys. Lett. B **317**, 227 (1993).
[20] P. L. Frabetti *et al.* (E687 Collaboration), Phys. Rev. Lett. **72**, 961 (1994).
[21] K. W. Edwards *et al.* (CLEO Collaboration), Phys. Rev. Lett. **74**, 3331 (1995).
[22] R. Ammar *et al.* (CLEO Collaboration), Phys. Rev. Lett. **86**, 1167 (2001).
[23] G. Brandenburg *et al.* (CLEO Collaboration), Phys. Rev. Lett. **78**, 2304 (1997).
[24] V. V. Ammosov, I. L. Vasilev, A. A. Ivanilov, P. V. Ivanov, V. I. Konyushko, V. M. Korablev, V. A. Korotkov, V. V. Makeev *et al.*, JETP Lett. **58**, 247 (1993).
[25] B. Aubert *et al.* (*BABAR* Collaboration), Phys. Rev. D **78**, 112003 (2008).
[26] R. Mizuk *et al.* (Belle Collaboration), Phys. Rev. Lett. **94**, 122002 (2005).
[27] T. Lesiak *et al.* (Belle Collaboration), Phys. Lett. B **665**, 9 (2008).
[28] P. L. Frabetti *et al.* (The E687 Collaboration), Phys. Lett. B **426**, 403 (1998).
[29] L. Gibbons *et al.* (CLEO Collaboration), Phys. Rev. Lett. **77**, 810 (1996).
[30] P. Avery *et al.* (CLEO Collaboration), Phys. Rev. Lett. **75**, 4364 (1995).
[31] S. E. Csorna *et al.* (CLEO Collaboration), Phys. Rev. Lett. **86**, 4243 (2001).
[32] J. P. Alexander *et al.* (CLEO Collaboration), Phys. Rev. Lett. **83**, 3390 (1999).
[33] B. Aubert *et al.* (*BABAR* Collaboration), Phys. Rev. D **77**, 012002 (2008).
[34] R. Chistov *et al.* (BELLE Collaboration), Phys. Rev. Lett. **97**, 162001 (2006).
[35] C. P. Jessop *et al.* (CLEO Collaboration), Phys. Rev. Lett. **82**, 492 (1999).
[36] B. Aubert *et al.* (*BABAR* Collaboration), Phys. Rev. Lett. **97**, 232001 (2006).
[37] J. Aichelin *et al.*, *The CBM Physics Book*, edited by B. Friman, C. Hohne, J. Knoll, S. Leupold, J. Randrup, R. Rapp, and P. Senger, Lecture Notes in Physics Vol. 814 (Springer, New York, 2011), pp. 1–960.
[38] W. Erni (PANDA Collaboration), arXiv:0903.3905.
[39] L. Tolos, J. Schaffner-Bielich, and A. Mishra, Phys. Rev. C **70**, 025203 (2004).
[40] M. F. M. Lutz and E. E. Kolomeitsev, Nucl. Phys. **A730**, 110 (2004).
[41] M. F. M. Lutz and E. E. Kolomeitsev, Nucl. Phys. **A755**, 29 (2005).
[42] J. Hofmann and M. F. M. Lutz, Nucl. Phys **A763**, 90 (2005).
[43] J. Hofmann and M. F. M. Lutz, Nucl. Phys. **A776**, 17 (2006).
[44] T. Mizutani and A. Ramos, Phys. Rev. C **74**, 065201 (2006).
[45] C. E. Jimenez-Tejero, A. Ramos, and I. Vidana, Phys. Rev. C **80**, 055206 (2009).
[46] J. Haidenbauer, G. Krein, U. G. Meissner, and A. Sibirtsev, Eur. Phys. J. A **33**, 107 (2007).
[47] J. Haidenbauer, G. Krein, U. G. Meissner, and A. Sibirtsev, Eur. Phys. J. A **37**, 55 (2008).
[48] J. Haidenbauer, G. Krein, U. G. Meissner, and L. Tolos, Eur. Phys. J. A **47**, 18 (2011).
[49] J.-J. Wu, R. Molina, E. Oset, and B. S. Zou, Phys. Rev. Lett. **105**, 232001 (2010).
[50] N. Isgur and M. B. Wise, Phys. Lett. B **232**, 113 (1989).
[51] M. Neubert, Phys. Rep. **245**, 259 (1994).
[52] A. V. Manohar and M. B. Wise, Cambridge Monogr. Part. Phys., Nucl. Phys., Cosmol. **10**, 1 (2000).
[53] C. Garcia-Recio, V. K. Magas, T. Mizutani, J. Nieves, A. Ramos, L. L. Salcedo, and L. Tolos, Phys. Rev. D **79**, 054004 (2009).
[54] D. Gamermann, C. Garcia-Recio, J. Nieves, L. L. Salcedo, and L. Tolos, Phys. Rev. D **81**, 094016 (2010).
[55] H. Toki, C. Garcia-Recio, and J. Nieves, Phys. Rev. D **77**, 034001 (2008).
[56] C. Garcia-Recio, J. Nieves, and L. L. Salcedo, Phys. Rev. D **74**, 034025 (2006).
[57] R. F. Lebed, Phys. Rev. D **51**, 5039 (1995).
[58] A. J. G. Hey and R. L. Kelly, Phys. Rep. **96**, 71 (1983).
[59] R. F. Dashen, E. E. Jenkins, and A. V. Manohar, Phys. Rev. D **49**, 4713 (1994); **51**, 2489(E) (1995).
[60] D. G. Caldi and H. Pagels, Phys. Rev. D **14**, 809 (1976).
[61] D. G. Caldi and H. Pagels, Phys. Rev. D **15**, 2668 (1977).
[62] D. Gamermann, C. Garcia-Recio, J. Nieves, and L. L. Salcedo, Phys. Rev. D **84**, 056017 (2011).
[63] C. Garcia-Recio, L. S. Geng, J. Nieves, and L. L. Salcedo, Phys. Rev. D **83**, 016007 (2011).
[64] C. Garcia-Recio, J. Nieves, and L. L. Salcedo, Phys. Rev. D **74**, 036004 (2006).
[65] T. Hyodo, D. Jido, and L. Roca, Phys. Rev. D **77**, 056010 (2008).
[66] C. Garcia-Recio, M. F. M. Lutz, and J. Nieves, Phys. Lett. B **582**, 49 (2004).
[67] C. Garcia-Recio and L. L. Salcedo, J. Math. Phys. (N.Y.) **52**, 043503 (2011).
[68] J. Nieves and E. Ruiz Arriola, Phys. Rev. D **64**, 116008 (2001).
[69] T. Hyodo, D. Jido, and A. Hosaka, Phys. Rev. C **78**, 025203 (2008).
[70] J. A. Oller and U. G. Meissner, Phys. Lett. B **500**, 263 (2001).
[71] S. Sarkar, B.-X. Sun, E. Oset, and M. J. Vicente Vacas, Eur. Phys. J. A **44**, 431 (2010).
[72] E. Oset and A. Ramos, Eur. Phys. J. A **44**, 445 (2010).
[73] K. Nakamura *et al.* (Particle Data Group), J. Phys. G **37**, 075021 (2010).

[74] C. Albertus, E. Hernandez, and J. Nieves, Phys. Lett. B **683**, 21 (2010).
[75] J. M. Flynn, E. Hernandez, and J. Nieves, Phys. Rev. D **85**, 014012 (2012).
[76] J. J. Dudek, R. G. Edwards, and D. G. Richards, Phys. Rev. D **73**, 074507 (2006).
[77] A. E. Blechman, A. F. Falk, D. Pirjol, and J. M. Yelton, Phys. Rev. D **67**, 074033 (2003).
[78] D. Jido, J. A. Oller, E. Oset, A. Ramos, and U. G. Meissner, Nucl. Phys. **A725**, 181 (2003).
[79] C. Garcia-Recio, J. Nieves, E. Ruiz Arriola, and M. J. Vicente Vacas, Phys. Rev. D **67**, 076009 (2003).
[80] L. Roca, S. Sarkar, V. K. Magas, and E. Oset, Phys. Rev. C **73**, 045208 (2006).
[81] A. F. Falk, Nucl. Phys. **B378**, 79 (1992).